Holocene Vegetation, Drought, and Fire Variability in the Northern Great Basin, Oregon

by

Chantel Victoria Saban

A dissertation accepted and approved in partial fulfillment of the

requirements for the degree of

Doctor of Philosophy

in Geography

Dissertation Committee:

Daniel G Gavin, Chair

Patricia McDowell, Core Member

Lucas de Carvalho Ramos Silva, Core Member

Edward Davis, Institutional Representative

University of Oregon

Summer 2023

DISSERTATION ABSTRACT

Chantel Victoria Saban

Doctor of Philosophy in Geography

Title: Holocene Vegetation, Drought, and Fire Variability in the Northern Great Basin, Oregon

The Northern Great Basin of south-central Oregon is ecologically diverse along elevational gradients. Generally, the area consists of sagebrush steppes and dry playas at the lowest elevations, mixed conifer dry forests at mid-elevations, and more mesic mixed forests to subalpine vegetation at high elevations. Ecosystems at all elevations have experienced significant climatic changes over the course of the Holocene, resulting at times in vegetational relocations. It has been unclear which environmental limiters have resulted in fire and ecological changes, and whether these controls differ among elevations and ecotones.

To reconstruct this environmental variability since the early Holocene, three sites located within 40 km of one another were selected to study environments located at different elevations over the Holocene. Two sites, Dog Lake and White Pine Marsh, provided sediment cores, and the third, Paisley Caves, used sediments and coprolites to reconstruct and contrast the low-elevation environment adjacent to the caves. Together these three sites grant a long-term view of environmental conditions over the last 10,000 years.

During the early Holocene, the area west of the Paisley Caves on slopes of Winter Rim saw significant *Abies* expansion, giving way eventually to *Pinus ponderosa* as *Abies* retreated upslope to the top of Winter Rim, indicative of little fire at lower elevations in the Paisley Caves region. Pollen assemblages of the coprolites differed from adjacent cave sediment, consistent with the selective ingestion of pollen by mammals.

The mid-elevation Dog Lake became so warm and arid during the early Holocene that fuel availability likely limited fire occurrence, and fire was very episodic through the remainder of the Holocene. High-elevation mixed forest site

White Pine Marsh experienced frequent and gradually increasing fires during the early Holocene. However, after the eruption of Mount Mazama in 7640 cal yr BP, 25 cm of lapilli tephra deposition there was greatly reduced fire for the remainder of the Holocene despite abundant fuels. Together, these records add to the understanding of the variability of drought, fire, and the forest/steppe landscapes of the Northern Great Basin.

Chapter 2 includes contributions from Daniel Gavin, Erin Herring, and Dennis Jenkins. At the time of writing the paper is in-press at Quaternary Research. Erin Herring processed the coprolites and provided analysis descriptions. Dennis Jenkins is the senior archaeological researcher at Paisley Caves and provided site expertise to this paper. Daniel Gavin and Chantel Saban conceptualized the study and devised the methodology of analysis. Saban analyzed the sedimentary pollen, while both Gavin and Saban analyzed the sedimentary lithological components. Saban wrote the original manuscript, with Gavin's help in the analysis and visualization of the data. Gavin also reviewed, edited, and contributed to the final manuscript.

In chapter 3 Saban and Gavin conceptualized the study and analyzed sediments, while Saban analyzed the pollen and charcoal. Analysis and data visualizations were significantly aided by Gavin while Saban wrote the original manuscript. Gavin further reviewed, edited, and contributed to the final manuscript. In chapter 4 Saban and Gavin conceptualized the study and devised the research methodology as well as analyzed the sediments, while Saban processed and analyzed pollen and charcoal. Saban wrote the original manuscript, and Gavin reviewed, edited, and contributed to the final manuscript.

CURRICULUM VITAE

NAME OF AUTHOR: Chantel Victoria Saban

GRADUATE AND UNDERGRADUATE SCHOOLS ATTENDED:

University of Oregon, Eugene
Oregon State University, Corvallis
University of Oregon, Eugene
Lane Community College, Eugene

DEGREES AWARDED:

Doctor of Philosophy, Geography, 2023, University of Oregon
Masters, Applied Anthropology, 2015, Oregon State University
Bachelor, Anthropology, 2010, University of Oregon

AREAS OF SPECIAL INTEREST:

Paleoecology
Fire History
Long-term Environmental Change
Early Human Migrations North America
Domestication Events

PROFESSIONAL EXPERIENCE:

Course Instructor, Department of Geography, University of Oregon
Introduction to Physical Geography, Spring 2021, 2022, Summer 2019, 2020, 2023
Geomorphology, Summer 2021

Graduate Employee, Department of Geography, University of Oregon
Introduction to Physical Geography, Fall 2018, 2022, Winter 2017, 2019, 2021, 2022
Spring 2017, 2019, 2020
Our Digital World, Spring 2018, Fall 2021
Biogeography, Fall 2016, 2017, 2020
Geomorphology, Spring 2023
Introduction to Environmental Studies, Fall 2019, Winter 2020

Watershed Science and Policy, Winter 2023
Field School Assistant Instructor, Museum of Natural and Cultural History
Connley Caves Archaeological Field School, Summer 2014, 2015, 2016

Archaeology Field and Lab Technician, Museum of Natural and Cultural History/OSMA, 2010 - 2015

GRANTS, AWARDS, AND HONORS:

Geological Society of America, Student Grant ($500), 2023

University of Oregon, Department of Geography
Rippey Dissertation Writing Grant, Summer 2022

University of Oregon Graduate Student Research Symposium, Group Award

PUBLICATIONS:

Saban, C.V., Herring, E.M., Jenkins, D.L., Gavin, D.G., 2023. Late glacial through early Holocene environments inferred using pollen from coprolites and sediments recovered from Paisley Caves, Oregon. *Quaternary Research.* In press.

ACKNOWLEDGMENTS

My deepest and most heartfelt gratitude goes to my adviser, mentor, and dear friend, Dan Gavin. It is not hyperbole to state that I would not have gotten through this process without your endless patience, expertise, and genuine kind guidance and encouragement. Words are not enough to express my gratitude, so I'll just have to show it in the future by continuing research and scientific stewardship to the best of my ability. To Pat McDowell who always expressed genuine enthusiasm and interest in my work, as well as gave great advice. I would also like to thank my other committee members, including Lucas Silva who graciously agreed to be on my committee early on and always has a kind word and a smile, which really means a lot. To Edward Davis, to whom I could turn to understand R just a little better and geek out with on Star Wars. These topics are absolutely related. And to Dennis L. Jenkins, my dear friend and mentor without whom I would have never even considered graduate school and who through the years has handed me opportunity after incredible opportunity like candy, always trusting me to see it all through. Hey Boss: I done made it!

Further thanks goes to Erin M. Herring, my dear friend, mentor, and mental health coach who always took time to train me in paleoecological methods in the early days and has since become like a sister. Thank you to the small army of incredible people that have gone on this journey with me. My field/ coring crew: R-P 'UTMs Are Life' Cromwell, Brianna 'Bilbo' Rollo, Kate "Sassface" Hayes, Jamila Baig. Makaela O'Rourke, and Brianna Rollo (again) for all their help processing charcoal. Rose Nittler for her hours of diligent lab work and incredible knit caps and shawls. Jamila Baig, my friend, confidant, and Gilgit sister who has always been here for me, and suspect, always will be. Ariana White who introduced me to paleoecology at the U of O in the

first place! Friends from OSU, particularly Alex Nyers who has reached out with friendly advice and warm connection since our OSU days. He is one of those people who underestimates his positive impacts on the lives of others. My MNCH people, including Jaime Kennedy and Tom Connolly, and most especially Katelyn McDonough, my dear friend and colleague whom I have had the pleasure of extensively adventuring with since forever.

Special thanks goes out to the Old Goat crew: my magnificent Bonnie Henderson-Winnie, Thomas Marsh, and the rest of the bunch. You all challenged me and lifted me higher than you all know, and I look forward to seeing what the next 30 years brings us! Thank you all for helping me become a better person. Further deep and loving thanks goes to Charlotte Mueller, Meisha Linwood, Sara Hescock, and Annie Caruso. Thank you to Steve Thoms Sensei, who has guided and supported me, my work, and my family in more ways than martial arts and academia. Thank you also goes to Collen and Don Murray, both of whom helped set me on this path.

To Pat Luther, my dearest friend and, if he could fly, would totally be my falcon. You have stood by me through every bad decision and hair-brained idea I have had for close to 3 decades now. I hope I have contributed even a mote of what you have always given me, Pat. Thank you for your constant love and support.

Thank you to the love of my life, Matthew Kale, who also has lovingly put up with all my shenanigans for the last three decades. We've been through the best and worst times together hon, and in the end, I know I am a worthwhile person because you love me. I love you always and I won!

Muchas gracias a mi mamá Olga Saban-Kaup, mi héroe, amiga, y mejor profesora. Gracias para todo tu amor y fuersa, mámi! Te quiero mucho y por siempre. Ya no necesito la chancla!

DEDICATION

This dissertation is dedicated to Marie Elizabeth Kale.

You are deeply loved and will be with us all, always.

TABLE OF CONTENTS

Chapter Page

Chapter Page

LIST OF FIGURES

Figure Page

APPENDIX

LIST OF TABLES

CHAPTER I

INTRODUCTION

The Northern Great Basin of Oregon is an area of diverse ecologies organized along elevational gradients and variable water sources. At the lowest elevations are the remnants of Pleistocene pluvial lakes, now deflated alkaline playas. Sagebrush (*Artemisia tridentata*) steppe dominates the region, and anywhere there is water at or very near the surface, marshes are present. At higher elevations open dry-forest systems begin appearing, composed primarily of *Pinus ponderosa,* but also including *Pinus contorta* and *Juniperus occidentalis. Populus tremuloides* is also found in greater abundance at these mid-elevation areas. High-elevation sites often host mixed conifer forests, subalpine forests, and some alpine conditions, with white-bark pine (*Pinus albicaulis)* found at some of the highest peaks. During the Pleistocene atmospheric conditions were cooler than present day, and evapotranspiration was much lower, resulting in the formation of large lakes. There were also glaciers present in some places, as well as locations too cold and dry to form glaciers.

Climatic conditions began changing rapidly beginning ca. 12,000 years ago (Mehringer 1987; Wigand 1987). Maximum insolation continued warming the planet and peaked by 11,000 years ago most of the continental ice sheets were rapidly retreating while montane glaciers in the NGB had already retreated (Osborn and Beavis, 2001). By 9000 years ago maximum air temperatures and increased aridity resulted in the Northern Great Basin pluvial lakes desiccating and many vegetation communities shifting upward in elevation. Such climate changes would also cause fire event frequency to also change during this time, resulting in conditions and disturbance timings very different than the current day.

Towards the end of the early Holocene the catastrophic eruption of Mount Mazama in ca. 7640 cal yr BP (Egan, 2015) would again alter vegetation communities and fire events to varying degrees depending on locations relative to the main eruption blast zone. Despite periodic droughts climatic conditions in the NGB have generally cooled through the late Holocene, with vegetation communities again responding. (Benson et al., 1997; Minckley et al., 2007; Marsicek et al., 2018).

With an emphasis on the Holocene, questions behind this dissertation were driven by asking 1) by how much did vegetation communities change in the Northern Great Basin responding to changes in climate and fire, 2) which taxa changed the least, which the most, and was it climate or fire that drove those changes, 3) by how much is it possible to observe regional or local drought severity, and 4) by how much and when did climatic timing in the Northern Great Basin differ from Central and Southern Great Basin regions, if at all? To address these broad questions three locations were identified as good study sites. These three locations are within 40 km of each other but at different elevations. Differing elevations were sought for the purpose of attempting to determine what the rate of ecological change was for each location.

There are few records showing continuous ecological and fire records at different elevations in the NGB from the early Holocene through to today, but of the records that do remain a rich history of variable timing for fire histories and ecological community structures are sharply delineated and preserved (Gruell, 1995; Minckley et al., 2007).

Environmental conditions were reconstructed using traditional and novel methods for three sites identified as ideal for contributing ecological perspectives that would overlap in time. To reconstruct ecological settings, pollen was the primary data source for all three sites. Pollen assemblages provide a view of the climatic conditions at a given point in time, but in some cases

may not reflect the full context of conditions as other variables such as tephra or charcoal may alter interpretations. Iin the case of coprolite pollen, a false sense of what vegetation is present on the landscape and in what abundances can occur. When available, carbon and nitrogen concentrations show how climate affected lake productivity, and charcoal provides insights on the fire-adapted landscape and how vegetation responded to changing arid conditions and fire events over time.

Chapter 2 examines the late Pleistocene through early Holocene environmental conditions at a low-elevation site by contrasting the regional pollen signal preserved in the sediments of Paisley Caves to the more focused and hyper-local pollen found in chronologically contemporaneous coprolites produced by medium to large-sized mammals as they moved across their ancient landscapes. The results show several consistent differences in pollen assemblage composition in the coprolites compared to the sediments, consistent with the coprolite producers favoring certain environments prior to depositing coprolites in a cave.

Chapter 3 examines the history of a rare mid-elevation freshwater lake in the NGB. Dog Lake is a landslide-formed lake whose lake level fluctuates annually, but remained very low during the early Holocene, followed by a period of low lake productivity and lower vegetation cover between 8700 and 8200 cal yr BP, then deepened to a point it resembled depths seen today. Using pollen, C and N concentrations, plant macrofossils, and charcoal, we found when lake productivity was low resulting from increased aridity in the early Holocene, there was also fewer fire episodes than expected from climate, likely due to low fuel availability and probably fewer ignition events. Fire frequencies increased with cooling temperatures and increased effective moisture during the middle Holocene.

Chapter 4 describes the fire and hydrological history of White Pine Marsh (WPMA), a high-elevation site located in a small cirque valley at the northern terminus of the Warner Mountains. The site is in a mesic, mixed conifer forest with the perennial marsh having formed after the Mazama eruption and subsequent deposition of tephra in the basin. Sediments also show the fire history was also altered by the tephra. Charcoal showed fires were more frequent and increased in intensity during the early Holocene, abruptly changing to lower intensity and longer fire intervals post-Mazama. Pollen showed mixed conifer conditions since 9500 cal yr BP with *Pinus ponderosa* always dominant with variable presence of *Abies*.

This dissertation includes published and unpublished co-authored material. At the time of writing Chapter 2 is in press at Quaternary Review. Co-authors include Daniel Gavin, Erin Herring, and Dennis Jenkins. Herring processed the coprolites and provided analysis descriptions. Jenkins provided site expertise to this paper. Gavin and Saban conceptualized the study and devised the methodology of analysis. Both Gavin and Saban analyzed the sedimentary lithological components. Saban wrote the original manuscript with Gavin's help in the analysis and visualization of the data. Gavin also reviewed, edited, and contributed to the final manuscript.

In chapter 3 Saban and Gavin conceptualized the study and analyzed sediments. Saban analyzed the pollen and charcoal. Analysis and data visualizations were significantly aided by Gavin while Saban wrote the original manuscript. Gavin further reviewed, edited, and contributed to the final manuscript. In chapter 4 Saban and Gavin conceptualized the study and devised the research methodology as well as analyzed the sediments, while Saban processed and analyzed pollen and charcoal. Saban wrote the original paper, and Gavin reviewed, edited, and contributed to the final manuscript.

CHAPTER II

LATE GLACIAL THROUGH EARLY HOLOCENE ENVIRONMENTS INFERRED USING POLLEN FROM COPROLITES AND SEDIMENTS RECOVERED FROM PAISLEY CAVES, OREGON

Published as Saban, Chantel V., Erin M. Herring, Dennis L. Jenkins, and Daniel G. Gavin. In press. Late Glacial Through Early Holocene Environments Inferred Using Pollen from Coprolites and Sediments Recovered from Paisley Caves, Oregon. Quaternary Research.

Saban and Daniel Gavin conceptualized the study and devised the methodology. Saban wrote the original manuscript, and Gavin reviewed, edited, and contributed to the final manuscript. Herring processed and analyzed the coprolites, as well as wrote descriptions of findings. Jenkins contributed site expertise and commentary. Saban acquired the funding while curation, analysis, and visualization of the data were done with the help of Gavin.

1. INTRODUCTION

The post-glacial vegetation history of the Northern Great Basin (NGB) has been strongly affected by the balance of moisture from the Pacific Ocean and continental dry and warm air masses moving north from the Central Great Basin (Wigand and Rhode, 2002; Minckley et al., 2007). Although large lakes persisted in the basins of the NGB through the late Pleistocene, decreased effective moisture and increased evapotranspiration since 11,000 cal yr BP have resulted in the desiccation of these pluvial lakes and subsequent deflation of Pleistocene sediments, generally precluding the use of these larger basins as reliable archives of post-glacial climate change (Allison, 1982; Cohen et al., 2000). Understanding post-glacial environments and

reconstructing the heterogeneity of this landscape has implications for understanding the environments experienced by humans and other animals, which is especially important as the NGB has evidence of some of the oldest human activity in North America (Gilbert et al., 2008; Jenkins et al., 2012; McDonough, 2019), as well as extinct and extant megafauna remains (McDonough et al.,2012; Jenkins et al., 2013).

Many post-glacial pollen records recovered from within the NGB have been studied at mid-to high-elevation sites, as low-elevation sites containing undisturbed sedimentary sequences that span the Holocene are uncommon (Cohen et al., 2000). The few low-elevation pollen records that do exist reveal the ubiquitous presence of xeric shrub-steppe vegetation since the Last Glacial Maximum (LGM) (Mehringer, 1987; Wigand, 1987; Wigand and Rhode, 2002; Mensing et al., 2013; Beck et al., 2018; Kennedy, 2018; McDonough et al., 2022). However, wetlands are embedded within this xeric landscape. In various places, drainages from mountains feed into seasonal or persistent wetlands, resulting in a sharp contrast between wet and xeric plant communities as hydrophytic plants respond rapidly to changes in water availability (Kovalchik and Chitwood, 1990; Nowak et al., 1994).

Terrestrial caves often serve as natural subaerial sediment traps and can preserve organic materials for thousands of years (White, 2007). Archaeological investigations of caves and rock shelters occasionally yield preserved mammalian coprolites, offering opportunities to gain information about the diet and health of animals, and to make inferences about past climates and environments (Bryant, 1974; Hofreiter et al., 2000; Carrión et al., 2001; Gilbert et al., 2008; Riley, 2008; Shillito et al., 2011; Wood and Wilmshurst, 2012, 2016; Beck et al., 2018, 2020; Blong et al., 2020). Coprolite studies have been an important component of Great Basin archaeological research since the early 20th century (Loud and Harrington, 1929; Heizer, 1969;

Heizer et al., 1970; Kelso, 1971; Thomas et al., 1983), and have since greatly expanded our understanding of past human behaviors and health (Jenkins et al., 2012; Jenkins et al., 2013; Dexter and Saban, 2014; Beck et al., 2018; Kennedy, 2018; McDonough, 2019; Blong et al., 2020; McDonough et al., 2022).

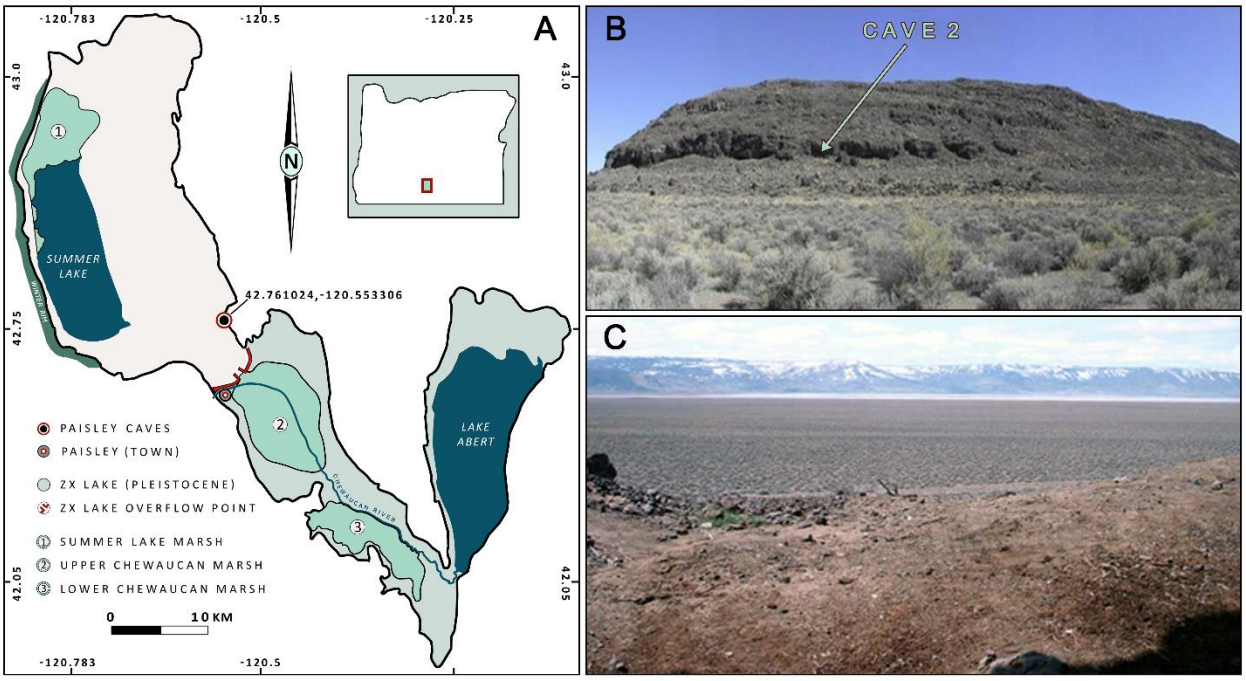

Figure 1. Location of 5-Mile Point Butte and Paisley Caves in the Chewaucan Basin of south-central Oregon. Black line shows the maximum high-water extent of pluvial lakes during the late Pleistocene. B. Looking east at 5-mile Point Butte with the caves. C. Winter Rim looking west as seen from Cave 5, Paisley Caves

Located in south-central Oregon within the NGB, the Paisley 5-Mile Point archaeological site (Paisley Caves) (Fig. 1A) produced a material assemblage that includes abundant coprolites, providing opportunities for expanding the interpretation of pollen records from cave sediments. Over 2800 mammalian coprolites were excavated from Paisley Caves between 2002 and 2011 (Jenkins et al., 2012, 2013), and each represents a point in time during the last >14,300 years. In this study, we assess the environmental conditions present during periods of wetland expansion and subsequent lake retreat in the Summer Lake basin between 14,000 and 6000 cal yr BP by

comparing pollen assemblages of coprolites and their associated sediments. With this approach, pollen recovered from sediments represents multi-decadal periods of sedimentation while coprolite pollen offers a different view of environmental conditions due to a short (several-day) "sampling" period. The Paisley Caves are situated in close proximity to three ecotones: lacustrine-wetland, sagebrush steppe, and conifer forest (Cronquist et al., 1972; Franklin and Dyrness, 1988; Anderson et al., 1998). Contrasting pollen assemblages of sediments and coprolites may help clarify the paleovegetation history, which is still not well understood at low-elevation NGB sites.

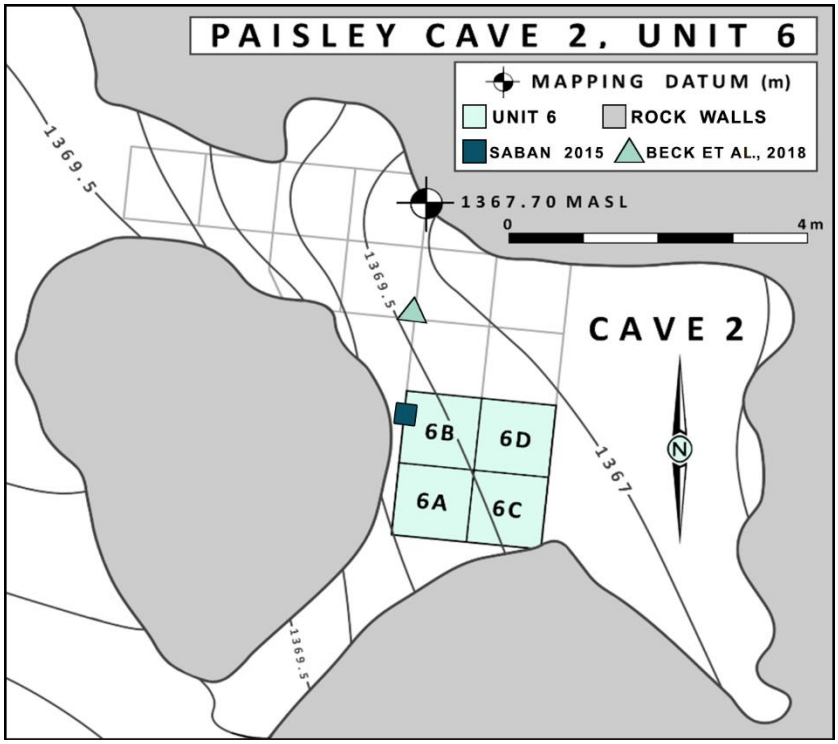

Figure 2. Cave 2 showing location of Unit 6 relative to datum and roof fall boulder at west end of the entrance. Map image redrawn from Jenkins et al. 2012.

Five previous studies of pollen and macrobotanical assemblages were conducted at Paisley Caves. First, Saban (2015) produced a pollen record from the same sampling unit (Cave 2, Unit 6B) as this study and is succeeded by the present study. Second, Beck et al. (2018)

produced a pollen record from the same cave as this study (Cave 2) but located one meter north of our sampled profile at a site with a different chronology and potentially different taphonomic processes (e.g., exposure to wind) (Fig. 2). Third, Kennedy (2018) identified macrobotanical remains from Cave 2 and developed a detailed description of local vegetation and cultural foods and plant resources. Fourth, Beck et al. (2020) at the same profile as Beck et al. (2018), compared *Neotoma* spp. (wood rat) coprolite pollen assemblages to sediment pollen assemblages. Due to the small mass of *Neotoma* coprolites, Beck et al. (2020) merged 57 coprolites into single samples resulting in a total of fifteen 0.25 g samples of packrat coprolites. Pollen assemblages of *Neotoma* coprolites were statistically very similar to those in associated sediments, but coprolite pollen assemblages were more variable than those from sediments possibly due to meal choice (Beck et al., 2020). Finally, Blong et al. (2020) examined contents of nine coprolites identified as originating from humans from the Younger Dryas through the Early Holocene for the purpose of reconstructing prehistoric human diets. That study found seeds, bones of small mammal and fish, and beetle remains in the coprolites, supporting foraging in marshes. Blong et al. (2020) also conducted limited pollen analyses, which found elevated percentages of insect-pollenated taxa and pollen aggregates, suggesting direct consumption of pollen.

DNA analysis of other coprolites from Paisley Caves have revealed coprolites associated with *Homo sapiens*, Camelidae, *Lynx*, *Ovis*, and *Panthera* (Jenkins et al., 2012). In addition to identifying the oldest human coprolites in North America, the Paisley Caves boast an extensive assortment of organic artifacts and materials that offer invaluable insights into the activities of humans and fauna from over 14,000 years ago. However, our comprehension of how humans and large mammals traversed the ancient landscapes of the NGB remains limited. Given the

limited past analyses of mammalian coprolite pollen at Paisley Caves (Blong et al., 2020), there remains a potential for this approach to provide us with a better understanding of how large mammals roamed the local environment and left behind evidence of their movements at the caves.

Traditionally, mammalian coprolite analysis from archaeological sites in North America has been used to reconstruct diet, health (Bryant and Holloway, 1983; Bryant and Reinhard, 2012; Blong et al., 2020), and human activities at a site (Gilbert et al., 2008; Jenkins et al., 2012; McDonough, 2019; Shillito et al., 2020). This study uses coprolite pollen solely as an environmental proxy to reconstruct conditions at and beyond the caves. Pollen found in coprolites represent short periods of time, approximately 19-37 hours (Kelso and Solomon, 2006), and is derived from various sources: pollen in drinking water, airborne pollen that entered nasal and esophageal mucus, pollen adhered to any food item, pollen in ingested flowers or pollen cones, or pollen in the stomach content of prey (Carrión et al., 2001; Chame, 2003). Thus, coprolite pollen represents a brief period that can potentially reveal different information than sediment pollen. This study is unique in using coprolites as distinct pollen samples for direct statistical comparison to contemporaneous sediments and considering all taphonomic pathways (not only diet) behind the formation of the coprolite pollen assemblage (Shillito et al., 2020).

Interpretation of pollen assemblages from cave sediments can be limited for several reasons. Caves often contain both aeolian and slope-wash sediment, filtered from the environment via the single depositional entry of the cave opening. Also, within the NGB redeposition of sediments blown off dry lakebeds may contribute pollen from prior climatic periods (Anderson, 1955). The location of the sediment samples relative to the layout of the cave may affect pollen assemblages due to, for example, pollen degradation due to temperature

exposure or physical degradation within a drip zone. Lastly, bioturbation of sediments by faunal or human activities can disturb or erase the chronological integrity of sedimentary sequences, resulting in time-averaged pollen assemblages.

We hypothesize that differences in the pollen assemblages between cave sediment and coprolites emerge primarily due to the unique "sampling" of the environment by a mammal. We therefore predict that 1) pollen assemblages will differ more between coprolites and associated sediments than between samples within either group, 2) pollen assemblage turnover (i.e. rate of change) will be greater for coprolites than in sediments due to the potentially stochastic processes that determine the coprolite pollen assemblage, and 3) pollen taxonomic diversity will be greater in sediments than in coprolites, as sediments sample a larger spatial and temporal window of pollen deposition than do coprolites.

2. SITE DESCRIPTION

2.1. Geologic setting

Summer Lake basin is located within the larger Chewaucan Basin, a V-shaped graben delineated by steep fault scarps and subdivided into 3 sub-basins: Summer Lake lies in the northwest portion of the “V”, with the basin that holds Upper and Lower Chewaucan Marshes in the south, and Lake Abert in the northeast (Fig. 1). The Chewaucan Basin graben dips northwest with the Summer Lake basin floor averaging 1275 m, Upper and Lower Chewaucan Marshes averaging 1314 m, and the Lake Abert basin averaging 1299 m.

The Paisley Caves are located on 5-Mile Point Butte, a scoriaceous basalt fault block butte located in the southeastern part of Summer Lake basin in south-central Oregon. This site is approximately 18 km east of the current Summer Lake shoreline and 8 km north of the

Chewaucan River (Fig. 1A). The caves are all on a southwest aspect, and their entrances are located midway up the butte at an average elevation of 1366 m above sea level (Fig. 1B). A series of eight wave-cut caves and rock shelters formed as a result of energetic wave action by Lake Chewaucan during periods of stable high lake stands (Allison, 1982; Friedel, 1993; Jenkins et al., 2013). Subsequent rockfalls at cave entrances have since resulted in some of the deeper caves developing into shallow rock shelters.

The current dry lakebed near 5-Mile Point Butte dips west at a 3.3° slope until the lakebed abruptly ends at the base of Winter Rim (Fig. 1C). The topography of the area north of 5-Mile Point Butte is characterized by dry lake flats, deflated playas, lunettes, and dune systems, with some small basalt fault block outcrops. East of 5-Mile Point Butte the topography rises in elevation above the lakebed floor and is less steep than the west side of Summer Lake basin. This east side is of fault block features that increase in elevation for 13 km up to approximately 1590 m after which the topography then slopes down 13 km east to Lake Abert. The Summer Lake lakebed slopes little south of 5-Mile Point Butte, where the topography is interrupted by the incised course of a stream that resulted from the overflow of ZX Lake into Summer Lake during the Younger Dryas (YD; Allison, 1982; Friedel, 1993; Hudson et al., 2021; Licciardi, 2001).

Pluvial Lake Chewaucan covered an area of 1243 km^2 at its maximum extent, with a surface elevation of 1381 m and a maximum depth of ca. 118 m (Allison, 1982; Cohen et al., 2000). The primary stream feeding Lake Chewaucan was the Chewaucan River, draining north through a steep river valley into the Chewaucan Basin. During the late Pleistocene Bølling-Allerød (BA) period, 14,700 to 12,900 cal yr BP (Sowers and Bender, 1995) water levels in Lake Chewaucan reached their last high stand by ca.14,500 cal yr BP, after which levels declined and Chewaucan River sediments formed the Paisley Fan (1323 m) at the south end of Summer Lake,

resulting in Summer Lake hydrologically separating from the rest of the Chewaucan basin (Allison, 1982; Licciardi, 2001). Basal sediments in this current study were dated to ca. 14,000 cal yr BP, at the time of the Chewaucan high stand.

The YD cold period (12,800 - 11,600 cal yr BP) is characterized by a return to cooler temperatures in the northern hemisphere (Mayewski et al., 1993; Rasmussen et al., 2014). At this time Summer Lake began receding due to lower precipitation and increasing insolation (Hudson et al., 2019, 2021). The climate began to warm after the YD, eventually resulting in climatic conditions being warmer during the earliest portions of the Holocene (11,000 – 9000 cal yr BP) with evidence of a brief period of increased precipitation that resulted in a transgression of Summer Lake to moderately high levels, although not as high as during the Bølling-Allerød (Hudson et al., 2021). Conditions reached thermal and aridity maximum after 9000 cal yr BP, after which climatic conditions began to cool but remained arid (Friedel, 1993; Bartlein et al., 1998, 2011; Cohen et al., 2000; Benson et al., 2002; Mensing et al., 2004; Minckley et al., 2007; Long et al., 2019; Hudson et al., 2021).

2.2. Climate and vegetation

The Summer Lake basin presently is located at a convergence zone of moist Pacific air parcels moving inland from the southwest and continental climate characterized by a high-pressure system centered above the Central Great Basin in Nevada to the southeast of the Chewaucan Basin, which has varied over the Holocene (Reinemann et al., 2009; Carter et al., 2017; Long et al., 2019). Geographically located in the rainshadow of the Cascade Range, the NGB region currently has warm summers and cold winters (mean July and January temperatures are 17.7°C and 2.2°C, respectively). Average annual precipitation is 33.9 cm with most

precipitation occurring from November through January and with afternoon thunderstorms during summer seasons.

Vegetation gradients in the region are primarily determined by elevation and its effects on orographic precipitation (Franklin and Dyrness, 1988; Kovalchik and Chitwood, 1990; Osmond et al., 1990). Current Summer Lake basin vegetation is high desert shrub-steppe dominated by *Artemisia tridentata* and salt-tolerant Amaranthaceae (*Chenopodium* and *Atriplex*; Franklin and Dyrness, 1988; St. Louis, 2021). The *A. tridentata* community includes an understory of the invasive *Bromus tectorum*, as well as *Elymus* sp., *Ericameria teretifolia*, *Sarcobatus vermiculatus*, and various other shrubs, forbs, and grasses adapted to sandy aeolian sediments and highly alkaline aridisols. At the base of 5-Mile Point Butte, the lakebed sharply transitions into a steep, rocky talus of basalt boulders with pockets of playa loess accumulating between the boulder gaps. Vegetation on the talus slope is primarily *Artemisia* and *Chrysothamnus* sp. with intermittent cespitose *Eriogonum* sp. and hemiparasitic *Castilleja angustifolia*.

The trees currently nearest to the caves are 8 km to the south at the town of Paisley, where riparian vegetation extends along the Chewaucan River into Upper Chewaucan Marsh. Modern-day trees and shrubs include *Pinus ponderosa, Alnus incana, Betula occidentalis, Juniperus occidentalis, Prunus virginiana, Salix* sp., *Populus tremuloides, Populus trichocarpa,* and non-native *Populus alba*. A very small population of *Quercus garryana* var. *semota* was reported on Gearhart Mountain at 1650 m (https://oregonflora.org/taxa/index.php?taxon=14318). Non-native *Medicago sativa* is grown in center-pivot irrigation fields within a few kilometers of the caves. Marsh plants are present in both Upper and Lower Chewaucan Marshes, near the Summer Lake Hot Springs ca. 8 km west of 5-Mile Point Butte, along most of the 40 km base of

Winter Rim, and at the north end of the Summer Lake basin at the Summer Lake Wildlife Area 24 km north of 5-Mile Point Butte. The marsh communities include a range of Poaceae, Juncaceae, Cyperaceae, *Ribes* sp., Typhaceae, and Asteraceae. Trees present 20 km west of 5-Mile Point Butte on the steep scarp of Winter Rim (2200 m elevation) include *Populus trichocarpa* and *P. alba, Prunus virginiana* at the base, *Pinus ponderosa, Salix* sp., *Juniperus occidentalis, Populus tremuloides* at mid-elevation, and *Pinus contorta* and *Abies concolor* at the Winter Rim summit.

2.3. Archaeological excavations at Paisley Caves

Sediments and coprolites used in this study were all collected during archaeological research at Paisley Caves between 2009 and 2011. Archaeological research began in 1938 under University of Oregon archaeologist Luther S. Cressman (Cressman, 1940; Jenkins et al., 2004), who numbered the caves sequentially from south to north. From 2002 to 2011 University of Oregon archaeologist Dennis L. Jenkins directed further excavations at the site. Materials recovered ranged from artifacts such as lithic tools and debitage, bone, antler, and wood tools, cordage, and grinding stones (manos and metates), as well as a rich array of organic materials that included plant macrofossils, insects, the bones of fish, waterfowl, small mammals, extant and extinct megafauna, reptiles, and 2533 coprolites of human and other mammalian origins. Gilbert et al. (2008) reported on the DNA sequencing of three ca. 14,000-year-old human coprolites which at the time of publication were the oldest confirmed human remains in the Western Hemisphere.

Materials dated to the YD period showed human activity was very high in Paisley Cave 2, with cultural material deposits becoming dense enough to create a culturally-formed

stratigraphic level referred to as the Botanical Lens (BL). BL deposits are composed primarily of a 5-8 cm thick mat of *Artemisia* twigs and shredded bark and contained a hearth dated to the YD (Jenkins et al., 2013). The BL is underlain by a 1-3 cm alluvial mud lens dated to ca. 12,930 cal yr BP and capped by a second 1-2 cm mud lens dated to ca. 11,500 cal yr BP.

The coprolites and sediments used in this study were excavated from Cave 2, Unit 2/6 (Fig. 2). Materials from this unit were selected for this project due to the high number of well-mapped, stratigraphically sequential, and large mammalian coprolites with associated sediments, as well as for the minimal westward slope of the cave floor (Fig. 3). Cave 2 is approximately 7 m long, 6 m wide, and 3 m deep; 30.3 m^3 of sediment over 22 m^2 has been excavated from this cave (Jenkins et al., 2013). The cave walls are composed of fine-grained basalts mixed with soft volcanic tuffs and breccias. Summer Lake basin is a seismically active area (Badger and Watters, 2004; Licciardi, 2001; Orr and Orr, 2012) resulting in roof falls being common in the caves. Roof fall materials range from small pebbles to multi-ton boulders, the most notable of which was once the outer ceiling of Cave 2 which now blocks most of the entrance to the cave. The age of the roof fall is ca. 2300 cal yr BP based on a radiocarbon date obtained from a human coprolite recovered from beneath a smaller boulder from the same event (Jenkins et al., 2013). In 1939 Luther Cressman excavated a trench in Cave 2 but missed unit 2/6 due to the presence of the roof-fall boulders. Looters who later dug up the Cressman trench also missed the 2/6 sediments for the same reason. The larger boulder remains in place, but the smaller one was removed in 2009. Cave 2 was divided into seven 2 m x 2 m plots that were further subdivided into 1 m x 1 m units (Fig. 2). By the end of Cave 2 excavations in 2011 the cave had been excavated in primarily 5 cm increments down to bedrock at a depth of ca. 308 cm.

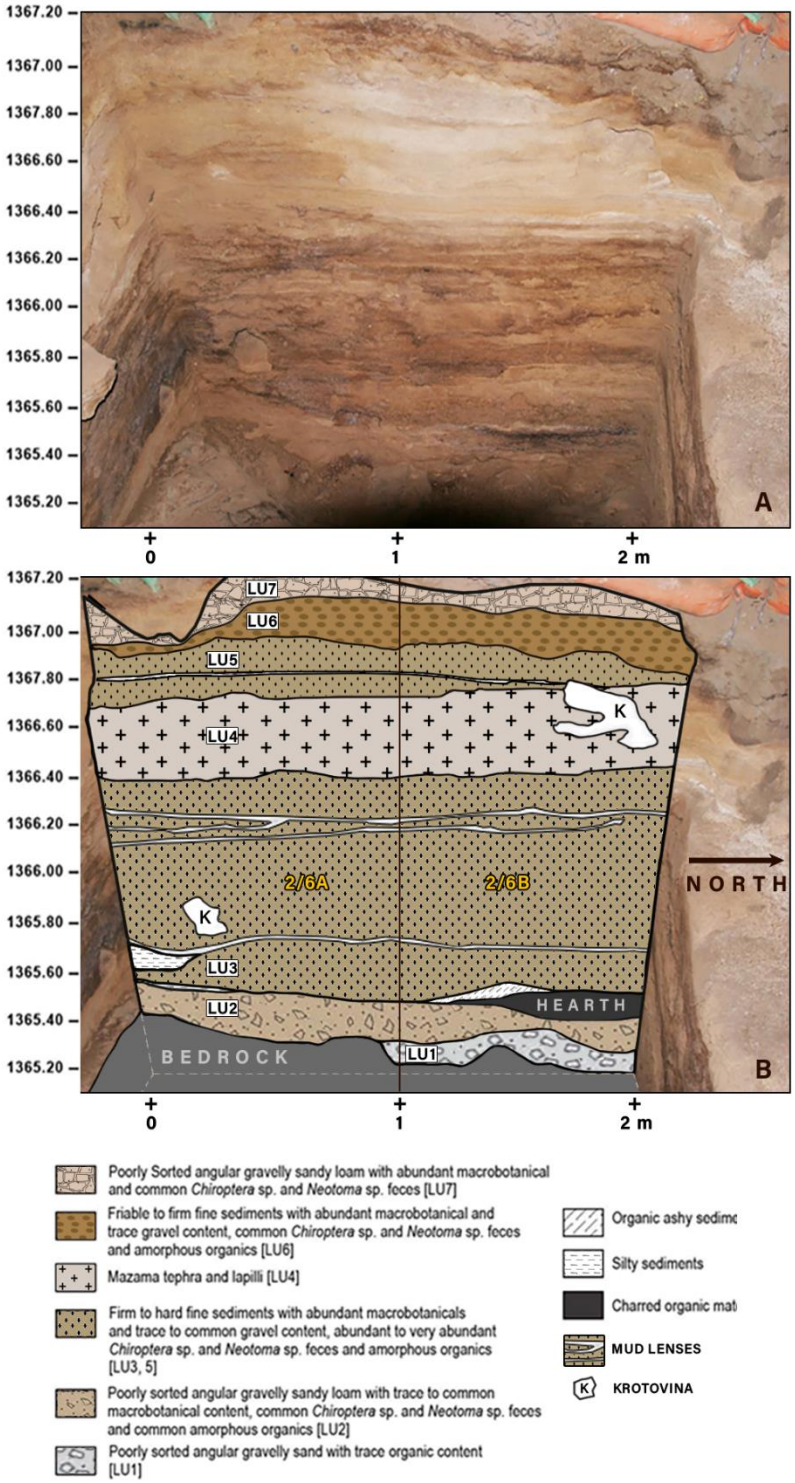

Figure 3. Remaining west wall of unit 2/6. This sediment wall is overlain by the roof collapse that occurred ca. 2 ka. Visible in the photo is the tephra layer, indurated laminations, the remains of a small hearth which is part of the Botanical Lens, and rodent holes (krotovina). Bottom image and description redrawn from Jenkins et al. 2012. Larger figure also in Appendix 25.

2.4. Sediment descriptions

Cave 2 sediments are comprised of both biological and exogenetic materials (Jenkins et al., 2012), and include varying amounts of aeolian deposits, rockfall, bat guano, rodent feces, deposited cultural materials, and vegetation blown in or brought into the rock shelter by *Neotoma* sp. Areas under smaller rockfall boulders not excavated by Cressman in 1938 were bioturbated by rodents or badgers or destroyed by looters in places, but overall the sediment matrices were well preserved and in excellent sequential order (Jenkins et al., 2012). This was largely due to millennia of urine accumulation forming hydrophobic and waterproof indurated sediments (Jenkins et al., 2012). A cross-section of the remaining 2/6 west sediment wall (Fig. 3) shows the stratigraphy before excavations. Cave 2 has an average sedimentation rate of approximately 50 years per centimeter, with the exception of the BL, which is primarily of anthropogenic origin, and the 30 cm of Mazama tephra representing a single event (Jenkins et al., 2016).

Lithostratigraphic units (LUs) are distinct sediment types that make up the matrices of sedimentary units and defined by their sediment characteristics (Gasche and Tunca, 1983; Stein, 1987). Seven LUs were identified in Cave 2, though only three are relevant here. LU1 overlays basement rock in a portion of 2/6B that was not sampled for this project. LU2 is a dark brown, poorly sorted gravelly sand approximately 30 cm thick overlying basement rock or LU1.

A distinct transition from LU2 to LU3 occurs at ca. 260 cm and has been dated to 12,500 cal yr BP. The transition is marked by a patchy occurrence of the BL (described above) and includes a small hearth of charred organic material overlain by ashy/organic sediment. LU3 extends up to the cataclysmic eruption of Mount Mazama ca. 7633 cal yr BP (Egan 2015). LU3 is a mix of fine aeolian deposited sediments, some smaller poorly sorted gravels mixed with angular roof fall, and heavy organic components of plant materials and bat guano (Jenkins et al.,

2012). LU3 sediments are firm to hard of polygenetic origins with abundant macrobotanical content, amorphous organic matter, and high amounts of *Neotoma* and *Chiroptera* feces (Jenkins et al., 2012).

Weakly consolidated Mazama tephra (152-180 cm) was assigned as LU4. Guano pellets from the base of the Mazama tephra were dated to 7633 cal yr BP (Jenkins et al., 2013). Laminations and fine ash capping and underlying the tephra suggests primary tephra deposition at the west end of Unit 2/6 (Fig. 3). The tephra in the 2/6 west wall ranges from fine ash to pale yellow rhyolitic lapilli from 1–1.5 mm in size. The topmost sediments for this unit are referred to as LU5, and contained little to no Mazama tephra (Jenkins et al., 2012).

3. METHODS

3.1. Material collection during excavations

All coprolites found *in situ* during excavations in Cave 2 from 2009 to 2011 were collected following strict protocols to limit their exposure to modern-day DNA contamination. These collection protocols included Tyvek hazmat suits, sterile gloves, forceps, and specimen cups. For most of the sampled coprolites, a sediment sample was also taken directly below the coprolite. Both samples were then sealed into sterile specimen cups and labeled. All coprolites selected for the study had an associated sample of sedimentary materials collected at the same time. No effort was made to distinguish human coprolites from those of other large carnivorous or omnivorous mammals. The coprolites were desiccated and ranged from very light tan to medium brown (Fig. 4). Faunal fragment analysis resulted in 6 to 20 bone fragments per coprolite sample, ranging from between 3-8 mm in size, and included mammalian and avian bone fragments (Cromwell, R.P., personal communication, 2016).

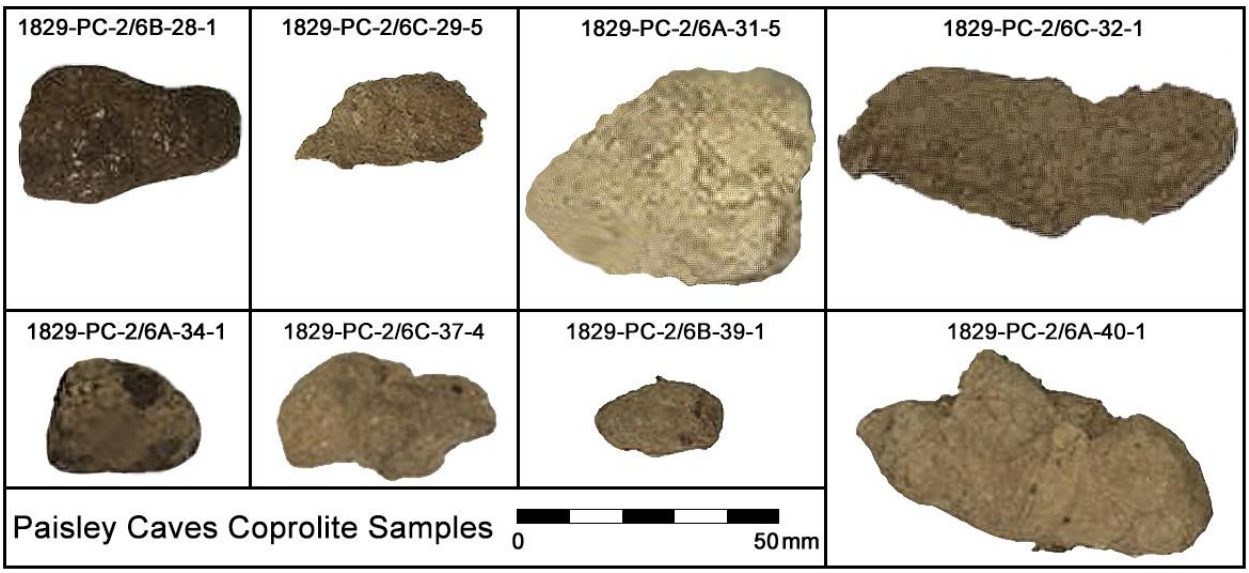

Figure 4. Photographs of a selection of the coprolites from Paisley Caves used in this study.

All the bones were fragmented except for one rodent left tarsal, several rodent molars, the dentin sheath of a rodent incisor, and two rodent claws. Artifact and radiocarbon date positions were changed from elevation (m) to cm below the modern cave floor (1368.3 m) for subsequent analyses. All samples in this study are from unit 6B (Fig. 2). In this portion of the cave, undisturbed sediments were excavated at depths of 120 to 320 cm below the 1368.3 m elevation.

3.2. Lab processing: coprolites

Sampling and chemical processing of both coprolites and sediments were conducted at the University of Oregon where strict sampling procedures were followed to protect the remaining materials from modern DNA contamination. Coprolites were subsampled for pollen following methods outlined by Wood and Wilmshurst (2012, 2016), except for sectioning the coprolites along a longitudinal axis rather than the center. An average dry weight of 1.6 g (ranging 0.668 to 3.638 g) was sampled from the center of each coprolite (Fig. 4). Coprolites lighter than 0.50 g were not processed.

The chemical process for pollen recovery from coprolites followed Pearsall (2016) and Smith (1998) but was modified to protect materials including bone and plant fibers for possible future radiocarbon dating. Chemical pollen extraction was performed inside a fume hood. Each coprolite subsample was placed in a 50 mL tube and spiked with one *Lycopodium* tablet to determine pollen concentration. Samples were rehydrated with 50 ml warm 10% sodium hexametaphosphate ($Na_6[(PO_3)_6]$) for 48-72 hours. Samples were sieved at 180 µm, and macrofossils were collected. Samples were treated with a 10% potassium hydroxide (KOH) at 80°C for 10 minutes, acetolysis (9:1 acetic anhydride:sulfuric acid, heated for 3 minutes). Samples were stained with Safranin and desiccated using ethyl alcohol and tert-butyl alcohol. Pollen was transferred into 2-dram glass vials with silicone oil used for suspension and preservation of pollen (Faegri et al., 1989).

3.3. Lab processing: cave sediments

Pollen recovery from the Paisley sediments required some minor adjustments to the chemical extraction process from Smith (1998) and Pearsall (2016). Sediments were wet-sieved using a 125 µm mesh until obtaining 20 cm^3 of the fine fraction. Each sample was added to a 1000 mL Nalgene beaker (12 samples per lab session) and spiked with one *Lycopodium* tablet to measure pollen concentrations. Samples were soaked in warm 10% $Na_6[(PO_3)_6]$. Sediments were agitated and allowed to settle for 8 hours, after which the water was partially decanted and refilled with distilled water (no additional $Na_6[(PO_3)_6]$ added), agitated, and allowed to settle for another 8 hours. This process was repeated for approximately 10-12 days until the water was clear. 10% KOH (80°C, 10 minutes) was used to remove remaining soluble organics followed by a 10% hydrochloric acid (HCl) treatment to remove carbonate minerals. A cold hydrofluoric acid

(HF) treatment for 24 hours reduced silicate content. Prior work on Cave 2 sediments showed that a cold HF treatment was more effective at removing silicates than a 45-minute hot HF treatment (Saban, 2015). Following a second 10% HCl treatment, the samples were rinsed with ultra-pure water.

Following the Smith (1998) protocols for processing dry sediments, a heavy liquid solution (1.9–2.0 specific gravity) of zinc bromide ($ZnBr_2$) was used to separate pollen from heavier materials. Following centrifuging, pollen suspended on the heavy liquid was decanted into 50 mL centrifuge tubes. $ZnBr_2$ heavy liquid suspension was repeated twice per sample. The remaining sediments in their original centrifuge tubes were filled with ultra-pure water, capped, and placed into storage boxes for possible future pollen recovery. The pollen fractions were diluted with water and centrifuged to remove the remaining $ZnBr_2$. Pollen was then transferred into 15 mL centrifuge tubes. Glacial acetic acid (GAA) was used to remove water, followed by acetolysis (as for the coprolite samples) to remove the remaining cellulose. Samples were stained, desiccated, and suspended in silicon oil as described for the coprolite pollen.

3.4. Identifications

Pollen from both coprolites and sediments were examined at 40X magnification. Pollen was identified to the highest taxonomic resolution possible using published keys (Faegri et al., 1989) and the modern pollen reference collection at the University of Oregon. Both coprolite and sediment slides were counted to a minimum of 350 grains per sample, with the exception of one coprolite with low pollen abundance where only 175 pollen grains could be identified.

3.5. Chronology

An age-depth model was constructed using the INTCAL20 calibration curve and the Bacon R package (Blaauw and Christen, 2011) (Reimer et al., 2020). The model is based on 16 radiocarbon dates available from unit 2/6 (Saban, 2015; Jenkins et al., 2016). We also obtained a new date on an unidentified plant macrofossil from a coprolite occurring above the Mazama tephra. A date of 7633 cal yr BP for the Mount Mazama eruption (Egan et al., 2015) was included in the age-depth model. In the Bacon model, we specified the Mazama tephra unit as an instantaneous event and placed a hiatus at 296.5 cm, where an abrupt change in ages corresponds roughly to the depth of the BL.

3.6. Statistical analyses

Raw pollen counts were transformed into percentages and diagramed using Tilia 3.0.1. Pollen assemblage zones of the sediment pollen record were determined using stratigraphically constrained cluster analysis. We used the rioja package in R statistical software to identify zones based upon the chord distance, calculated as the Euclidean distance of square-root-transformed pollen proportions. The number of significant pollen zones was determined using the broken stick method (Bennett 1996).

Non-metric multidimensional scaling (NMDS) gradient analysis was used to compare sediment and coprolite assemblage relationships. NMDS is an indirect gradient ordination analysis using a dissimilarity matrix that describes a pairwise difference between taxa assemblages. Pollen assemblage dissimilarity was measured using the chord distance using the vegdist and metaMDS functions in the vegan package in R (Oksanen et al., 2020). Both

coprolites and sediments were included in the ordination, using the 29 taxa found in three or more samples.

Chord-distance dissimilarity was summarized between coprolites and adjacent sediment and between adjacent sediment and coprolite samples as a measure of stratigraphic turnover. Pollen taxa richness of coprolite and sediment samples was estimated using rarefaction for a sample of 175 pollen grains, using the rarefy function in vegan. The difference of rarefied pollen richness between coprolites and corresponding sediment samples was tested using a paired t-test.

4. RESULTS

4.1. Sediment age-depth model and pollen assemblage zones

Thirteen of the 17 radiocarbon ages occur in the lower 40 cm, surrounding the BL, several of which were out of stratigraphic order. The Bacon age-depth model provides a best estimate of ages through periods of overlapping radiocarbon dates at the base of the section as well as interpolation between ages at the top of the section (Fig. 5; Table 1).

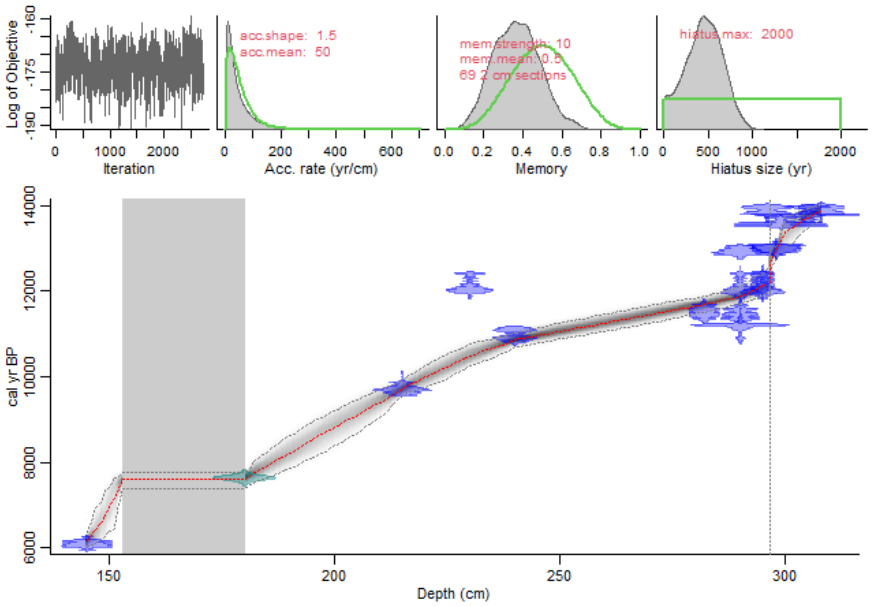

Figure 5. Bacon age-depth model for Paisley Cave 2, Unit 6B (Blaauw, M. and Christen, JA. 2011, Reimer et al. 2020). The grey area on the graph represents sediments enriched with Mazama tephra.

Table 1. Radiocarbon dates from Paisley Cave 2, unit 6. Depths are in relation to datum at 1367.70 m elevation.

Depth (cm)	Material	Lab number	Radiocarbon age	Calibrated 2σ age range	Source
145	amorphous coprolite plant matter	CAMS-176969	5305 ± 30	6190-5950	This study
152-180	Mazama tephra	-	-	7682-7584	Egan et al. 2015
215	*Artemisia* wood	UGAMS-14472	8740 ± 20	9890-9560	Saban 2015
230	*Artemisia* wood	UGAMS-14473	10,310 ± 20	12,440-11,940	Saban 2015
240	*Artemisia* wood	UGAMS-14474	9630 ± 20	11,170-10,800	Saban 2015
282	*Artemisia* charcoal	UCIAMS-98931	10,020 ± 30	11,710-11,320	Jenkins et al. 2016
290	*Artemisia* charcoal	D-AMS 1217-410	9774 ± 46	11,260-11,110	Jenkins et al. 2016
290	*Atriplex* bark cordage	UCIAMS-85337	9995 ± 25	11,680-11,280	Jenkins et al. 2016
290	*Atriplex* bark cordage	UCIAMS-87420	10,920 ± 35	12,890-12,760	Jenkins et al. 2016
290	*Artemisia* charcoal	UCIAMS-90577	11,005 ± 30	13,060-12,830	Jenkins et al. 2016
295	bone Artiodactyl	UCIAMS-103089	10,290 ± 30	12,440-11,830	Jenkins et al. 2016
295	*Artemisia* wood	UCIAMS-103086	10,365 ± 30	12,470-12,000	Jenkins et al. 2016
296	bone *Camelops* carpal	UCIAMS-103085	11,980 ± 35	14,020-13,780	Jenkins et al. 2016
298	*Artemisia* charcoal	UCIAMS-102110	11,055 ± 35	13,090-12,850	Jenkins et al. 2016
298	*Artemisia* charcoal	D-AMS-1217-406	11,098 ± 45	13,100-12,900	Jenkins et al. 2016
299	bone *Equus* sp. Maxilla	UCIAMS-86251	11,740 ± 25	13,740-13,500	Jenkins et al. 2016
305	bone unknown mammal	UCIAMS-90593	11,930 ± 25	14,010-13,610	Jenkins et al. 2016
308	bone Leproid humerus	D-AMS-024767	12,008 ± 35	14,020-13,800	Jenkins et al. 2016

The basal age at 308 cm was modeled to 13,900 cal yr BP. Very slow accumulation occurred from 300 to 296 cm (encompassing 700 years). Furthermore, a hiatus was required to fit the age model to a step change in the radiocarbon dates at 296.5 cm (12,700 to 12,200 cal yr BP), which corresponds to the BL between units LU2 and LU3. This hiatus does not appear to be present in other portions of Paisley Cave 2 (Beck et al. 2018). Instead of containing sediments, the BL is composed of organic materials including artifacts, macrobotanicals, and coprolites. There were coprolites available from the BL, but as there were no corresponding sediments they were not used in this study. Above this hiatus, fewer ages constrain the age-depth model, but they show a generally fast sedimentation rate (20 yr/cm) which declined upward to the Mazama tephra (70 yr/cm).

Overall, pollen preservation was very good, with <2% being indeterminable. There were no pollen aggregates identified within the coprolites, which have been used to support direct consumption of pollen (e.g., Blong et al., 2020). The stratigraphically constrained cluster analysis identified three zones in the sediment record, with breaks at 252 cm (11,100 cal yr BP) and 172 cm (within the Mazama-enriched sediment). The break at 252 cm corresponds roughly with the LU2/LU3 boundary. Pollen concentrations were sufficient for pollen analysis in the Mazama-enriched zone (LU4, 180-152 cm).

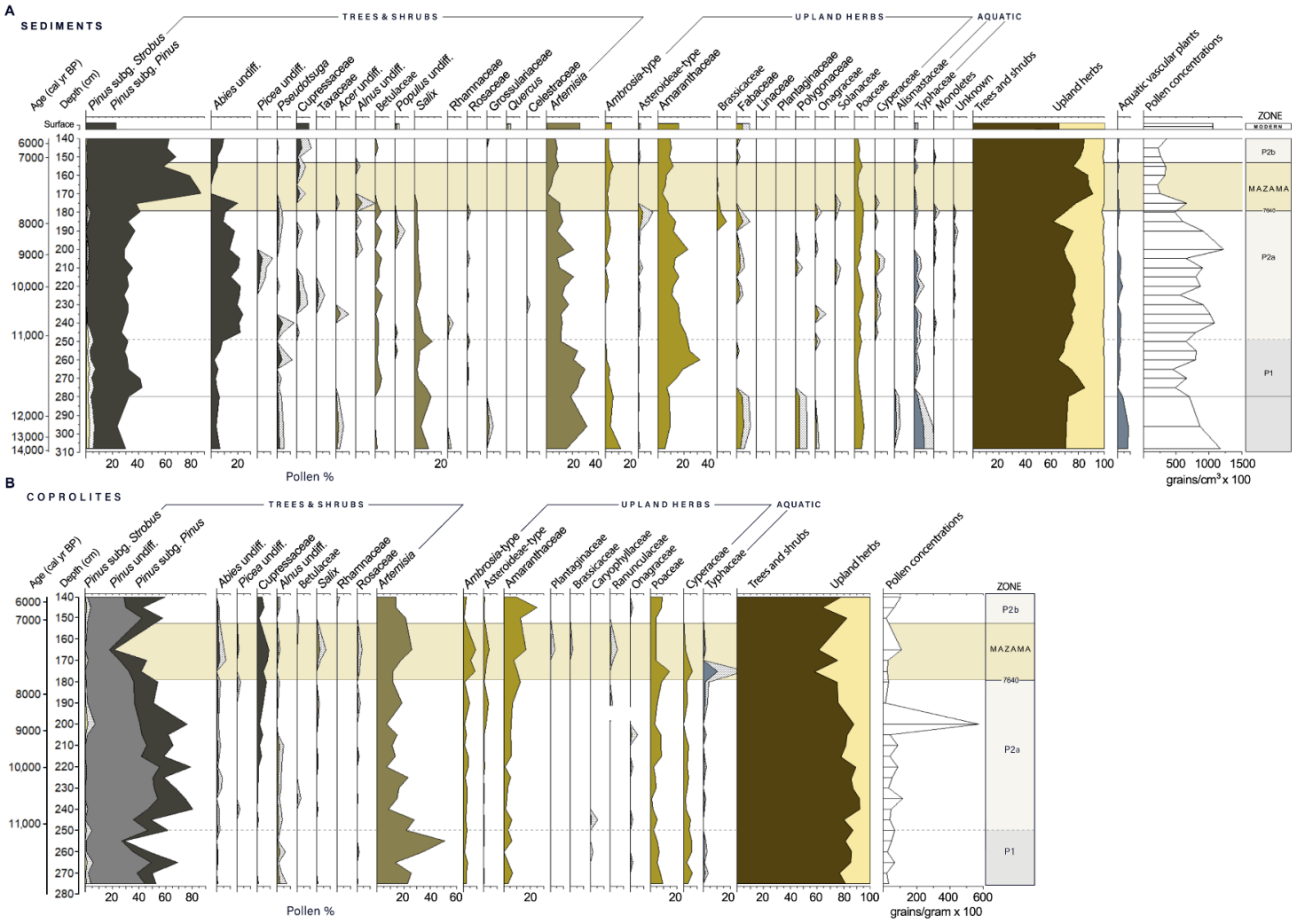

Figure 6. A. Sedimentary pollen diagram from Paisley Cave Unit 2/6. Included in the diagram is the pollen from a sediment sample taken 10 cm below the modern surface immediately in front of Cave 2. Sediments from the Younger Dryas period (~12.8- 11.5 ka) were missing from the sediments sampled for this project. B. Coprolite pollen diagram from coprolites adjacent to sediment samples. The spike in pollen concentrations seen in zone P2a is the result of the ingestion of pollen-enriched water. Both diagrams also shown larger in Appendix Figures 26 and 27.

4.2. Sediment pollen record

4.2.1. P1: Late Pleistocene Bølling-Allerød to early Holocene

Period P1 covers a 2700-year timespan from 13,900 cal yr BP during the Bølling-Allerød (B-A) warm period, and following a sediment hiatus, to the early Holocene (11,100 cal yr BP). A total of 20 taxa were identified (Fig. 6A). Common pollen types during P1 included *Pinus* subg. *Pinus* (increasing from 25% to 45% then returning to 30%), *Pinus* subg. *Strobus* (1-2%), *Abies* (3-6%), *Pseudotsuga* (1-2%), *Acer* (1-2%), Betulaceae (1%), *Salix* (4-10%), Grossulariaceae (1%), Rhamnaceae (1%), *Artemisia* (15-28%), *Ambrosia*-type (11% decreasing to 1%), Asteroideae-type (1%), *Amaranthaceae* (5% increasing to 30%), Fabaceae (3-5%), Polygonaceae (3%), Onagraceae (1%), Typhaceae (3-4%), Alismastaceae (1%), and Poaceae (4%). Pollen concentrations declined from 120,000 grains/cm^3 in the sample before the hiatus to 50,000 grains/cm^3 after the hiatus, then increased to 80,000 grains/cm^3.

4.2.2. P2a: Early Holocene to the Mazama tephra

P2a ranges from the early Holocene at 11,100 cal yr BP to the Mazama tephra at 7633 cal yr BP. Thirty taxa were identified. *Abies* increased sharply from 7% to 21% at the start of P2a and remained at approximately 20% until the Mazama tephra. During this time *Artemisia* declined from 24% to 10%. *Pinus* subg. *Pinus* pollen remained consistently between 28-35%, and *Pinus* subg. *Strobus* declines to below 1%. Conifers also include *Picea* (0-4%) and *Pseudotsuga* (1%). Other taxa include Taxaceae (1-2%), Cupressaceae (1-2%), Betulaceae (1-5%), *Alnus* undiff. (1-2%), *Salix* (1-5%), *Populus* undiff. (1-3%), Aceraceae (3%), Celestraceae (1%), *Artemisia* (9-20%), Asteroideae-type (1-5%), *Ambrosia*-type (1-4%), *Amaranthaceae* (8-23%), Brassicaceae (1-7%), Fabaceae (2-5%), Onagraceae (1-2%), Solanaceae (1%), Typhaceae

(1-4%), Cyperaceae (0-4%) and Poaceae (2-7%). Pollen concentrations were generally high (>90,000 grains/cm^3) before the Mazama unit and were lower (21,000-60,000 grains/cm^3) within the Mazama unit.

4.2.3. P2b: Mazama tephra to middle Holocene

P2b ranges from 7633 to 5800 cal yr BP. This pollen period included samples within the upper portion of the Mazama unit and three samples above it. Only 15 taxa were identified in P2b. At the start of this zone, *Pinus* subg. *Pinus* increased abruptly from 38% to 87%, *Pinus* subg. *Strobus* remained below 1%, and *Abies* declined to 0-8%. Other taxa included Cupressaceae (1-4%), Betulaceae (1-5%), *Salix* (2-12%), *Populus* undiff. (2%), Grossulariaceae (1%), *Artemisia* (1-8%), *Ambrosia*-type (2-6%), *Amaranthaceae* (4-12%), Brassicaceae (2%), Solanaceae (1%), Typhaceae (0.3-1%), and Poaceae (2-6%). Only trace amounts of *Pseudotsuga* and Fabaceae were present. Pollen concentrations were low within the Mazama unit (21,000 grains/cm^3) but increased to 36,000 grains/cm^3 above the unit.

4.2.4. Modern pollen

The modern pollen included 14 taxa, including *Pinus* subg. *Pinus* (19%), *Pinus* subg. *Strobus* (<1%) Cupressaceae (9%), *Populus* undiff. (2%), *Quercus* (2%), *Artemisia* (31%), *Ambrosia*-type (6%), *Amaranthaceae* (18%), Boraginaceae (1%), Fabaceae (5%), Linaceae (2%), Plantaginaceae (1%), Typhaceae (1%), and Poaceae (3%). The modern assemblage differed from the pre-Mazama zones primarily due to the dominance of *Artemisia* sp., far lower *Pinus* subg. *Pinus*, higher Fabaceae (presumably *Medicago;* alfalfa), and the occurrence of *Quercus.*

4.3. Coprolite pollen

The coprolite pollen assemblages were more variable and less species-rich than the sediment pollen samples (Fig. 6B). We describe the coprolite pollen following the same zones identified for the sediment pollen record. All coprolites analyzed post-date the hiatus in the age-depth model.

4.3.1. P1: post-Younger Dryas to Holocene

Seventeen pollen taxa were identified in the five analyzed coprolites from P2. These coprolites were dominated by *Pinus* subg. *Pinus* (30-70%) and *Artemisia* (14-51%) pollen. Other common pollen taxa were Poaceae (7%), Cyperaceae (5%), *Amaranthaceae* (4%), *Ambrosia*-type (2%), and *Alnus* (1%). Pollen concentrations ranged from 21,000 to 70,000 grains/g.

4.3.2. P2a: Early Holocene to Mazama tephra

Nineteen pollen taxa were identified in the 14 analyzed coprolites from P2a. These coprolites are dominated by *Pinus* subg. *Pinus* (declining from a high of 80% to 41%) and *Artemisia* (7-28%). Cupressaceae (likely representing *Juniperus*) increased from trace levels to 7%. Other common pollen taxa were Poaceae (6%), Cyperaceae (3%), *Amaranthaceae* (4%), *Ambrosia*-type (3%), and *Alnus* (1%). *Abies* is notably rare (<1%), and Typhaceae were overall rare but was abundant (10%) in the uppermost coprolite of this zone. Pollen concentrations were generally ca. 50,000 grains/g, but two samples (200 and 235 cm) have very high concentrations (570,000 and 110,000 grains/g, respectively).

4.3.3. P2b: Mazama tephra to middle Holocene

Twenty-one pollen taxa were identified in the five analyzed coprolites from the second half of P2b. These coprolites were also dominated by *Pinus* subg. *Pinus* (21-60%) and *Artemisia* (14-26%). Other common pollen taxa were *Amaranthaceae* (14%), Poaceae (6%), Cupressaceae (6%), *Ambrosia*-type (4%), and Asteroideae-type (1%). Only trace amounts of *Abies*, Cyperaceae, and *Alnus* were present.

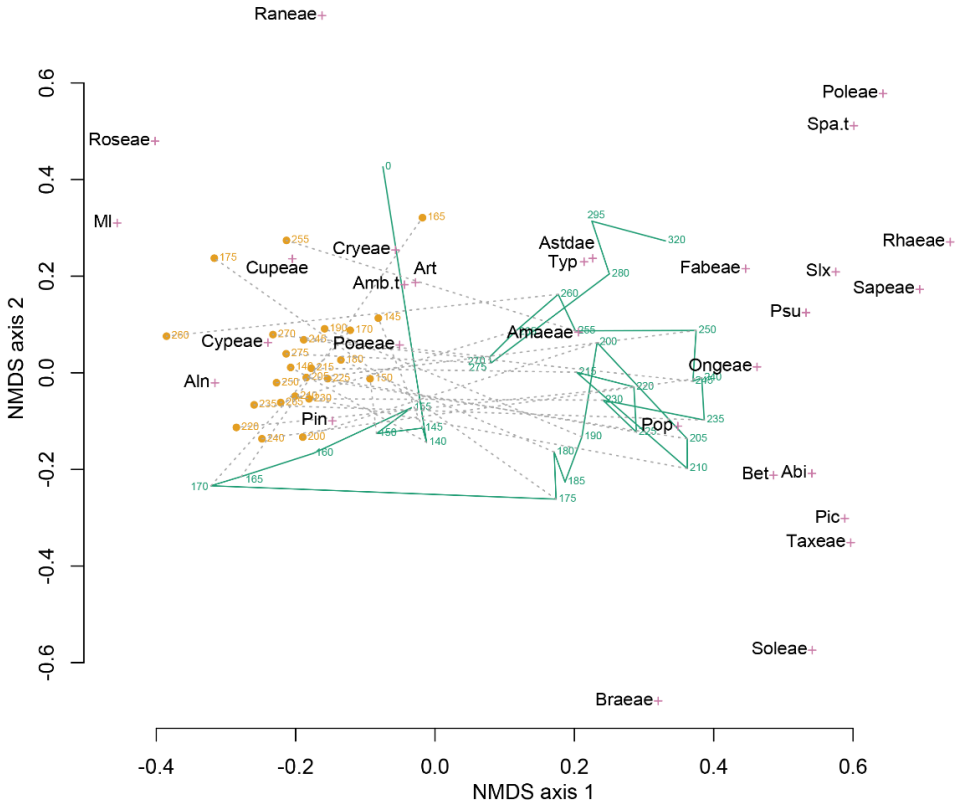

Figure 7. Non-metric multidimensional scaling (NMDS) of the combined coprolite (brown circles) and sediment (green line) pollen assemblage data set. Sample depths (cm below cave floor) are shown for both coprolite and sediment samples. Green line connects sediment pollen samples in stratigraphic order. Gray dashed lines connect coprolite and adjacent sediment samples. The species scores of the 29 pollen taxa are shown by magenta crosses. Abi=Abies, Aln=Alnus, Cheno-t=Chenopodium-type, Amb.t=Ambrosia-type, Art=Artemisia, Astdae=Asteroideae, Bet=Betula, Braeae=Brassicaceae, Cryeae=Caryophyllaceae, Cup=Cupressaceae, Cypeae=Cyperaceae, Fabaeae=Fabaceae, Ml=Pteridophyta (monolete), Ongeae=Onagraceae, Pic=Picea, Pin=Pinus, Poaeae=Poaceae, Poleae=Polemoniaceae, Pop=Populus, Psu=Pseudotsuga, Raneae=Ranunculaceae, Rhaeae=Rhamnaceae, Roseae=Rosaceae, Sapeae=Sapindaceae, Slx=Salix, Soleae=Solanaceae, Spa.t=Sparganium-type, Taxeae=Taxaceae, Typ=Typha. 90% of the variation in differences in pollen assemblages (defined by the chord distance) is explained by the two dimensions of the NMDS ordination. Larger figure also in Appendix 28.

4.4. Statistical analysis

In the joint ordination of the pollen assemblages from the sediments and coprolites, the two groups do not overlap in ordination space (Fig. 7). The ordination space occupied by the sediment samples is larger than that occupied by coprolite samples, indicating greater taxonomic turnover among the sediment samples. The coprolite and sediment samples fell into distinct groups along NMDS axis 1, with coprolite samples located closer to the taxa scores for *Pinus*, Poaceae, Cupressaceae, and Cyperaceae. In contrast, the sediment samples start in the upper right and, for periods P1 and P2, decreased on NMDS axis 2 as influenced by a variety of herbaceous taxa arrayed along that axis. Sediment samples moved close to coprolite samples after the large increase in *Pinus* in the sample at 170 cm.

Examination of pollen-assemblage turnover shows the degree of change of pollen assemblages between adjacent samples for coprolites and sediments and contrasts these changes with differences between coprolites and associated sediments (Fig. 8). We found that the dissimilarity of pollen assemblages between coprolites and associated sediments (chord distance ca. 0.6) was greater than the serial dissimilarity (turnover of pollen assemblages between stratigraphically adjacent samples) within either group (chord distances ca. 0.2-0.4), supporting our first hypothesis. However, we did not find that serial dissimilarity was greater for coprolites than for sediments. Rather, the opposite pattern emerged for most of the P2 zone, thus not supporting the second hypothesis.

Pollen taxonomic richness, estimated by rarefaction to a 175-grain count, was greater in the sediment samples ($\bar{x}$ = 11.3) than in the coprolite samples ($\bar{x}$ = 10.2). While richness was greater in the sediment than adjacent coprolites for 20 of the 24 analyzed coprolites, a paired t-

test showed only marginal significance (t = -1.8, p = 0.08; Fig. 9), thus not fully supporting the third hypothesis.

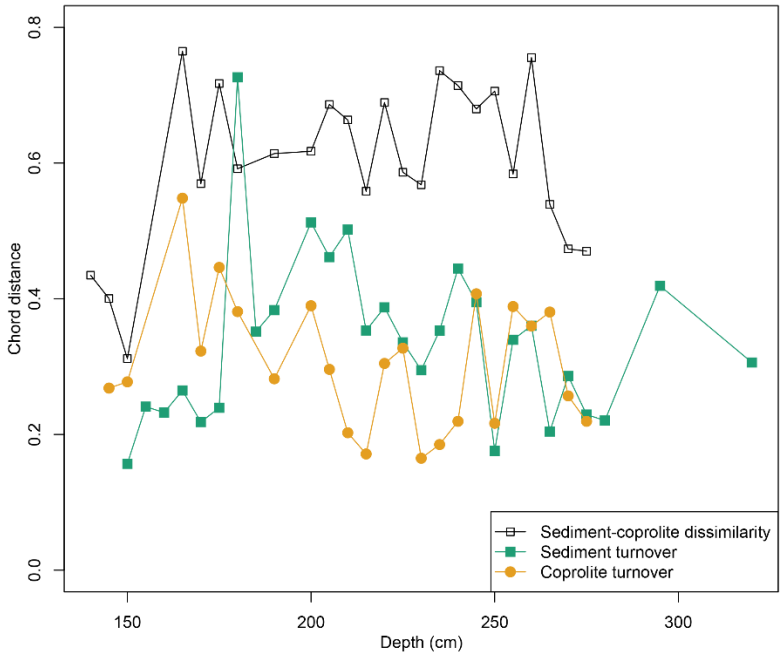

Figure 8. Chord distance analysis over time. The combination of sediment-coprolite pollen is structurally closer to the sediment assemblage than to the coprolite pollen assemblage, but distances between sediment and coprolite pollen show some overlap.

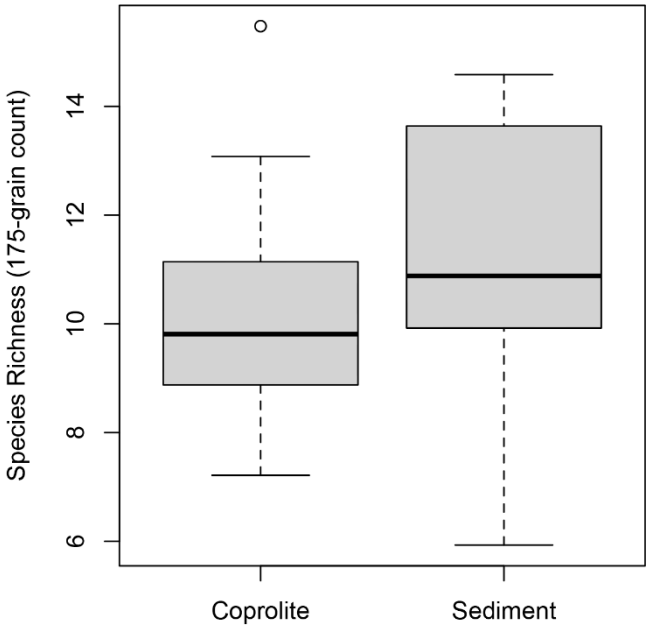

Figure 9. Pollen taxonomic richness in 24 coprolite samples and 24 adjacent sediment samples.

5. DISCUSSION

5.1. Sediment pollen assemblage

Pollen assemblages at Paisley Caves are influenced by the proximal sagebrush steppe, the wetlands of the Chewaucan Basin and lake edge, and the conifers of the forested uplands west of the caves. Adjacent to Paisley Caves, Summer Lake changed in size and salinity throughout the Holocene. Thus, the pollen record should also have been influenced by the changing riparian, lake shore, and wetland vegetation through time. Surrounding these wetlands, a mix of steppe vegetation, common to the lower elevations of the NGB, graded into juniper woodlands and forest, with sharp community changes occurring within a few hundred meters of elevation, particularly in wetter areas or on north-facing aspects (Wigand and Rhode, 2002; Grayson, 2011).

The sedimentary pollen analyzed in this study represents over 7000 years of deposits that may reflect local climate, hydrology, and Summer Lake's transgressive and regressive shorelines. Our pollen record from cave sediments is similar to the adjacent record developed by Beck et al. (2018) with the exception of much higher *Abies* and *Salix* pollen percentages in our profile. In contrast, our mammalian coprolite pollen record differs substantially from the adjacent *Neotoma* coprolite pollen record developed by Beck et al. (2020). Below we discuss the causes of these differences and examine the environmental drivers of the changes in the sediment pollen record in the context of prior studies in the NGB.

5.1.1. P1: Late Pleistocene Bølling-Allerød to Holocene

Hudson et al. (2019, 2021) characterize conditions in the Chewaucan Basin during the terminal B-A (ca. 13,000 cal yr BP) as warming with high effective moisture and a deeper lake

than immediately prior, with the shoreline only 17 m below and within 100 m horizontally of the base of 5-mile Point Butte. This time period is poorly represented in the unit 2/6 record with a modeled hiatus (Fig. 6A). As no hiatus exists in other portions of the cave, this hiatus may be due to a localized impact such as high foot-traffic. Our single pollen sample from this time contains a good representation of the riparian and lake-shore taxa of *Salix* and Typhaceae. In contrast, the high abundance of *Artemisia* and *Ambrosia*-type pollen in this zone suggests arid steppe conditions. As is the case today near riparian settings, riparian and arid steppe taxa are closely juxtaposed; our results are consistent with geological evidence for freshwater being much closer to the caves than it is today. Our findings correspond well with results from other pluvial lake basins near the Chewaucan Basin, including pollen and highwater stand timings from Warner Valley to the east (Wriston and Smith, 2017) and pollen, macrobotanical analysis, and highwater stand timings from Fort Rock Basin to the north (Friedel, 1993; Egger et al., 2021; McDonough et al., 2022).

The YD is well represented archaeologically through a rich cultural assemblage (Jenkins et. al., 2013, 2016), but based upon the sediment chronology, there was little sediment material from this time in our sampled Unit 6. This contrasts with Unit 4, where Beck et al. (2018) inferred a continuous record through the YD. It is possible that cave habitation and hearths eroded and consumed this layer in Unit 6. The YD is generally described as cool and dry in western North America (Mitchell, 1976; Allison, 1982; Licciardi, 2001; Vacco et al., 2005; Carlson, 2013; Jenkins et al., 2016). The YD is characterized in the Summer Lake basin as a period of cooler conditions and increased aridity, ultimately resulting in Summer Lake receding (Cohen et al., 2000; Hudson et al., 2019, 2021). After the YD, there was warming and increased effective moisture in conjunction with increasing insolation during northern hemisphere

summers (Kutzbach et al., 1998). While the YD shorelines are poorly constrained at Summer Lake, it appears likely that Summer Lake levels rose at the start of the Holocene (Hudson et al., 2021), as has been suggested for nearby Warner Lake (Wriston and Smith, 2017).

Although truncated by a hiatus, the remainder of zone P1, from 12,100 to 11,100 cal yr BP appears consistent with the YD having been in a period of high aridity. *Artemisia* and Amaranthaceae pollen increase and *Pinus* subg. *Pinus* decreases. Comparing the relative amounts of the two Asteraceae subgroups, *Ambrosia* spp. (ragweed) can at times be indicative of high arid conditions (Thompson, 1996; Dennison-Budak, 2010), while the Asteroideae-types can be indicative of wetter or cooler conditions (Heusser et al., 1995; Thompson, 1996; Mudie et al., 2007). Post-YD *Ambrosia*-type asters are in high abundance until ca. 11,100 cal yr BP, indicative of continuing aridity and increasing temperatures.

Pinus subg. *Pinus* (representing *Pinus ponderosa* and *Pinus contorta*) remained fairly low (ca. 20-30%) through P1. *Pinus* species are highly prolific pollen producers, contributing significantly to the regional pollen signal (Minckley et al., 2008). While *Pinus* percentages were higher than the surface sample (Fig. 6A), they were like that of other surface pollen assemblages from Paisley Caves (Beck et al., 2018) and much lower than *Pinus* percentages at sites closer to current *Pinus* population (Beck et al., 2018, 2020), supporting the conclusion of Beck et al. (2020) that pines were not substantially closer than present to Paisley Caves during this period.

Highly notable is the presence of pollen from *Pinus* subg. *Strobus* (<2%) in the P1 pollen assemblage. In the NGB this pollen type represents *Pinus albicaulis* (white-bark pine) and *Pinus monticola* (western white pine). Both species are indicative of higher moisture and lower summer temperatures than those occurring at basin floor today, as *P. albicaulis* is found at

elevations at or above 2100 m, and *P. monticola* grows between 1700 and 2000 m. The presence of *Pinus* subg. *Strobus* in P1 indicates lower aridity and cooler temperatures at lower elevations during the terminal Pleistocene relative to later periods.

Also notable is the absence of Cupressaceae (*Juniperus occidentalis*) pollen in P1 samples, indicating either low abundance of Cupressaceae in the basin during P1, or poor pollen preservation within 2/6 sediments. That Cupressaceae was present in the Summer Lake area at this time has been established, as *Juniperus occidentalis* seeds were recovered from unit 2/6 from both pre-and post-YD deposits (Kennedy, 2018) and a trace of Cupressaceae pollen during P1 was reported by Beck et al. (2018) in a different area of Cave 2. The seeds were recovered primarily from hearth deposits and showed signs of charring (Jenkins et al., 2013; Kennedy, 2018). The presence of *Juniperus* macrobotanicals within P1 and P2 deposits was likely due to human seed transport to the caves from distances further than what is traveled by rodents and is consistent with what is known about human foraging habits at the time (Grayson, 1993; Kennedy, 2018; Longland and Ostoja, 2013).

5.1.2. P2a: Early Holocene to Mazama tephra

P2a covers the period from 11,100 to 7633 cal yr BP. Summer Lake levels were moderately high during the early Holocene (Hudson et al., 2019, 2021), but after 9000 cal yr BP lake levels receded rapidly. Pollen-based climate reconstruction from other regional sites show that temperature and aridity peaked at ca. 9000 cal yr BP (Mehringer, 1987; Minckley et al., 2007). However, the Paisley pollen record for P2a shows increased and sustained high *Abies* pollen (ca. 20%, from 11,000 to 8000 cal yr BP) and periods of elevated *Picea* and Cyperaceae

pollen (>3%), while more arid-adapted taxa (Amaranthaceae and *Artemisia*) remain steady at ca. 20%.

Abies grandis x *concolor* (white fir) is currently present on Winter Rim between 1700 and 2000 m. A decrease in temperature and fire episodes would facilitate the expansion of *Abies* below 1700 m. *Abies grandis* x *concolor* is a shade-tolerant species when young and can remain in the understory for many years until a disturbance opens the tree canopy, after which rapid growth can ensue (Lanner, 1984; Howard and Aleksoff, 2000; Arno, 2007). Reduced fire frequency would also favor *Abies* relative to *Pinus*.

An alternative explanation for the increase in *Abies*, a pollen grain that is poorly dispersed due to its thick exine (Bagnall 1975), is increased westerly flow during the pollen-producing season. Increased westerly flow, due to a deepening low pressure over the NGB, may have more effectively transported *Abies* pollen the >20 km from its nearest populations located at higher elevations. Changing strength in westerlies has been invoked to explain an increasing occurrence of coastal western hemlock pollen in interior British Columbia between 9000 and 8200 cal yr BP (Spooner et al., 2003).

Picea peaks at 9000 cal yr BP during the P2a period. Beck et al. (2018) reported very low *Abies* and *Picea* pollen percentages from the unit 2/4, and *Picea* was also reported from higher elevation sites such as Deadhorse Lake (2200 m elevation) on Gearhart Mountain (2440 m elevation) 30 km south of Paisley (Minckley et al., 2007). It is probable that the *Picea* pollen at Paisley Caves originated from Gearhart Mountain.

Typhaceae species are associated with marshy, perennially wet areas. Typhaceae counts decreased throughout P2 and remained low after the Mazama eruption. Waning Typhaceae concentrations in the sediments is a clear indicator of Summer Lake recession moving marshy

areas further away from the caves. *Typha latifolia* and *T. angustifolia* are both currently present in the Summer Lake basin, but *T. latifolia* is at a far higher abundance. The genus *Sparganium* has recently been added to the Typhaceae family, with *Sparganium euricarpum* present in Summer Lake Marsh. While *Sparganium* pollen is distinct from *Typha*, we merged it into Typhaceae as it was only present in the lowermost two samples. Both genera occupy similar wetland habitats, although *Sparganium* requires deeper water than *Typha* sp. (Dennis and Halse, 2008).

5.1.3. P2b: Mazama tephra to middle Holocene

P2b (7633 - 5800 cal yr BP) includes sediments from the Mazama tephra unit. The presence of sedimentary pollen and the occurrence of coprolites within the Mazama tephra unit suggest downward percolation of pollen and/or multiple tephra deposition events. In all sediments other than the Mazama unit, the cave sediment is dense and cemented by *Neotoma* fecal pellets. However, the Mazama tephra is coarse (>1 mm grain size) and loosely consolidated with no cementation. This would suggest the pollen stratigraphy within the ca. 26 cm deep tephra units is mixed. However, we also found an abrupt increase of *Pinus* within the tephra layer, perhaps attributable to Mazama deposition occurring in at least two phases (Buckland et al., 2020). In a study of pollen concentration of the Mazama tephra, Mehringer et al. (1977) interpreted an increase in *Pinus* pollen from 10% to 60% as an initial, rapidly deposited tephra layer followed by a second event during the *Pinus* pollen season. The pattern of pollen in the Paisley Cave Mazama unit is consistent with multiple ash depositions in different seasons (Mehringer, 1987; Egan et al., 2015). However, the coprolite assemblages do not show a similar increase in *Pinus* as would be expected if the tephra affected the regional vegetation.

The remainder of P2b shows an increase in Cupressaceae, likely indicating an increase in juniper woodland in the middle Holocene, as well as an increase in *Abies*. Some herbaceous plant types, such as Brassicaceae and Fabaceae, thrived in response to the tephra deposition. Such plants have adaptations to disturbance, including, in the case of Fabaceae, the ability to fix nitrogen from the atmosphere.

5.2. Coprolite pollen assemblage

The amount of pollen present within a coprolite reflects seasonality and the natural pollen-rain, various dispersal forms including anemophily (wind-dispersed), entomophily (insect-dispersed), and zoophily (animal-dispersed), the types of plants contributing to ambient pollen, and the amount of pollen output by different plant species (Shillito et al., 2020). Intake into an organism's mucus system occurs either through passive or intentional ingestion. Passive ingestion occurs through respiration, drinking water with pollen present, eating plant materials with pollen present on the plant surfaces (Wood et al., 2012; Shillito et al., 2020), or through the predation and consumption of the digestive organs of plant-consuming prey (Carrión et al., 2001). Pollen has also been intentionally ingested as a food source by Native American people throughout North America, with examples including *Typha* and *Populus* pollen used as food seasoning and thickeners, as well as used in cultural customs and rites (Williams-Dean and Bryant, 1975; Euler, 1986).

Our hypotheses regarding the pollen assemblages of coprolite versus sediment samples were largely supported. First, the dissimilarity between sediment and coprolite pollen assemblages (chord distance between coprolite and associated sediments) was much greater than the serial dissimilarity (chord distance between stratigraphically adjacent samples) within

sediments or coprolites (Fig. 8). This pattern is expected because the sediment pollen assemblage represents a larger area over a longer time, thus capturing regional pollen more consistently. The coprolite assemblage represents a brief temporal window while the sediment assemblage integrates a decade or more of pollen deposition. Second, the serial turnover among coprolites was not greater than that among sediments. We hypothesized that the "sampling" of pollen by a foraging human or another large mammal would result in a stochastic pattern from feces "spiked" with variable amounts of pollen in the gut that were inhaled and ingested, while cave sediment pollen represents a much greater spatial and temporal smoothing. However, the turnover in coprolite assemblages was often less than that of sediment samples. Such a pattern might result from a selection of certain pollen types from the environment based on foraging or hunting behaviors. Third, pollen taxonomic diversity was slightly lower in the coprolites than in the sediment samples. This is consistent with sediment samples representing many years of pollen accumulation from a broad regional source, while the coprolite pollen "samples" only a portion of the landscape and over a brief period of time.

Compared to sediment pollen assemblages, the coprolite pollen has higher abundances of lighter pollen types (*Pinus*, Cupressaceae, and in P1 and P2b, *Artemisia*) and wetland pollen types (Cyperaceae and in P2b, Typhaceae) and lower abundances of heavy pollen types, including *Abies*, *Pseudotsuga*, and Amaranthaceae. The higher occurrence of lighter pollen types (e.g., *Pinus* relative to *Abies*) in the coprolites than in the sediments is consistent with pollen being inhaled, then moved into the gut by mucus transport. Pollen which remains airborne for longer periods would be more likely to be inhaled. Seasonality may also play a role in the coprolite pollen assemblages. For example, the high abundance of *Artemisia* in some coprolites may be due to seasonal use of the caves timed with the late-summer flowering of *Artemisia*. As

the production of *Pinus* and the other regional conifers all occur in the late spring months (Burns and Honkala, 1990; Osmond et al., 1990), we can surmise that there were two seasonal occupational periods of the caves. Further, all of the coprolites examined for this study contained pollen, suggesting no winter occupation of Cave 2.

The higher abundances of wetland taxa, such as Cyperaceae, in coprolites than in sediments is best explained by people and other animals traveling to marsh areas and ingesting pollen in water. The fact that this difference between coprolites and sediments was observed for all time periods suggests that the phenomenon occurred regardless of the distance of the wetlands from the caves. *Typha* pollen has a similar abundance (~0.5-2%) in sediment and coprolites, with the exception of one coprolite with 10% *Typha* pollen. This particularly high abundance of *Typha* may be attributable to the intentional consumption of *Typha* pollen, as was practiced by the Native people of the region (Euler, 1986).

Cupressaceae (*Juniperus*) pollen percentages are higher in coprolites than in sediments throughout zones P2a and P2b. This could indicate intentional human or other large mammal interaction with *Juniperus* woodlands some distance to the caves. This is consistent with human activity at the time, as *Juniperus* was an important dietary and medicinal resource (Euler, 1986; Kennedy, 2018). This is also consistent with the seasonal timing of *Pinus* pollination in late spring, as *Juniperus occidentalis* also begin producing cones in late spring (Miller and Rose, 1995; Adams, 2019). An increase in Cupressaceae through the early Holocene has not been described before in the NGB (Miller and Wigand, 1994). The increase may represent either an expansion of *Juniperus* woodlands, the increased use of juniper woodlands by humans or other large mammals, or both.

The Amaranthaceae pollen present in Cave 2 coprolites is likely derived from an alkaline-tolerant *Chenopodium*. During P1 and P2a, this taxon has low abundance in the coprolites, while in P2b there is an increased amount relative to the sediments. This change may indicate a change from avoidance of saltbush-dominated playa areas to increased travel through such areas as playas increased in extent through the early Holocene. The organism that ingested the pollen would have done so in the early to mid-summer when *Atriplex* pollen is produced (Hitchcock and Cronquist, 1976).

The concentration of pollen in the coprolites varied, with the majority being relatively low pollen concentration, indicative of passive pollen ingestion. There is a major spike in pollen in a coprolite at 200 cm (8800 cal yr BP), matching a spike in sediment pollen concentration at the same depth. The coprolite spike was driven by a high *Pinus* influx while the sedimentary spike was the result of high *Artemisia* and Amaranthaceae pollen, perhaps reflecting a brief cold period. Perhaps the coprolite producer was near *Pinus* stands, as such places may have provided mesic conditions at a time when Summer Lake was all but desiccated (Cohen et al., 2000; Friedel, 1993; Hudson et al., 2021; Licciardi, 2001)

6. CONCLUSIONS

The pollen record from Paisley Cave 2 in south-central Oregon is consistent with prior studies showing steppe conditions persisting throughout much of the Northern Great Basin during the Pleistocene and into the Holocene (Mehringer, 1986). However, differences in climate, the presence of large freshwater lakes, and changes in insolation timing and intensity mean that there are no analogous ecological conditions today for the region. By contrasting the degree of changes between adjacent pollen sample types, this study found that the dissimilarity

of pollen assemblages between coprolites and associated sediments was greater than the serial dissimilarity between stratigraphically adjacent samples within either group. However, serial dissimilarity within types was not greater for coprolites than sediments. The coprolites showed localized pollen assemblages related to mammalian survival strategies within a 1 to 2-day period, resulting in less taxonomic variability over time than sedimentary pollen.

Survival decision-making by the coprolite producers is suggested by the high percentage of aquatic/wetland pollen in the coprolites. As large mammals need to drink water frequently, as do potential prey animals, it is reasonable to assume the water sources would be in relatively closer proximity to the caves. Overall, the coprolite pollen shows a strong seasonal signal, with late spring and late summer equally strong, but there are components of early spring and midsummer as well. If the coprolite producers were present at Paisley Cave in late fall or winter, we would expect no pollen in the coprolites, which was not the case for any of the coprolite samples.

Taphonomy and careful excavations at Paisley Caves provided the rare opportunity to analyze two pollen sources from the same location. Rarer still was to have both preserved in a long chronological sequence. Pollen from cave sediments can provide a regional environmental reconstruction over time (White, 2007), but it is by contrasting sediment pollen with chronologically related coprolite pollen, additional angles of ecological interactions related to changing climates and ecosystems can be determined. The results of these types of studies can then be applied to questions regarding diet, health, mobility, and other topics relating to past human or other mammalian behaviors, as well as to other ecosystems in the region. Ultimately we contrast the Paisley results to a 10,000 year long mid-elevation lake core from Dog Lake south of Summer Lake, and found very different climatic effects between the two sites.

CHAPTER III

RECONSTRUCTION OF HOLOCENE ARIDITY, FIRE, AND VEGETATION PATTERNS USING LAKE SEDIMENTS FROM DOG LAKE, SOUTH-CENTRAL OREGON

Co-authored by Saban, Chantel V. and Daniel.G. Gavin. Reconstruction of Holocene Aridity, Fire, and Vegetation Patterns Using Lake Sediments from Dog Lake, South-central Oregon. In preparation for The Holocene.

Chante Saben and Daniel Gaivn conceptualized the study and devised the methodology. Saban and Gavin analyzed sediments. Saban processed and analyzed pollen and charcoal. Curation, analysis, and visualization of the data were done with the help of Gavin. Saban wrote the original manuscript, and Gavin reviewed, edited, and contributed to the final manuscript.

1. INTRODUCTION

Extended periods of heightened aridity over the last 10,000 years have been well documented for most of western North America (Cook & Irwin, 1992; Benson et al., 1997; Bartlein et al., 1998; Shinker, 2010; Herweijer et al., 2007; Cronin, 2009; Shuman et al., 2009; Hermann et al., 2018; Cook et al., 2022). Much of our understanding of past arid periods east (Mehringer, 1986; Mehringer, 1987; Wigand, 1987; Booth et al., 2005; Minckley et al., 2007; Mensing et al., 2008; Reinemann et al., 2009; Walsh et al., 2010; Thompson, 2012; Long et al., 2019) and west of the Cascade Range (Sea & Whitlock, 1995; Worona & Whitlock, 1995; Long et al., 1998; Grigg & Whitlock, 1998; Briles et al., 2005; Gavin et al., 2007; Walsh et al., 2008, 2010) comes from pollen, stable isotopes, and lithological materials preserved in freshwater lake

sediments. Lake water levels of closed lake basins are highly sensitive to changes in the balance of precipitation and evaporation (Anderson et al., 1988). Similarly, pollen assemblages in arid regions reflect regional changes in effective moisture (precipitation minus evaporation).

The Northern Great Basin (NGB) is an area that has experienced great variation in Holocene aridity and temperature. Precipitation in the region is derived from winter Pacific storm tracks moving inland (Lyle et al., 2008; Hudson et al., 2019). The NGB is generally arid with an annual precipitation average of 40 mm over the last 100 years (PRISM), supporting few perennial streams and fewer locations with natural surface water during the summer. Most examples of fresh surface water are small springs or pools within marshes or small intermittent streams and springs. Thus, few lakes with a well-preserved sediment record exist in the lower elevations of the NGB, such that the Holocene history of fire and vegetation is poorly understood.

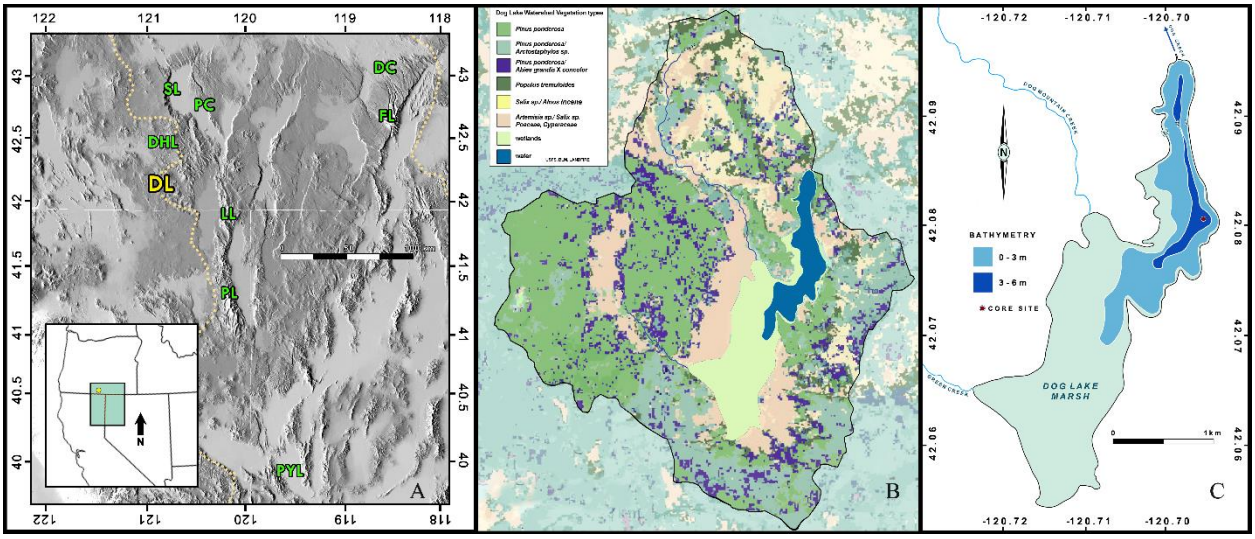

Figure 10. A) Map of Northern Great Basin region with sites cited in paper marked. Hydrologic Great Basin outlined as yellow dotted line. Dog Lake (DL), Summer Lake (SL), Lake Abert (LA), Dead Horse Lake (DHL), Diamond Pond (DC), Fish Lake (FL), Lily Lake, Patterson Lake (PL), Pyramid Lake (PYL) B) Dog Lake watershed with primary vegetation types. C) Dog Lake bathymetry with marsh. Figure 2a shows the marsh in early spring flooded, but for the majority of the year the marsh is not inundated. Larger figure also in Appendix 29.

This study examines the vegetation, drought, and fire history of Dog Lake, a small freshwater lake located on the western edge of the NGB located approximately 30 km west of Lakeview, Oregon (Fig. 1A). It is one of the lowest elevation (1580 m above sea level, masl) perennial freshwater lakes in the Northern Great Basin, situated near a lower treeline and thus at a location suitable for recording a range of ecological and climatic variability. The lake is naturally eutrophic and therefore should have a sedimentation rate that produces a sediment record with high temporal resolution (i.e., <10 yr/cm).

While paleoclimatic and paleoecological research has been conducted in the NGB (Mehringer and Wigand, 1986; Cohen et al., 2000; Mensing et al., 2004; Minckley et al., 2007; Mensing et al., 2008; Reinemann et al., 2009; Hudson et al., 2019, 2021), this high-resolution sediment core can fill gaps in understanding the climatic variability of the NGB, particularly for a mid-elevation site near lower treeline. In addition, near the lower treeline in ponderosa pine woodland, fires are common and fuel loads vary greatly over time and space; thus fire history is likely to be dynamic over the Holocene.

Our primary goal is to document the evolution of a mid-elevation natural lake in the NGB by reporting the history and magnitude of variable aridity during the early to mid-Holocene by using vegetation, fire history, and sediment composition analyses. Given the ecotonal position of the study site, we hypothesized the effect of past climate on fire history was mediated by fuel availability. The secondary goal was to identify the effect Mount Mazama tephra had on the vegetation of Dog Lake Basin through the use of a high-resolution pollen analysis immediately preceding and following the tephra layer. Given the importance for soil texture on plant communities in this region (Hopkins, 1979), we hypothesized tephra addition would increase the apparent aridity inferred from the pollen record.

1.2. Site description

Dog Lake (42.079859°N, 120.70005°W, 1585 m masl) is a landslide-formed, freshwater lake (ca. 84 ha) within a 3890 ha catchment basin located in the Fremont-Winema National Forest of south-central Oregon (Fig. 10A) on the western periphery of the hydrologic Northern Great Basin. The lake is managed by the USFS in cooperation with the Nature Conservancy. The conditions are semi-arid to mesic, with annual average precipitation varying between 290 - 790 mm per year (1980-2020; PRISM), with the majority (73%) falling during winter months (November-April). Mean January and July temperatures are -0.5°C and 18.1°C, respectively (OSU-PRISM).

Winter Pacific storm tracks from the west are the primary precipitation source for the NGB (Hirschboek et al., 1991), and precipitation in the Dog Lake area of the NGB is ultimately determined by the strengths of the North Pacific Subtropical High and Aleutian Low (Thompson et al., 1993). In contrast, 60 km east the precipitation regime is more greatly influenced by variations in the Central Great Basin high-pressure region (Mensing et al., 2019).

The lake is fed primarily by Green Creek and Dog Mountain Creek, both located on the west side of the lake, and several unnamed annual springs and seeps (Fig. 10C). Dog Lake outflows north as Dog Creek into Drews Reservoir. The lake level drops below the outlet each summer. Maximum water depth in mid-spring is ca. 8 m and the maximum lake extent is ca. 200 ha (Johnson et al., 1985) but can drop by as much as 3 m in late summer. The lake is stratified during the summer, with near-zero dissolved oxygen below 5 m measured during site visits in late August 2016 and 2017.

Dog Lake is naturally eutrophic resulting from high nutrient input from forested slopes and the presence of K-feldspar basement rock of Miocene origin (DOGAMI, 2023), although

cattle grazing in the adjacent wetlands likely also contribute to the nutrient-enriched water. Other bedrock in the basin includes rhyolite, basalt, and welded tuffs ranging from Miocene to Pliocene in age (Walker, 1963). The rhyolite is rich in silica, sodium, and potassium. In lower areas of the basin the igneous rocks are overlain by Quaternary sedimentary deposits.

Soils of the Dog Lake basin have not been thoroughly mapped, however, mapped soils of adjacent areas show common soil types (USDA Web Soil Survey). Soils are primarily of the suborder Xeroll, a temperate Mollisol found in areas of very dry summers and moist winters. The Xerolls include the Winterim Series, a deep, well-drained, gravelly loam derived from basalt and tuffs, the Lorella series, similar to Winterim but shallower in depth and typically on south-facing slopes, and the Booth series, a moderately deep, well-drained soil formed in colluvium derived from tuff or basalt. All 3 series are located on slopes ranging from 0 to 65 percent. Mazama tephra is also a major component of the soil.

Vegetation communities are vertically sharply stratified in the Great Basin, by elevation as well as by soil texture and distance to streams (Dyrness 1973; Hopkins 1979; Grayson 1993,2011). Current vegetation in the Dog Lake watershed (Fig. 10B) consists of *Pinus ponderosa* dry forest at lower elevations of the basin (<1600 masl). *Juniperus occidentalis* (juniper) trees are common on more well-drained soils. Tree cover becomes sparse near the floors of the larger basins, below 1500 masl. At elevations above 1600 m, vegetation changes to more mesic, mixed conifer forest including *Abies grandis* x *concolor*, *Calocedrus decurrens,* and *Pinus contorta*. Hardwood trees and large shrubs include *Populus tremuloides, Alnus incana,* and *Sambucus mexicana*. Scattered throughout the basin on coarse (sandy) soils are open dry grass and sagebrush meadows. *Arctostaphylos patula* in fire-cleared areas at elevations above 1,600 m,

with occasional wet meadows dominated by *Carex* are also present. *Cercocarpus ledifolius* is present on rocky outcrops primarily at lower elevations between 1590 m and 1650 m.

Dog Lake has extensive wetlands of several types. “Wetlands” are defined as transitional lands between terrestrial and aquatic where the water table is typically near the surface or the land is covered in shallow water (<2500 m) (Cowardin et al. 1979, Dodson 2005; Dennis and Halse 2008). Dog Lake wetlands are in the category of lacustrine to littoral with classes including emergent wetland, aquatic bed, and unconsolidated shore. Using Cowardin definitions, Dog Lake wetland descriptions are further simplified into 3 classes: perennial submerged substrates, annual emergent wetlands, and wet meadows.

Perennially submerged substrates support obligate water-supported macrophytes including *Sagittaria* spp., *Nuphar* spp. and *Chara* spp. Annual emergent wetlands support emergent hydrophytes which include graminoids (Cyperaceae, Juncaceae, Poaceae), Sparganium sp., and *Typha* sp. The south end of the basin is a combination of seasonally inundated grassy meadow and an emergent wetland of ca. 240 ha (Fig. 10B). A similar wetland is present at the north terminus of the lake where Dog Creek flows north to Drews Reservoir. Wet meadows flood annually, but typically dry by August through late September. Plants include graminoids, *Salix* sp., *Ranunculus* sp., *Veronica* sp., *Camassia* sp., *Iris* sp., *Ribes* sp., and others. Other vegetation requiring a high water-table or nearby water sources include *Populus tremuloides*, *Salix* sp., *Sambucus* sp., *Alnus incana*, and *Betula* sp. This type of wetland is common on the west side of the lake, where alluvium slopes at a gentle angle eastward until abruptly deepening toward the center (Fig. 10C). The deepest portions of the lake are flat and uniform in depth, possibly a result of a previous stream channel and floodplain or terraces prior to the lake formation.

Fire was historically frequent in the Dog Lake basin, with burn intervals currently ranging between 5-10 years (Crawford 2015). However, fire intensity during fire events has likely been exacerbated over the last 100 years as a result of increased juniper expansion and cheatgrass (*Bromus tectorum*) invasion (Hann et al. 1999; Miller and Rose 1999), resulting in a more flammable forest understory (Pilliod et al., 2017). Over the last 20 years, fire events in 2014 and 2018 were particularly severe. Increased grasses and fire severity appear to support the position that an increase in grass and *Artemisia* would result in more continuous fire events as opposed to periods of low grass, meaning the basin is fuel limited. Remains from a recent high intensity fire can be seen in a panorama photo of Dog Lake looking west March 2020 at an altitude of 1600 m shows trees burned in 2018 (Fig. 11A). Figure 11B shows late spring flooding of the south wet meadow.

Figure 11 A) Dog Lake panorama showing remains of a severe fire looking southwest to northwest. Dog Mountain, the source of the lake-forming slide is visible in the top right of photo a. The fire burned in 2018. B) Dog Lake at flood-stage looking south towards area that is wet meadow most of the year. Photo taken in March 2020. Larger figure also in Appendix 30.

2. METHODS

2.1. Field sampling

Two 12.8-m sediment cores were collected from the deepest section (6 m) of Dog Lake in late August 2016. The top 1 m of the surface was collected using a plastic tube surface sampler and sub-sampled in the field at 1 cm intervals. The remaining 11.8 m was cored using a Livingston square rod piston corer. Sediments were extruded into plastic-wrap lined, halved PVC pipes, measured and described, then covered with the other portion of the PVC, sealed, and labeled. The core sections were refrigerated and stored at the University of Oregon until subsampling could begin.

2.2. Sediment density from computed tomography (CT) scan

CT scans of radiodensity (expressed as Hounsfield Units, HU) were obtained on each Livingstone core drive using a Toshiba Aquilion 64-Slice at the Oregon State University College of Veterinary Medicine. The data files (two per 1-m core drive) were processed using SedCT software (Reilly et al., 2017). SedCT trims out voids and outlier values to produce a mean down-core radiodensity at equal 0.25 mm depth intervals. The radiodensity series from the two parallel Livingstone core drives were correlated and the data sets stitched together, resulting in a continuous sediment sequence.

2.3. Age-depth model

Accelerator mass spectrometry (AMS) radiocarbon dates were obtained on plant macrofossils (n = 5) and bulk sediment (n = 5). All samples were cleaned with warm 10% KOH and 10% HCl rinses before submitting to the dating facility (NOSAMS, Woods Hole, MA;

Direct AMS, Bothell, WA, or Center for Accelerator Mass Spectrometry, Livermore, CA). An age-depth model was constructed using the CLAM model in R (Blaauw 2010), with the INTCAL20 calibration curve (Reimer et al., 2020) modified to use a monotonically increasing spline curve fit (Schworer et al. 2017) to the 10 radiocarbon dates, the Mazama tephra (7633 ± 25 cal yr BP; Egan 2015), and the core top. The Mazama tephra unit was specified as an instantaneous event within the CLAM model.

2.4. Pollen

Pollen recovery followed protocols described by Smith (1998) and Pearsall (2016). Sediments (n = 56 1-cm3 subsamples) were obtained roughly evenly-spaced down-core (averaging a sample every 300 yr), with the exception of 20 pollen samples at 1-cm intervals preceding and following the Mazama tephra. Samples were added to 15 ml test tubes together with one Lycopodium tablet per tube to measure pollen concentrations. Chemical pollen extraction was performed inside a fume hood. 10% KOH was used to remove remaining soluble organics followed by a 10% HCL treatment to remove carbonate minerals. Hot hydrofluoric acid (HF) treatment for 40 minutes reduced silicate content. A second 10% HCL treatment sample was followed by glacial acetic acid (GAA), followed by acetolysis to remove the remaining cellulose. Samples were stained with safranin and desiccated using ethyl alcohol (ETOH) and tert-Butyl alcohol (TBA). Pollen was transferred into 2-dram glass vials with Si oil used for suspension and preservation of pollen. Pollen was examined at 400x magnification and identified to the highest taxonomic resolution possible using published keys (Faegri et al., 1989) and the modern pollen reference collection at the University of Oregon. Pollen was identified to a minimum of 350 grains per sample. Stratigraphically constrained cluster analysis (CONISS) was

performed in Tilia 3.0.1 (Grimm 1987) to aid in pollen zonation. A cluster analysis of the Mazama-period samples was conducted separately from other pollen samples.

2.5. Charcoal

Charcoal sampling followed protocols described by Rhodes 2016. 1 cm3 of sediments were subsampled at 1 cm increments the length of the core (12.8 m). Each subsample was placed into a 12 ml vial and soaked for 12 hours in 10% sodium hexametaphosphate (Na-HMP). Sediments were then gently rinsed with water using 250 µm and 125 µm 8 cm diameter mesh sieves. All large identifiable charcoal pieces or macrobotanicals were saved, and the remaining charcoal was placed back into 12 ml vials. The 125-250 µm fraction was soaked overnight in 7% hydrogen peroxide (H2O2) to partially digest and bleach organic materials. Samples were then rinsed using a 125 µm mesh sieve. Charcoal particles were counted using a Bogorov counting chamber under 10X-25X magnification. During sieving for charcoal analysis, aquatic macrofossils were saved and identified using keys and online sources.

Charcoal data were analyzed using the CharAnalysis software (Higuera et al. 2008) where the sedimentation rate obtained from the age-depth model output was used to convert the raw charcoal concentration into accumulation rates. CharAnalysis then identified charcoal peaks above “background” background charcoal accumulation rates (BCHAR). BCHAR, calculated as a mean charcoal accumulation in a moving window, and interpreted as biomass burning in a region near the lake (Marlon et al. 2009; Long et al. 2019). A background window of 1000 years produced a high signal-to-noise ratio (>3 throughout the core), suggesting peak identification was statistically robust. CHAR peak events are punctuated charcoal accumulation events that

likely represent one or more fires within, at the most, several kilometers of the lake (Higuera et al., 2010).

2.6. Organic carbon and nitrogen and carbon mass accumulation rates

Concentrations of total organic carbon (TOC) and nitrogen (N) were obtained on 171 samples. Samples were acid-rinsed (0.5N HCl) to remove carbonates, then dried in a drying oven and ground into fine powder. Subsamples of 3 to 7 mg were then weighed to the nearest microgram and packed in tin capsules. Percent C and N were measured at the Stable Isotope Facility at the University of California Davis. Stable isotopes of C and N were measured but are not reported in this study.

Carbon mass accumulation rate (CMAR, $mg/cm^2/yr$) was calculated as the product of the proportion TOC, the sedimentation rate from the age-depth model, and the sediment bulk density. The bulk density was estimated from the CT scan data, in which the measured bulk density of 120 samples was strongly linearly correlated with the corresponding radiodensity ($r = 0.98$).

3. RESULTS

3.1. Chronology and sediment descriptions

The 10 radiocarbon ages and the Mazama tephra (13-cm thick) occurred in stratigraphic order (Fig. 12; Table 2). The chronology of the 1276-cm, 9600 cal yr BP core revealed a high average sedimentation rate (0.16 cm/yr or 6.25 yr/cm) but which varied greatly over the Holocene (0.04 to 0.34 cm/yr; Fig. 12). The base of the core below 1040 cm had the highest sedimentation rates.

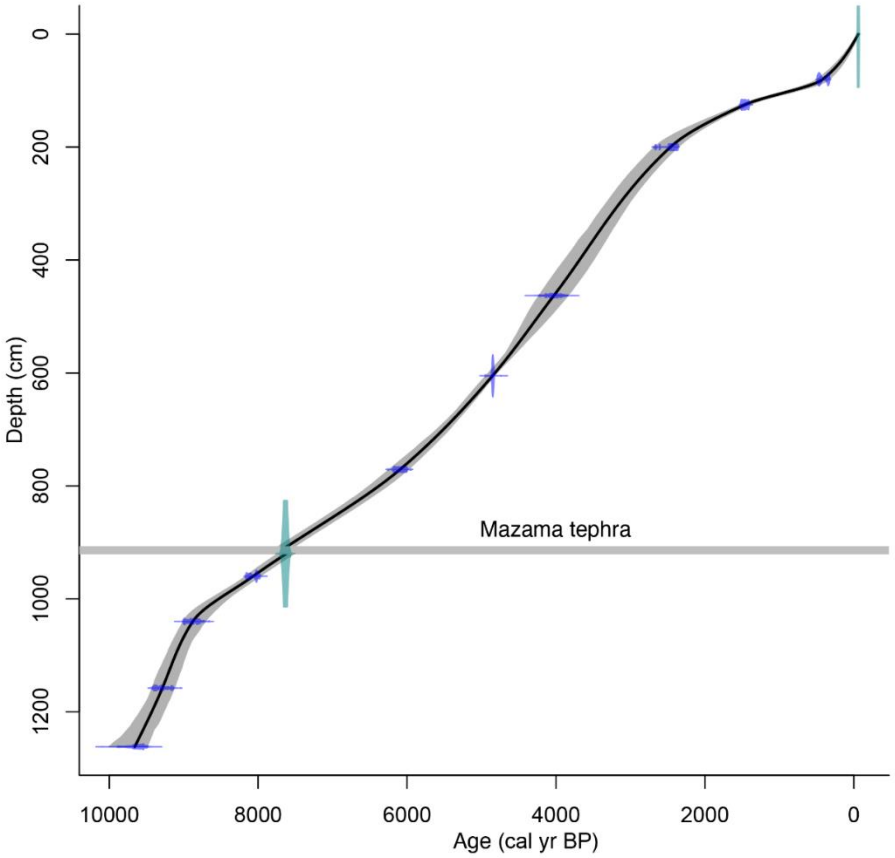

Figure 12. Age-depth relationship for the Dog Lake sediment core, fit using a monotonic spline.

Table 2: Radiocarbon dates for Dog Lake.

Depth (cm)	Material	Lab number	^{14}C age	Calibrated age (± 2 SD age range)
80	sediment organic material	D-AMS 042762	371±21	463 (x-x)
125	wood	NOSAMS-169245	1580±20	1453
200	Sediment organic material	D-AMS 042763	2422±23	2405
463	wood	NOSAMS-169246	3690±70	4025
605	sediment organic material	D-AMS 042764	4285±27	4874
771	sediment organic material	NOSAMS-166894	5310±35	6080
920	Mazama tephra	Egan et al. 2015	-	7633
960	sediment organic material	D-AMS 042765	7241±36	8016
1040	wood	NOSAMS 163363	8020±40	8729
1158	*Scirpus* seed	NOSAMS 163364	8290±40	9346
1262	conifer cone material	CAMS 176970	8620±90	10,052

The majority of the core (200-1040 cm; 2300-8800 cal yr BP) showed a fairly constant sedimentation rate (0.14 cm/yr). The upper 60 cm had a sedimentation of 0.2 cm/yr, but two radiocarbon dates at 80 to 125 cm depth differed by more than 1000 yr, which resulted in the lowest sedimentation rates in the core.

Sediment descriptions (Fig. 19) follow Schnurrenberger et al. (2003). Overall, the 1276 cm core is low in TOC (normally < 10%) and is generally high in diatom content with low carbonates and silt content. Only a few fine laminations were visible in the core, mostly in the period following the Mazama tephra. The lowest segment of the core, from 1276 to 1263 cm is a sandy paleosol (with a distinct A horizon) that predates the landslide and inundation by Dog Lake. The paleosol interpretation is supported by very high charcoal counts (>1500 pieces/cm^3, 125 µm mesh) recovered from the paleosol immediately underlying the lake sediments. The radiocarbon date on a macrofossil at 1263 cm dates the landslide at 9600 cal yr BP (2-sigma range of 9890-9460 cal yr BP). The remainder of the core is described as four lithological units related to sedimentation rates and sediment Characteristics which are ascribed to lake level history. Photographs of actual core sediments are in the Appendix (Fig. 25).

3.1.1. Zone 1a (lake formation)

The Initial Lake Formation (ILF) period at the base of the core from 1263 to 1152 cm (9600 - 9300 cal yr BP) consists of sediments ranging from dark olive-brown to dark brown and light brown and with high CT density values (HU > 400 corresponding to > 0.35 g/cm3). The carbon content is very low (2-4% TOC) but due to the high sedimentation rate, CMAR is comparable to much of the Holocene (ca. 3 mg/cm^2/yr). C:N fluctuates around a value of 12.

Lake organic matter that is primarily aquatic in origin have C:N values of >10 (Meyers and Teranes, 2001).

3.1.2. Zone 1b (low lake period)

Sediment from 1152 to 1130 cm (9300 - 8700 cal yr BP), the Low Lake Period (LLP), is marked by highly compacted charophyte matting consisting of *Chara* vulgaris and *C. globularis*. The algae was well preserved and showed no signs of humification into peat. These mats resulted in highly fluctuating TOC from 4 to 16% which caused CMAR to vary from 3 to 23 mg/cm^2/yr. CT density was also lower (250 HU) with several sharp peaks to 700 HU. C:N values also fluctuated greatly, from 11 to 14.

3.1.3. Zone 2a (early Holocene arid period)

Sediments from the early Holocene arid period 1030 to 920 cm (8700 - 7600 cal yr BP) consisted of dark-brown to olive-brown fine detrital sapropel. This period began with some of the lowest TOC in the core (3%) increasing to 6%, also with low carbon accumulation (CMAR <2 mg/cm^2/yr). No *Chara* was present at these depths. C:N was at the lowest value in the core (10) until the Mazama eruption, and the CT density is high (350 HU). Smear slides of the sediment from this unit indicate high amounts of silt-sized silicates. The C:N ratio, ca. 8.5, was near the lowest of the record.

The Mazama tephra spans from 920 to 908 cm (7640 cal yr BP). The tephra has abrupt contact with the lake sediment. In addition, the tephra showed fine (<1-cm) layering consistent with multiple deposition events. Very thin laminations (<1 cm) were visible in the 4 cm of organic sediment above the Mazama tephra.

3.1.4. Zone 2b (middle to late Holocene)

Sediments from the mid–late-Holocene begin at 908 cm (7600 cal yr BP) post-Mazama through the late Holocene (present-day) and consist of massively bedded (>100 cm) biogenic sapropelic ooze. The sediments include irregular silt deposits but are otherwise uniform in light-brown color and texture. However, the sediments exhibit a long-term decrease in density

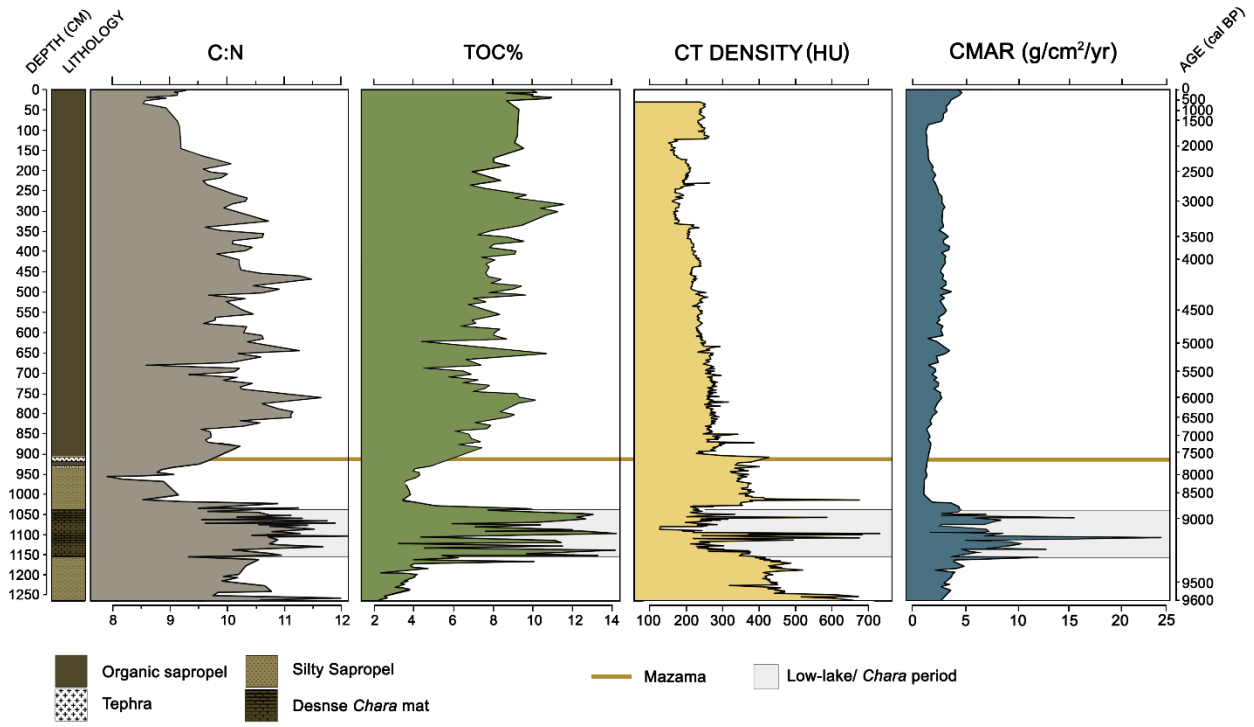

Figure 12. Sediment lithology, organic content, and density. Lithology was primarily composed of organic sapropel. From 908 - 903 cm are laminations directly above the Mazama tephra (too fine to depict in the lithology diagram). The Mazama tephra (920-908 cm) was preceded by a narrow tephra band at 928-927 (also too fine to depict in the diagram), likely from the Llao Rock eruption (Baig and Gavin 2023). The CT density is from a CT scan of the cores and shown as Houndsfeld units (HU). Larger figure also in Appendix 32.

(Fig. 13). In the upper portion of the core, TOC remained between 6 and 10% while CMAR tracked the sedimentation rate, decreasing to 0.77 mg/cm2/yr in the low-sedimentation rate periods from 125 to 80 cm. C:N declined from a value of 12 to 10 within this period. CT density declined steadily from 300 to 150 HU.

3.2. Pollen

Two pollen zones were identified through sum-of-squares analysis and correspond to the zones described by sediment characteristics. Zone 1 extends from 9600 to 8700 cal yr BP, and Zone 2 between 8700 cal yr BP to 150 cal yr BP (Fig. 14A). Taxa percentages are based on the sum of terrestrial pollen per each level. The pollen diagram shows a diverse range of vegetation consistent with wetlands surrounded by conifer woodlands. Current-day basin vegetation is sharply divided between wetland and upland forest vegetation.

Pinus pollen in the assemblage was entirely *Pinus* subg. *Pinus* or undifferentiated *Pinus* (representing *P. ponderosa* and *P. contorta*), although currently there is *Pinus* subg. *Strobus* (*P. monticola*) at elevations above >1600 masl. Cupressaceae pollen likely represents *Juniperus occidentalis*, however, *Calocedrus decurrens* is occasionally present in the Dog Lake basin. *C. decurrens* is most common in the Cascade Range ca. 120 km west of Dog Lake. "Graminoids" include true grasses (Poaceae) as well as sedges (Cyperaceae) and rushes (Juncaceae). The relatively high and steady amounts of Rosaceae pollen strongly indicates the presence of primarily anemophilous *Cercocarpus ledifolius*, despite being rare near Dog Lake today.

3.2.1. Zone 1 (lake formation and low-lake periods) 1263 - 977 cm (9.6 - 8700 cal yr BP)

There were 23 taxa in this period. Pollen influx averaged 32,000 grains/cm^2/yr and declined over the period. *Pinus* was low relative to the rest of the record (25-30%), Cupressaceae was steady (6%), *Abies* increased from 1 to 5% by 9300 cal yr BP then declined, while *Populus* remained steady around 6%.

Upland shrubs, particularly Rosaceae (likely *Cercocarpus*), increased from 7% to 10%, and upland herbs increased from 40% to 50%. *Artemisia* fluctuated between 5% to 18%, its

highest level in the record. Other shrubs increased (Ericaceae: 0 to 3%) or decreased (*Salix*: 8% to 2%; *Alnus*: 4% to 1%; Grossulariaceae: 4% to 2%). Poaceae fluctuated between 9% and 15%, Cyperaceae increased from 3% to 13% then abruptly declined to 4%. Aquatic vascular plants remain steady overall, dominated by *Typha* (4%). *Sparganium* appeared at the end of the LLP (>1%). *Nuphar* appeared at the end of the LLP (>1%).

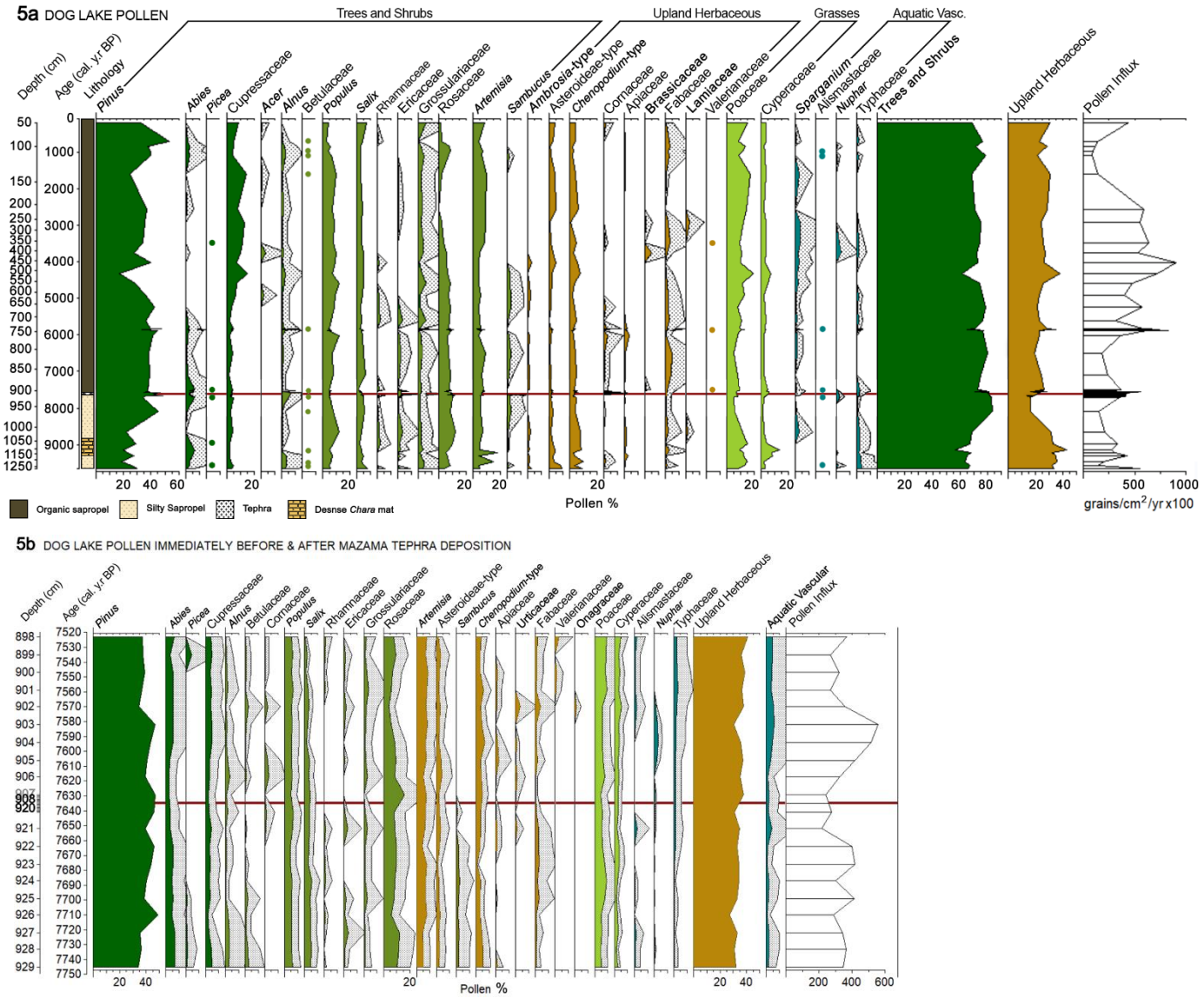

Figure 14. A) Sediment pollen diagram from Dog Lake, Oregon. B) Pollen record at 1-cm (ca. 10-yr) resolution for the 100-year period before and after the Mazama tephra. Larger diagrams also in Appendix 233 and 34.

3.2.2. Zone 2 (8700 cal yr BP to present)

Twenty-five taxa were identified in this zone. Pollen influx, beginning at 21,000 grains/cm^2/yr, peaked at 90,000 grains/cm^2/yr at 4000 cal. yr BP then declined to a very low rate (8000 grains/cm^2/yr) at 1000 cal. yr BP during a period of low sedimentation rate.
The zone is marked by a sharp increase in *Pinus*, 23% to 40%, beginning at 8700 cal yr BP and remaining between 30-40% for the remainder of the record. *Abies* increased to 10% up to the Mazama tephra, declined to 3 - 4% until 5300 cal yr BP, then declined to 0 - 2% for the remainder of the record. Cupressaceae remained low up to 5300 cal yr BP ranging from 5 - 8%, but after 5300 cal yr BP Cupressaceae increased steadily and averaged ca. 16% for the remainder of the record.

Populus changes little over the zone (7 - 12%) until declining to 4% at the core top. Shrubs show some marked patterns over the last 8700 cal yr BP. Rosaceae (likely *Cercocarpus*) peaks at 8700 cal yr BP at 12%, then remains very steady at ca. 6 - 9% until 2800 cal yr BP when Rosaceae declines to <2%. In contrast, *Salix* (3 - 6%) and *Alnus* (1-2%) were consistent through the zone. *Artemisia* increased from ca. 4% to 8% at 4300 cal yr BP. *Sambucus* (2%) was present throughout the first part of the zone, but disappears from the assemblage after 4300 cal yr BP.

Upland herbs were low (15%) pre-Mazama tephra but were around 25% for most of the record. Most notably, *Chenopodium*-types increase from 2% to 8%, similar to Poaceae (12% to 19%) and Cyperaceae (2-7%). Graminoids as a whole increase from 14% to 26% between 4.9 and 4300 cal yr BP. Graminoids include Poaceae (11%) and Cyperaceae (2%) lower than previous to 8700 cal yr BP. Aquatic vascular taxa include *Nuphar* and *Typha*ceae, which reached their highest levels (5%) at ca. 3700 cal yr BP.

3.3. Pollen assemblages before and following the Mazama tephra deposition

The 20 pollen samples below and above the Mazama tephra encompass the 100 years before and following the tephra deposition (Fig. 14B). Pollen influx increased from 30,000 to 56,000 grains/cm^2/yr over fifty years, then declined to pre-tephra levels. The cluster analysis showed that there was no statistically significant pollen zonation within these samples. Pollen percentages were consistent across the Mazama tephra for nearly all taxa, except for *Sambucus* which was consistently present before the tephra and absent after.

3.4. Fire history

Background charcoal accumulation rate (CHAR) levels were stationary over the last 9600 yr, fluctuating around 1 particle/cm/yr, despite variable sedimentation rates. In contrast to background CHAR, the variation in peak frequency and peak height varied greatly over time (Fig. 15A).

The Dog Lake fire history is divided into two zones, following the zone boundary determined from pollen analysis: Zone 1 from 9600 - 8700 cal yr BP, and Zone 2 from 8700 - 125 cal yr BP. The division also coincided with a major lithological transition from *Chara* mats to deeper-lake sediments with more dense and less organic sediment. The fire return interval (FRI) for Zone 1 was 15 years, whereas the fire return interval for Zone 2 is 47 yrs (Fig. 15A). Zone 1 is *Chara*cterized by frequent CHAR peaks that decrease in magnitude over time. Zone 2 begins, between 8700 - 7900 cal yr BP, with very low CHAR levels and only one identified peak. During the mid-Holocene fire frequency was highly variable with two periods of especially high fire frequency from 5800 to 5200 cal yr BP and from 4800 to 4300 cal yr BP. After 2 cal yr BP and until 0.4 cal yr BP the sedimentation rate was very low precluding inferences about the

fire history. After 0.4 cal yr BP, the sedimentation rate increases, providing the resolution to identify seven more peaks.

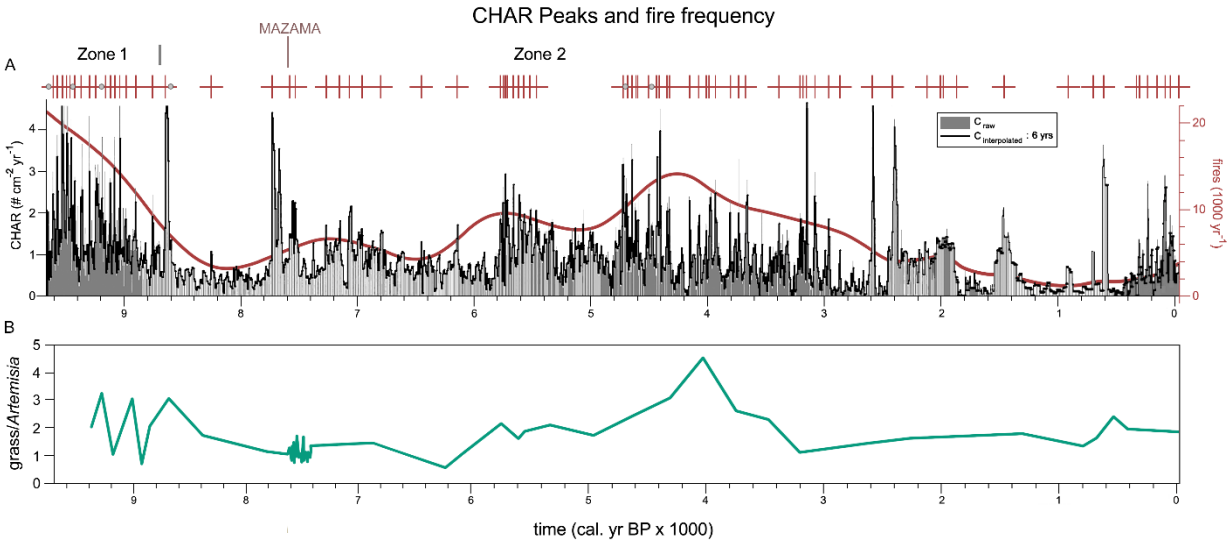

Figure 15. A) Charcoal accumulation rate (CHAR) from Dog Lake, Oregon. Peak identification (red crosses) were determined by CharAnalysis (Higuera et al.). The smoothed fire frequency (red line) is overlaid by the CHAR data. Note that low sedimentation rate from 2.4 to 0.4 ka precludes detection of many fire events. B) Poaceae:Artemisia ratio from the Dog Lake pollen diagram (Fig. 14A). Figures larger in Appendix 35.

4. DISCUSSION

The Dog Lake sediment record has a dynamic history reflecting fluctuating water level, productivity, and vegetation and fire history. The eutrophic lake has a high sedimentation rate due to the high-nutrient input from forested slopes of the basin, nutrient-rich runoff from the wetlands south of the lake, and perhaps due to pockets of K-feldspar basement rock of Miocene origin (DOGAMI). Thus, the 13-m sediment core has the resolution to resolve a frequent-fire regime for most of the past 9600 yr, with the exception of a low-sedimentation period during the last 2000 yr. The effect of temperatures and precipitation fluctuations seen elsewhere in the Great Basin (Mensing et al., 2004, Reinemann et al., 2009) are expressed in Dog Lake record's coherent history of lake level, vegetation change, and fire history.

The fire history at Dog Lake is extremely dynamic with periods of short fire intervals (15 yr) and some multi-centennial periods with no fire. An inverse pattern is observed in which Poaceae (grass):*Artemisia,* is positively correlated with more frequent fire events (Fig. 15B). In the NGB, grasses are indicative of a cooler or wetter spring climate, with *Artemisia* indicative of warmer and drier climate. Grasses produced in the year of the fire, or in preceding years, provide fuel for fire spread. In contrast, *Artemesia* shrublands may have barren ground and less continuous fuels. High Poaceae:*Artemisia* may also indicate grassy fuels under pine forest (a similar result is obtained with a Poaceae:*Pinus* ratio). Thus, the pollen evidence suggests fuel limitation for the fire regime at Dog Lake. During frequent-fire periods, there was likely sufficient precipitation in the winter and early spring to produce grass cover, yet late summers were quite dry, allowing the lake level to drop to lower than it reaches today. Such fluctuating conditions support frequent fire in grassland ecosystems (Brown et al. 2005).

4.1. Initial lake formation and low-lake periods

The initial lake formation (ILF) period from 1252 cm/9600 cal yr BP to 1152 cm/9300 cal yr BP occurred after a landslide blocked the northeastern flow of Dog Creek. The sharp transition from soils to lake sediment (Appendix Fig. 25) suggests that the lake outlet was high enough after the landslide to support deep water. The C:N ratio of 10.5 indicates primarily aquatic productivity, and the low organic matter (TOC < 4%) and higher sediment density indicate high detrital mineral matter. Erosion of the new lakeshore combined with a high fire frequency and post-fire erosion contributed to the high sedimentation rate at this time.

The low-lake period (LLP) is between 1152 cm/9300 cal yr BP and 1130 cm/8700 cal yr BP. A dark and fibrous *Chara* mat is present in the sediment core. This genus of algae

proliferates in water as shallow as 5 cm to as deep as 6 m depending on water clarity. The density of *Chara* stems combined with continued high input of inorganic matter (organic matter did not reach more than 30% given the 14% peak % TOC; Fig. 13 suggests that Dog Lake was likely between ca. 10 - 50 cm deep during the summer, much lower than the 6 m depths of Dog Lake in recent years. *Chara* growth was likely promoted by intermittently very low late summer water levels, resulting in the rapidly fluctuating values in CMAR and TOC (Fig. 13). Lower precipitation and a lower late summer water table could have dropped Dog Lake levels much lower than the lowest levels reached in recent decades. The lower water level was due to a reduction in precipitation causing reduced flow from the primary stream sources of Green Creek and Dog Mountain Creeks (Fig. 10C). Pollen indicators of lower lake levels are from proximal littoral species, such as *Typha* and Cyperaceae, that were closer to the core site at the time. In addition, fire frequency declined during the low-lake period, consistent with a fuel limitation hypothesis for the fire regime control at this site.

4.2. Early Holocene arid period

The period from 8700 to 8200 cal yr BP, marked by fine lacustrian sapropel with silt, is sharply delineated from the previous *Chara* mats. The lake may have had fewer extremely low stands, precluding *Chara* growth at the core site, but many other indicators point to this time as very arid. There was lower lake productivity as seen in low TOC and CMAR (Fig. 13) and C:N values were higher, indicating a higher proportion of terrestrial organic matter. High-density values (HU) and an increase in silt deposit likely originated from the local watershed as well as from the now-dry Goose Lake playa 20 km east of Dog Lake. Salt-tolerant *Chenopodium,* common on the playa, is also more abundant at this time. This time period also saw very little

fire, a result of less available herbaceous fuel (and the lowest upland herbaceous pollen percentages in the record) on the landscape and perhaps also fewer ignition events if summer thunderstorms were less frequent.

4.3 Vegetation pre- and post-Mazama tephra deposition

The high-resolution sampling of pollen analysis (every 1-cm or ca. 11 yr) before and after the Mazama eruption (Fig. 14B) showed little definitive plant response to the tephra deposition with the exception of *Sambucus* (elderberry), Rosaceae, and vascular aquatic vegetation including Alismastaceae and *Typha*ceae. *Sambucus* disappears from the record at the time of tephra deposition. This would not be due to a change in soil chemistry as *Sambucus* tolerates alkaline and acidic soils (USDA). This selective loss of *Sambucus* is thus difficult to determine.

Vascular aquatic vegetation (hydrophytes) increased slightly as a result of the tephra deposition. The substrate of the lake shore may have been raised by several centimeters, creating new substrates suitable for hydrophytic rooting. It is likely that the sudden slope wash of tephra into the lake may have increased the littoral area, increasing area for hydrophytic propagation. In addition, the increase in aquatic productivity, seen as a 1 cm section of laminations, was the result of Si-fertilization of diatoms. In contrast to Dog Lake, tephra affected vegetation further north and northeast of Mount Mazama in regions with thicker tephra fall (Long et al., 2014; Egan et al., 2016; Baig and Gavin 2023)

4.4. Vegetation middle to late Holocene

The pollen record shows minor changes following the deposition of the Mazama tephra despite large millennial-scale changes in fire frequency. Two millennial-scale patterns emerge from the pollen record. First, Cupressaceae pollen increases through the mid-Holocene from 5% to >15%. The most prolific pollen producer is *Juniperus occidentalis*, a species easily killed by moderate-severity fires. Cupressaceae pollen begins its increase at 5000 cal yr BP during a minimum in fire activity. Second, Rosaceae pollen declines from 10% to <1% at ca. 3000 cal yr BP. Rosaceae pollen likely represents *Cercocarpus*, a wind-pollinated species that would be represented in lake sediments to a much greater extent than other insect-pollinated Rosaceae.

The period of Rosaceae decline follows a long period of higher fire frequency from 4500 to 3000 cal yr BP. *Cercocarpus* increases in abundance during long fire intervals, but in the event of a moderate to severe disturbance it can take several decades for *Cercocarpus* to re-establish as a result of a long sexual maturity period (Gruell et al., 1982, Gucker 2006) This means if fire intervals were shorter than the time-to-reproductive maturity, then it could explain the decline of this species in the watershed. Why these two fire-avoiding species respond differently to the same fire regime changes is difficult to determine from our data, but differences in drought tolerance during the decreasing summer insolation of the late Holocene may play a role.

Populus pollen, likely *P. tremuloides* due to altitude, is steady through the Holocene. *Populus* tremuloides today is around the Dog Lake lakeshore and there are also stands at higher elevations. In the intermountain west of North America, *Populus* occurs as both seral stands following fire or edaphically controlled sites in locations with higher water availability (DeByle and Winokur, 1985; Shinneman et al., 2013). That *Populus* pollen does not track the fire regime

suggests that edaphically supported populations, rather than seral stands, were supported in the Dog Lake watershed through the Holocene.

4.5. Regional synthesis

Several other paleoenvironmental studies from eastern Oregon and the NGB provide support for the record from Dog Lake. The arid periods of the early Holocene at Dog Lake fit within the regional millennial scale period of increased aridity in the Pacific Northwest peaked at ca. 11,000 cal yr BP, when summer-season insolation was highest (Hermann et al., 2018) and combined with warm, dry air from a strong and persistent Pacific sub-tropical high-pressure system, the combination of which intensified evapotranspiration rates inland (Hirschboeck, 1991; Thomson et al., 1993; Minckley et al., 2007). In particular, the distinct lithological unit encompassing 8700 to 8200 cal yr BP was an exceptionally dry period within the early Holocene. Summer Lake/Lake Abert experienced peak heat and aridity between 8700 and 8200 cal yr BP (Cohen et al., 2001, Hudson et al., 2021), with the lake completely desiccating by the mid-Holocene. At Skull Creek Dunes in Catlow Valley, this time period of low-vegetation cover resulting in dune-erosion (Mehringer and Wigand, 1984).

In the eastern and Central Great Basin, the timing of maximum aridity was out of phase with Dog Lake. Pyramid Lake shows high drought as a result of Lake Tahoe not overflowing to feed the Truckee River in the middle Holocene (Benson et al. 2002; Mensing et al., 2004). The Ruby Marshes, located southeast of Dog Lake near central Nevada also showed peak aridity closer to the mid-Holocene. Overall, droughts occur earlier in the Holocene the further north the site is located.

Later in the Holocene, the sediment composition (and inferred lake levels) changed little at Dog Lake, but the variable fire history suggests distinct millennial-scale variability (Fig. 15). The temporal resolution of the Dog Lake record is significantly higher resolution than previous charcoal-stratigraphic studies in the region and from a lower elevation. Pollen-based precipitation and effective moisture reconstructions from nearby Lilly and Patterson lakes show increased moisture developing from 7000 to 5000 cal yr BP (Minckley et al., 2007), a time period when fire overall increased dramatically at Dog Lake. This is consistent with the fuel-limitation inference and the Poaceae/*Artemisia* pollen ratio at Dog Lake. The highest annual precipitation values were reported between 3900 - 3000 cal yr BP at Lilly Lake. Further east, decreased aridity values at Diamond Pond were reported from 3600 - 2200 cal yr BP (Wigand 1987). Changes in regional aridity occur earlier in the NGB than further east or south in the Great Basin. Changes in aridity at Steens Mountain are more synchronous with the Central Great Basin than the northwest portion of the Great Basin where Dog Lake is located (Mensing et al., 2008).

Regions east of the Warner Mountains show drier conditions during the mid-Holocene (Hermann et al., 2018). At Diamond Pond peak aridity was measured at ca. 5000 cal yr BP (Mehringer, 1987; Wigand, 1987) with high amounts of *Artemisia* and Atriplex. Between 4000 - 3700 cal yr BP *Artemisia* and Atriplex decreased rapidly and were replaced by grass, juniper, and aquatic plant seeds, all indicators of a reduction in aridity. This trend continued from 3600 - 2200 cal yr BP, a period *Chara*cterized as a high-water period at Diamond Pond (Wigand 1987). The timing of these variations in effective moisture appears to be out of phase and slightly later than at Dog Lake.

In the Central Great Basin south of Dog Lake, several periods of punctuated and persistent aridity were documented, but a mid-Holocene dry period ca. 7500 - 5000 cal yr BP was found at many sites (Lindström, 1990; Benson et al., 2002; Mensing et al., 2004, 2008; Reinemann et al., 2009; Grayson, 2011). Portions of Lake Winnemucca was present from 4300 - 3900 cal yr BP based on artifact ages (Long & Ripparteau, 1974), fish vertebrae, primarily tui chubs (*Siphateles* sp.) and western pond turtles (*Actinemys marmorata*) (Mensing et al., 2013) (Hattori, 1982). Thompson (1992) reported that between 7600 and 5400 cal yr BP sedimentation rates in the Ruby Marshes of west-central Nevada decreased rapidly in response to increased aridity. Grayson (2000) used a well-dated mammal sequence from Homestead Cave, Utah, to show faunal species decrease from 9200 to 3500 cal yr BP in response to more xeric conditions. Pika (*Ochotona princeps*), a genus incapable of tolerating temperatures above 25^{o}C, disappeared from low-elevation Great Basin sites ca. 7800 cal yr BP (Grayson, 2005).

Additionally, in the southern Great Basin, black mats formed by spring discharges into wet meadows and shallow ponds were absent between 7200 to 2500 cal yr BP, indicating a period of high aridity (Quade et al., 1998). Punctuated aridity at Owens Lake was *Chara*cterized by TIC and $\delta^{18}O$ values which showed 7700 - 3200 cal yr BP as highly arid and a sediment hiatus between 6500 - 3900 cal yr BP suggests complete lake desiccation below coring site elevation (Benson et al., 1997, 2002; Lund & Benson, 2021). Evidence from Walker Lake, Nevada shows evidence of complete desiccation at or before 5000 cal yr BP (Yuan et al., 2006). On the east slope of the White Mountains of California, the tree-line elevation at Sheep Mountain was relatively high between ca. 5700 and 4100 cal yr BP, falling 100 meters between 4100 and 3500 cal yr BP, indicating a 1^{o}C decrease in warm-season temps and another 70 m around 900 cal. yr BP (La Marche 1973).

5. CONCLUSIONS

The formation of Dog Lake coincided with a period of increased insolation, higher temperatures, and lower annual precipitation. The first 400 years showed high mineral inclusions followed by diatomaceous sapropels. This formation of the sapropelic sediments was interrupted by a shallow lake period and the formation of dense *Chara* mats between 9200 - 8700 cal yr BP. At 8700 cal yr BP the *Chara* mats abruptly disappear. Between 8700 and 8200 cal yr BP conditions were so warm and dry that dust deposition into the lake increased as a result of lower vegetation cover and desiccating regional lakes. The *Chara* mats indicated low water levels at the deepest part of the lake, perhaps less than a meter in depth. The lower organic productivity is interpreted as being the result of reduced precipitation, high temperatures, and high evaporation rates. After 8200 cal yr BP high organic sapropels return, indicating a deeper water column. The Mazama tephra deposition resulted in little vegetation changes in the Dog Lake basin. The remaining core is characterized by a steady, high sedimentation rate through to the current day.

The high sedimentation rate offered the opportunity for a high-resolution CHAR analysis in a high fire-frequency setting. Fire intervals were far shorter during Zone 1 (9600 - 9300 cal yr BP) averaging a 15-year FRI. Fire intervals were very episodic over the last 8700 years. From 8700 to 8200 there was low fire activity in the basin. Post-Mazama periods of more frequent fire episodes were recorded during the mid-Holocene from 5700 - 5400 and 4700 - 3700 cal yr BP, periods of time coinciding with higher grass pollen percentages. Thus, increased early summer moisture and increased grass productivity likely contributed to increased fire spread. We conclude that this lower-treeline site is precipitation or climate-limited (with respect to fine grass fuels) on millennial time scales. This is in contrast to the more mesic, high-elevation site of White Pine Marsh, which was found to be fuel-limited over the same time periods.

CHAPTER IV

CONTRASTING THE HOLOCENE FIRE AND VEGETATION HISTORY OF LOW AND HIGH-ELEVATION MIXED-CONIFER FORESTS IN SOUTH-CENTRAL OREGON, USA

Co-authored research by Saban, Chantel V. and Daniel G. Gavin. Contrasting the Holocene Fire and Vegetation History of Low and High-elevation Mixed-conifer Forests in South-central Oregon, USA. In preparation for Palaeogeography, Palaeoclimatology, Palaeoecology.

Chantel Saban and Daniel Gavin conceptualized the study and devised the methodology. Saban and Gavin analyzed sediments. Saban processed and analyzed the pollen and charcoal. Curation, analysis, and visualization of the data were done with the help of Gavin. Saban wrote the original manuscript, and Gavin reviewed, edited, and contributed to the final manuscript.

1. INTRODUCTION

Studies using lake sediments recovered from various sites throughout the Northern Great Basin (NGB) region have primarily focused on the timing of late Quaternary climate changes (Mehringer, 1986; Mehringer and Wigand, 1986; Cohen et al., 2000, Wigand, 1987; Minckley et al. 2007; Reinemann et al., 2009). Research across the NGB has shown that there is a difference in timing on when climatic changes affect the vegetation (Wigand and Rhode, 2002; Mensing et al., 2004; Minckley et al., 2007, 2008) versus when it affects hydrological systems, primarily the large-scale, low-elevation pluvial lakes, of the NGB (Allison 1984; Friedel 1994, Cohen et al., 2001; Wriston and Smith, 2017; Adams and Rhodes, 2019; Hudson et al., 2019, 2021).

Closely related to vegetation and climate changes are questions regarding possible variability in the fire history of mid- and high-elevation forests over the Holocene. There remains an opportunity to contrast fire history across the range of forested elevations in the NGB to better understand the role of fuel vs climate limitation in Holocene fire history. For example, it is widely postulated the fire history at lower treeline is fuel-limited and fire is promoted by wet periods that promote grassy fuel development, while higher elevation forests are limited by the length of the fire season (Falk et al., 2011). This is supported by Minckley et al. (2007) who found Holocene fires in the NGB were more frequent in mid-elevation forests and rare in high-elevation forests.

High-elevation mixed montane forests, located in areas of orographic precipitation, are rare in the NGB (Wolf and Cooper, 2015). The northern Warner Mountains receive approximately 1200 - 1500 mm precipitation annually at elevations ranging between 2000 - 2400 m (OSU-PRISM). This research concentrates on materials recovered from White Pine Marsh (Fig. 16), located at the northern terminus of the Warner Mountains, and contrasts vegetation and fire results from White Pine Marsh with Dog Lake, a lower elevation site closer to the lower elevational limit of forests in the NGB.

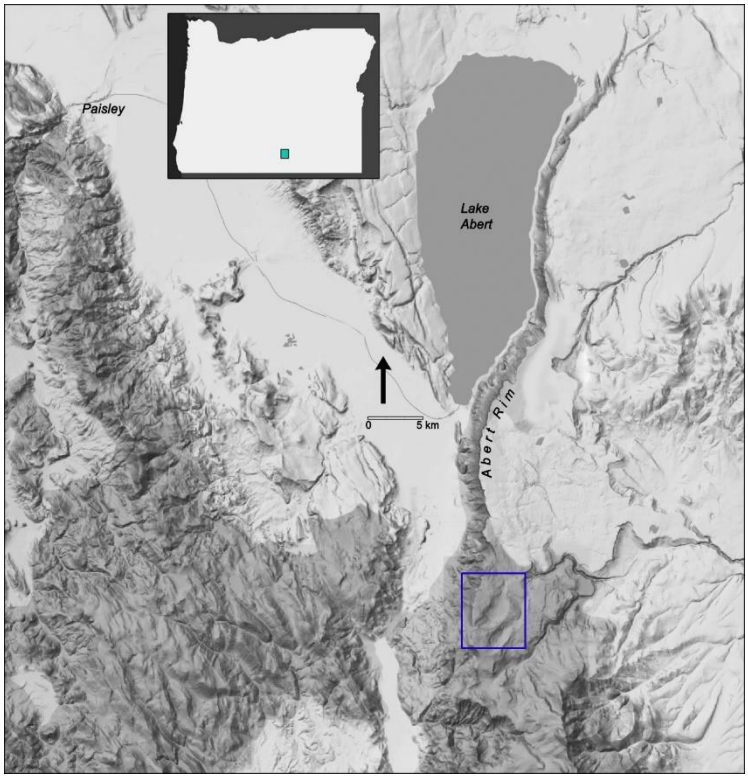

Figure 13. Location White Pine Marsh (outlined in blue), south-central Oregon.

White Pine Marsh is a high-elevation wetland located within a small glacial cirque at a mean elevation of 2053 meters above sea level (masl). This is a high biodiversity area sensitive to changes in climate, with vegetation communities being precipitation or moisture limited rather than temperature-limited (North et al., 2016). Combined with the floristic variability not common at lower elevations in the NGB, WPMA is an excellent location for identifying changes in precipitation and ecological communities over the course of the Holocene. While marshes and wetland systems are common throughout the NGB at all elevations (Allison, 1982; Hattori, 1982; Smith and Street-Perrott, 1984; Oetting, 1989; Thompson, 1992; Crowe & Clausnitzer, 1997; Cohen et al., 2000; Wigand & Rhode, 2002; Adams et al., 2008), no research has been conducted on determining the evolution of marsh development in a high-elevation systems in the northern Warner Mountains. Additionally, no research has been conducted on the Holocene history of vegetation or fire in the high-elevation mixed dry-forest of the northern Warner Mountains, although work has been done in the central (Minckley et al., 2007) and southern Warner Mountains (Vale, 1977; Di Orio et al., 2005; Howard, 2018). The biodiversity of the northern Warners is high given its location at the junction of the Great Basin and proximity to the Cascade Range. The position of multiple ecologically distinct biomes sharply delineated within elevational meters instead of latitudinal kilometers makes this area of south-central Oregon worthy of further paleo-studies.

This project seeks to address the dearth of paleoenvironmental data available for a high elevation forest in the terminal northern Warner Mountains by 1) determining the vegetation and wetland history of White Pine Marsh, and 2) determine limiting factors for fire at WPMA and 3) contrast the Holocene fire history preserved in sedimentary charcoal of White Pine Marsh with a fire history from a nearby mid-elevation mixed forest.

2. METHODS

2.1. Site description

White Pine Marsh (hereafter WPMA; 42.400880°N, 120.213456°W) is located at the northern terminus of the Warner Mountains within a small glacial cirque valley with a mean elevation of 2053 masl (m) (Fig. 17A and 17C) within a shallow lake basin. The WPMA valley is flanked by a small lateral moraine on the southeast side of the marsh and a small terminal moraine at the north end of the marsh. The glacial head was located at 2198 m. The valley trends southwest to northeast and is approximately 3 km long southwest to northeast, and ca. 1.2 km wide. The marsh itself covers an area of approximately 110 ha (23B). The marsh is fed by precipitation and groundwater, draining north into Little Honey Creek, which itself drains northeast into Hart Lake in Warner Valley.

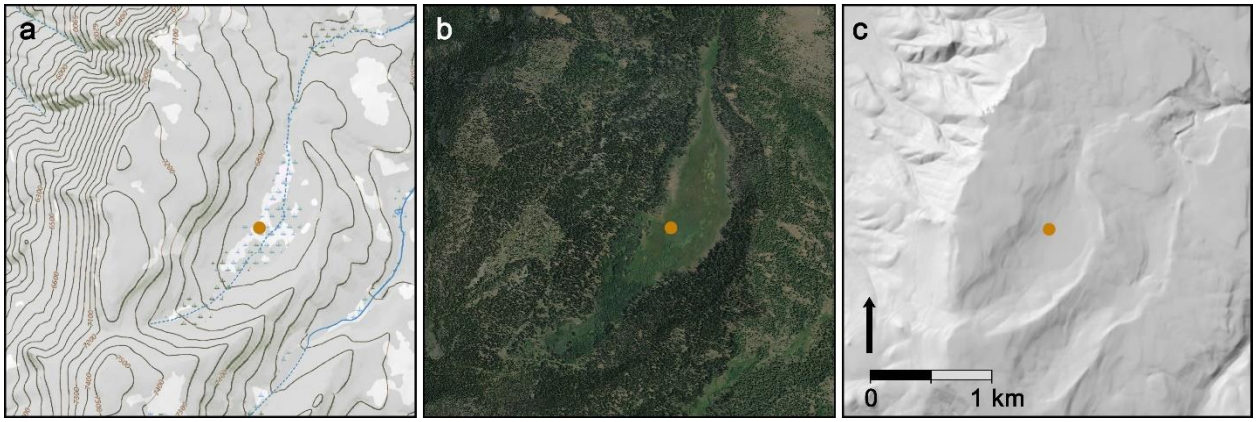

Figure 17. White Pine Marsh a) topography map, b) satellite image, and c) shaded relief. Yellow dot is coring site. Larger figure also in Appendix 36.

The dominant bedrock is olivine basalt and andesites originating during the Paleogene (Walker 1963). The soil of WPMA is perennially saturated, with a narrow margin of annually saturated wet meadow around the perimeter. The marsh is perhaps better described as a basin fen, a perennial wetland with alkaline, neutral, or slightly acidic peaty soil (Dodson 2005). Basin

fens are common in the Warner Mountains and Sierra Nevadas above 1600 m elevation, as well as areas west of WPMA (Wolf and Cooper, 2015).

The majority of precipitation in the north Warner Range comes from winter storm fronts moving east from the Pacific Ocean, with summer precipitation sourced from convection cells resulting in thunderstorms. The average precipitation range is from 1270-1520 mm (OSU-PRISM), sharply contrasting to lower elevations surrounding the WPMA area, some receiving < 500 mm annually.

2.2. Field Sampling

A combination of topographic maps and ground truthing resulted in the selection of a site in the center of the marsh for coring. In July 2018 sediment cores were recovered using an 8-cm diameter Livingstone piston corer followed by a 5-cm piston corer for deepest coring depths. A cable held by a tripod aided in the recovery of two staggered core sections totaling 182 cm (Fig. 18). Sediments were extruded into plastic-wrap lined, halved PVC pipes (Fig. 19), measured and described, then covered with the other portion of the PVC, sealed, and labeled. The cores were refrigerated at the University of Oregon until subsampling could begin.

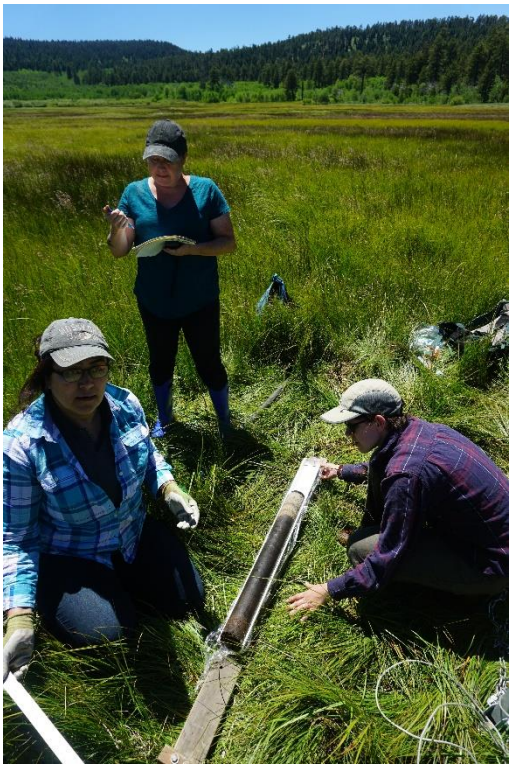

Figure 18. Extraction of core, WPMA, July 2018.

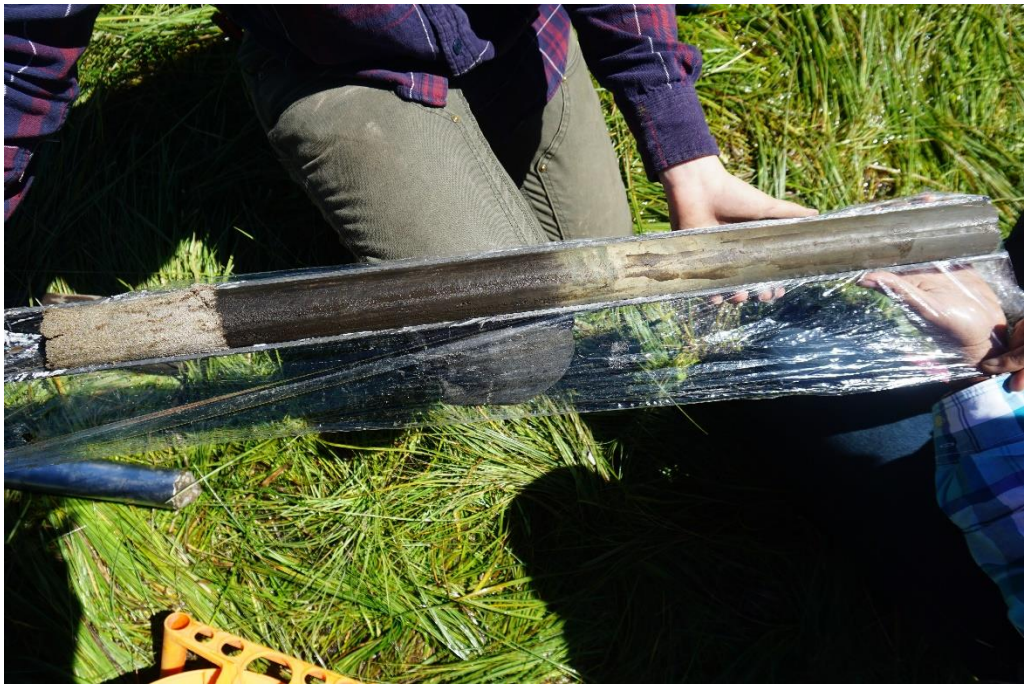

Figure 14. Portion of extracted core. Note tephra/lake sediment transition (left) and high aridity period sediments (right of center.)

2.3. Age-depth model

Accelerator mass spectrometry (AMS) radiocarbon dates were obtained from amorphous bulk organic matter (n = 4) (Table 3). All samples were pretreated with warm 10% KOH and 10% HCl rinses before submitting to the dating facility. An age-depth model was constructed using the CLAM model in R (Blaauw 2010), with the INTCAL20 calibration curve (Reimer et al., 2020) modified to use a monotonically increasing spline curve fit (Schworer et al. 2017) to the four radiocarbon dates, the Mazama tephra (7640 ± 25 cal yr BP; Egan 2015), and the core top. The Mazama tephra unit was specified as an instantaneous event within the CLAM model (Fig. 20).

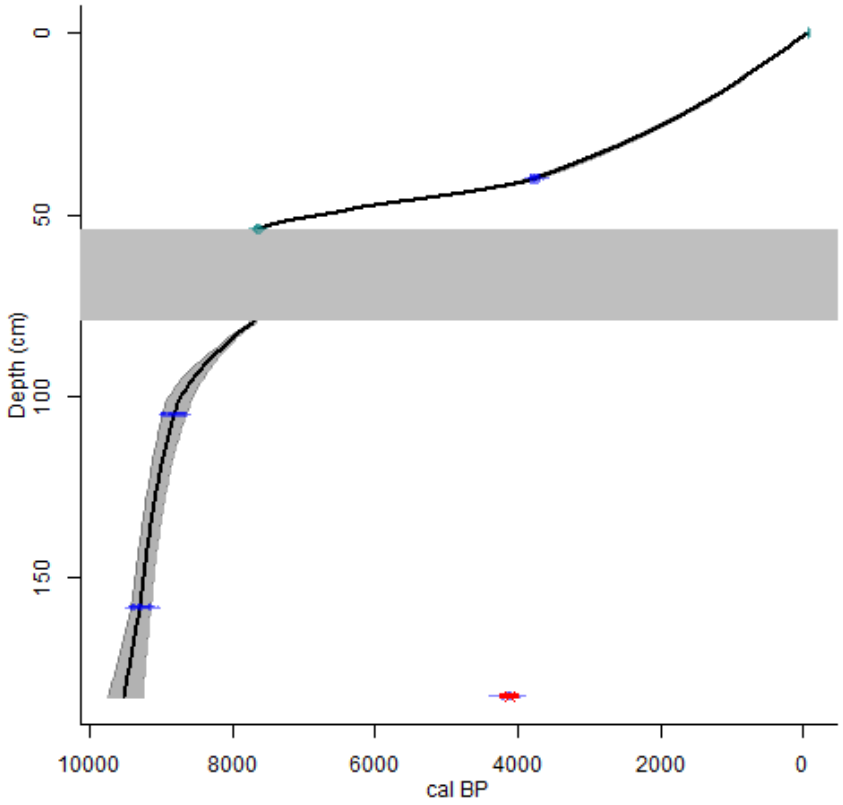

Figure 20. Age-depth relationship for White Pine Marsh core.

Table 3. Radiocarbon dates from White Pine Marsh.

Depth (cm)	Material	Lab number	^{14}C age	Calibrated 2σ age range	Source
0	amorphous pretreated organic	surface	-	-	-
40	amorphous pretreated organic	D-AMS 042766	3482 ± 22	3660 – 3830	*This study*
54 - 80.5	Mazama tephra	-	-	7682 – 7584	Egan et al. 2015
105	amorphous pretreated organic	D-AMS 042767	7939 ± 30	8642 – 8973	*This study*
158	amorphous pretreated organic	D-AMS 042768	9283 ± 38	9128 – 9420	*This study*
182.5	amorphous pretreated organic	D-AMS 042769	9505 ± 35	9238 – 9734	*This study*

2.4. Pollen

Pollen recovery followed protocols described by Smith (1998) and Pearsall (2016). Sediments (n = 11 1cm^3 subsamples) were obtained every 10 cm down-core (averaging a sample approximately every 900 yr). Samples were added to 15 ml test tubes together with one *Lycopodium* tablet per tube to measure pollen concentrations. Chemical pollen extraction was performed inside a fume hood. 10% KOH was used to remove remaining soluble organics followed by a 10% HCL treatment to remove carbonate minerals. Hot hydrofluoric acid (HF) treatment for 40 minutes reduced silicate content. A second 10% HCL treatment sample was followed by glacial acetic acid (GAA), followed by acetolysis to remove the remaining cellulose. Samples were stained with safranin and desiccated using ethyl alcohol (ETOH) and tert-Butyl alcohol (TBA). Pollen was transferred into 2-dram glass vials with Si oil used for suspension and preservation of pollen. Pollen was examined at 40X magnification and identified to the highest taxonomic resolution possible using published keys (Faegri et al., 1989) and the modern pollen reference collection at the University of Oregon. Pollen was counted to a minimum of 350 grains

per sample. In addition to graphing the pollen results a stratigraphically constrained cluster analysis (CONISS) was calculated in Tilia 3.0.1 (Grimm 1987) to aid in pollen zonation.

2.5. Charcoal

Charcoal sampling followed protocols described by Rhodes 1998. 2 cm^2 of sediments were subsampled at 0.5 cm increments the length of the core (182 cm) except for the segment of Mazama tephra. Each subsample was placed into a 12 mL vial and soaked for 12 hours in 10% sodium hexametaphosphate (Na-HMP). Sediments were then gently rinsed with water using a 250 µm and 125 µm 7.6 cm diameter mesh sieves. All large identifiable charcoal pieces or macrobotanicals were saved, and the remaining charcoal was placed back into 12 mL vials. The 125-250 µm fraction was soaked overnight in 7% hydrogen peroxide (H_2O_2) to partially digest and bleach organic materials. Samples were then rinsed using a 125 µm mesh sieve. Charcoal particles were counted using a Bogorov counting chamber under 10x-25x magnification. Charcoal counts were converted to percentages of sediment collected per sample and graphed.

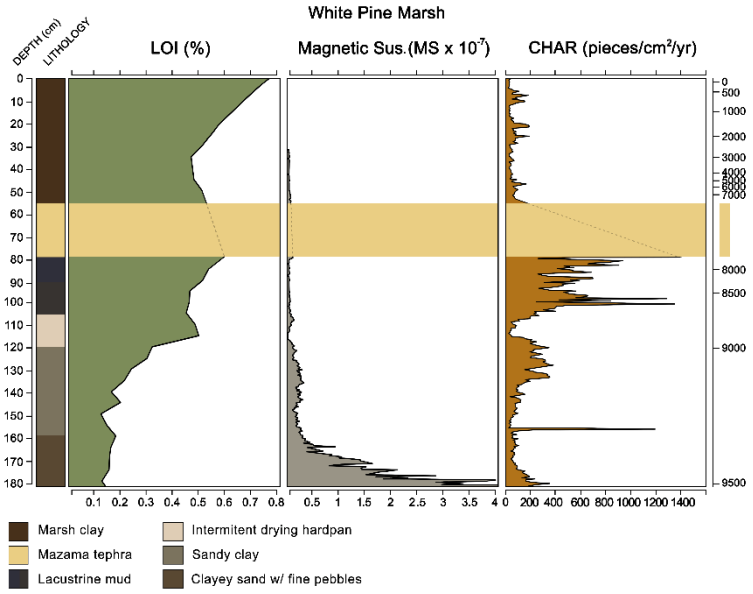

Figure 21. LOI, magnetic susceptibility, and charcoal. Dog Lake carbon mass accumulation rate (CMAR) on right. Sediment descriptions in text. Larger figure also in Appendix 37.

2.6. Loss on Ignition

To measure organic matter content, loss on ignition (LOI) was conducted on 31 samples for the purpose of measuring bulk density and organic matter content (Fig. 21). Ceramic crucibles (10 ml) were washed and dried in a drying oven at 95°C, then weighed. Wet 1 cm^2 samples were placed into the labeled crucibles and weighed again. Crucibles were then placed back in the drying oven for eight hours to desiccate the sediments completely, after which samples were once again weighed. Crucibles were then put in a muffle furnace and sediments were combusted at 550°C for 2 hours. Crucibles were cooled in a bell desiccator and then weighed a final time. Testing with 10% HCl showed little to no carbonates, so no further combustion at a higher temperature (950°C) was conducted.

2.7. Statistics

Raw pollen counts were transformed into percentages and diagrammed using Tilia 3.0.1. Pollen assemblage zones of the sediment pollen record were determined using stratigraphically constrained cluster analysis (CONISS). The WPMA results were then compared to Dog Lake CHAR results.

3. RESULTS

3.1. Chronology and sediment descriptions

A total of 182 cm of sediment were recovered from WPMA. The age-depth relationship is shown in Figure 20. Four radiocarbon ages and the Mazama tephra (25-cm thick) age occurred in chronological order. An abrupt change in sedimentation rate (Fig. 20) occurred at the point of Mazama tephra deposition 7640 cal yrs BP. The sedimentation rate averaged 0.0946 cm/year or

10.6 yrs/cm pre-Mazama tephra deposition, slowing to 0.00916 cm/yr or 109.2 yrs/cm post-Mazama. The following sediment descriptions follow Schnurrenberger et al. (2003) and divisions are shown in Figure 21.

Sediments show very different conditions present in the basin since the early Holocene. Forested systems combined with near-constant water inputs have been constants in the marsh. It is currently unknown what conditions were like immediately post-glaciation, although sediments from 182-160 cm/ 9500-9300 cal yr BP shows sediments consistent with open forest conditions present at the current marsh site. These earlier sediments were reddish, slightly clayey with rounded clasts throughout between 2 mm to 1 cm, as well as obsidian (<2 mm) and mica <1 mm).

From 160-120 cm/ 9300-9000 sediments turned light brown, reflecting a dry, open meadow or grassland. This transitioned into a light gray aridisol-type sediment from 120-105 cm/ 9000-8800, a highly arid period in the NGB. This material showed little reaction to HCL, meaning carbonates were low. The sediment does not appear to be saline like the playas located in lower elevations and is likely silt deposits precipitated in a very shallow occasional lake preserved as hardpan through desiccation. A similar hardpan sediment structure was recovered in 2018 from Colvin Lake, a small body of water near the summit of Abert Rim and fed by groundwater. and 5 km north of WPMA. The extremely hard 40 cm of sediment recovered from Colvin (C. Saban, unpublished data) is a possible modern analog for the past condition at WPMA: a body of water prone to frequent desiccation.

Above the desiccated lake section from 105-90 cm/ 8800-8300 cal yr BP sediments turn dark brown and consist of low-clastic materials combined with sapropels. This form of sediment is consistent with a highly organic, clayey, shallow lake (Dodson, 2005). This is a particularly

arid period at lower elevations in the NGB (Chapter III), so it is slightly anomalous that a shallow lake would appear at this time. However, WPMA is situated in a highly tectonically active area, so it is likely that an earthquake resulted in increased groundwater flow into the WPMA basin. Sediments turned very dark brown between 90-79 cm/ 8300-7640 cal yr BP. This sediment is more sapropelic and with no clasts larger than silt. Sediments from 79-54 cm are all well-defined tephra originating from Mount Mazama, located 157 km northwest of WPMA. The tephra consisted primarily of lapilli 1-2 mm in size, with fine ash present at 79 cm.

Sediments from 54-0 cm are clayey marsh soils with roots throughout. Between 40-54 cm there are few to no modern roots, and the texture and color remain dark brown and a silty clay. The upper 30 cm of the core is hydric silty clay, dark brown in color with modern grass and sedge roots throughout. There was little odor to the upper 30 cm soil, indicating anaerobic conditions with little or very slow decomposition, suggesting that the wetland soils remain wet year-round.

3.2. Pollen

A sum of squares analysis divided the pollen assemblage into two zones (Fig. 22) at ca. 3700 cal yr BP, although significant enough differences are evident at the eruption of Mount Mazama at ca. 7640 cal yr BP that the eruption can be considered a division between the two zones as well. Taxa percentages are based on terrestrial pollen sums of each level. The overall pollen diagram shows a highly diverse range of vegetation consistent with fen wetlands surrounded by mixed conifer woodlands. Of the entire assemblage, only *Pseudotsuga* is not found in the greater WPMA region today.

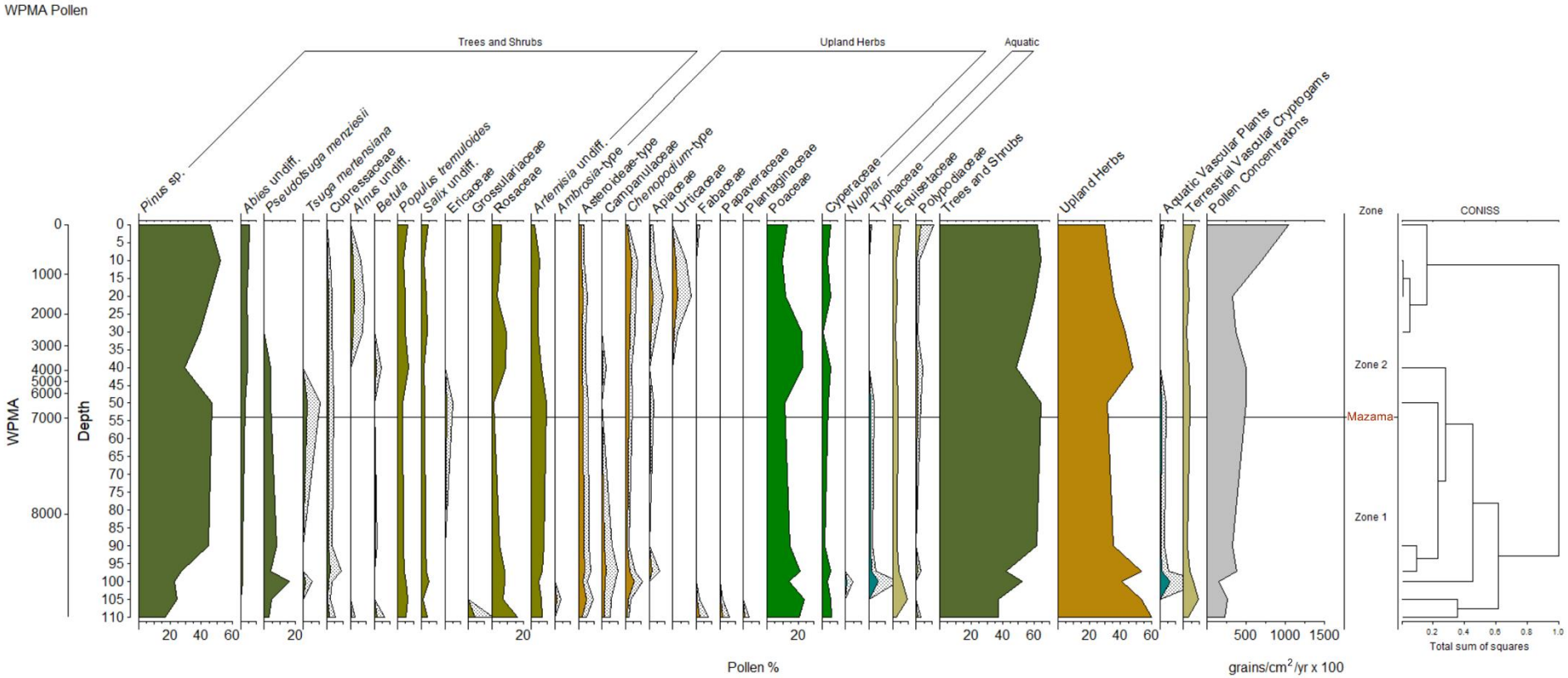

Figure 22. Sediment pollen diagram for White Pine Marsh, Oregon.

Pinus pollen consisted primarily of *Pinus* subg. *Pinus* or undifferentiated *Pinus* (representing *P. ponderosa* and *P. contorta*), with lesser amounts of *Pinus* subg. *Strobus* (*P. monticola*) and perhaps *P. albicaulis*. *Abies* was low in pre-Mazama samples (<5%), increasing sharply post-Mazama and remaining steady at near 10% through to current day. *Pseudotsuga* was present pre-Mazama with values nearing 20% at times but declines sharply post-Mazama and disappears from the WPMA record at ca. 3000 cal yr BP. *Tsuga* pollen also occurred briefly pre-Mazama ca. 8800 cal yr BP at <5%, later reappearing immediately following the Mazama eruption until ca. 5000 cal yr BP. *Tsuga mertensiana* is currently present regionally, but infrequent and further west and south relative to WPMA. Cupressaceae was present but remained low (<5%) through the entire assemblage, with lowest values from ca. 200 cal yr BP up to current-day. This is likely *Juniperus occidentalis*, however, *Calocedrus decurrens* is occasionally present in the Dog Lake basin 40 km east of WPMA so it is possible the species was in the WPMA area. Hardwoods are well represented at WPMA through the Holocene. *Alnus* appeared in the later Holocene, and *Betula* was present early through mid-Holocene. *Populus* remained steady through the assemblage, and is likely *P. tremuloides*, as *P. trichocarpa* is found in the region but only below 1500 masl. Graminoids include true grasses (Poaceae) as well as sedges (Cyperaceae).

3.2.1. Zone 1 (110-79 cm) 8900-7640 cal yr BP

There are 23 taxa identified during the 1260-year-long pre-Mazama period covering the early Holocene. During Zone 1, upland herbs were relatively more common until ca. 8300 cal yr BP, after which trees and shrubs surpassed upland herbs. During the Zone 1 period *Pinus* undiff. has the highest pollen percent counts (27.2%). *Pinus* began low (17%) at 8880 cal yr BP, nearly doubling between 8800 (25%) and 8600 (27%). By 8330 *Pinus* reached near-modern values at

45%. *Pseudotsuga* averaged 8%, beginning at 8880 cal yr BP (5.1%), reaching the highest percent at 8700 cal yr BP (16%), and ending Zone 1 at 8330 cal yr BP at 8.2%. *Abies* began low (0.8%), increasing to 1% beginning at 8700 cal yr BP and remaining there through the remainder of Zone 1. Cupressaceae averages 1%, maxing out at 2% by 8600 cal yr BP then decreasing to ca. 1% by 8330 cal yr BP. *Abies* is low throughout Zone 1, beginning at 0.2% and ending at ca. 1%. *Tsuga* ($\overline{x}$ = 0.3%) appears only once (1.4%) at 8700 cal yr BP.

Hardwood trees and shrubs include Rosaceae ($\overline{x}$ = 9%), likely *Cercocarpus ledifolius* which is currently found at lower elevations within a short distance of WPMA but not currently in the WPMA basin itself. Rosaceae ($\overline{x}$ = 9%) began Zone 1 at 16%, decreasing to 5% by 8330 cal yr BP. *Artemisia* ($\overline{x}$ = 6.7%) began at 7% and remains there until increasing to 8% at the end of Zone 1. *Populus tremuloides* averaged 5% during Zone 1, beginning at 5%, increasing slightly to 7% and ending the zone at 3%. *Salix* ($\overline{x}$ = 3%) began at 4%, decreased to 1% by 8800 cal yr BP then increased to 5% by 8700 cal yr BP, decreasing to ca. 3% by the end of Zone 1. Remaining pollen types include Grossulariaceae (($\overline{x}$ = 0.8%), *Betula* ($\overline{x}$ = 0.4%), and *Alnus* ($\overline{x}$ = 0.1%)

Upland herbs are dominated by Poaceae at 19% during Zone 1. Poaceae begins at 20%, increasing to 24% by 8800 cal yr BP, decreasing to 14% by 8700 cal yr BP and ending the zone at 15%. Cyperaceae is second to Poaceae, but only averaging 4.5%. Cyperaceae began at 6%, remaining there until 8330 cal yr BP where the percentage went down to 2%. Asteroideae-type ($\overline{x}$ = 3.5%) pollen began at 3%, increased to 5% then decreased to 3% by the end of Zone 1. *Chenopodium*-type (($\overline{x}$ = 2.4%) began low (1%), increased to 5% by 8.7 cal yr BP, and ending the zone at 1%. Averages for remaining herbaceous taxa include Campanulaceae (2.4%),

Fabaceae (0.5%), Papaveraceae (0.4%), Apiaceae (0.3%), *Ambrosia*-type (0.2%), and Plantaginaceae (0.2%).

Aquatic species are not included in the statistical analysis, but they inform on the overall environmental conditions within assemblages. Two hydrophytes were identified from WPMA: *Nuphar* and *Typha*. *Camassia* was predicted to be potentially present, but it was not, a result of perennially wet conditions of WPMA as opposed to annual. *Nuphar* appears once at 8900 cal yr BP. Typha begins at 8% at 8900 cal yr BP, declining to <2% for the remainder of Zone 1.

3.2.2 Zone 2 (54 - 0 cm) 7640 - -60 cal yr BP

Zone 2 has 21 taxa identified and covers the pollen assemblage for the last 6900 years post-Mazama eruption, although the sum of squares shows the primary division as being at 3700 cal yr BP. The pollen influx began higher at the start of Zone 2 than the previous Zone 1, beginning with an influx of approximately 60,000 grains/cm^2/yr at 6800 cal yr BP, decreasing beginning at 3700 cal yr BP to 45,000 grains/cm^2/yr through to ca. 900 cal yr BP, then sharply increasing up to 120,000 grains/cm^2/yr through current day. Higher pollen influx was driven by trees and shrubs in the period immediately after the Mazama eruption (7640-6000 cal yr BP). From 6000 to 3700 cal yr BP upland herbs were most represented in pollen concentrations, decreasing to be replaced by trees and shrubs as dominant from 900 cal yr BP to the current day.

Pinus during Zone 2 once again have the highest pollen percentages ($\overline{x}$ = 43%), with values beginning at 47% after Mazama and dropping to 29% by 3750 cal yr BP, then increased to 52% in 670 cal yr BP. *Pinus* current-day values are 45%. Abies averages much higher than Zone 1 at 4%. *Abies* began at 3% post-Mazama, increasing to 5% and remaining at ca. 5% thorough current-day. *Pseudotsuga* averaged 1%, beginning at 4% from post-Mazama through

3700 cal yr BP, then disappearing from the pollen record. Other conifers include Cupressaceae (0.67%) which began low and remained low through to 670 cal yr BP (<1%) and no longer present current-day, and *Tsuga* (3%) present only at 6844 cal yr BP and then gone from the record.

Hardwood trees and shrubs include Rosaceae, averaging at 9%, beginning low at 6800 cal yr BP (1.3%), increasing by 3700 cal yr BP peaking at 2500 cal yr BP (9%). Current values began at ca. 670 cal yr BP (6%), remaining at 6% through to current-day. *Artemisia* was slightly lower than seen in Zone 1 at 5%. *Artemisia* begins high at 9% post-Mazama, then slowly decreases resulting in current-day values of 2%. *Populus* averages did not change from Zone 1 (5%), beginning at 3%, increased to 5% by 2500 cal yr BP, and current-day *Populus* is at 7%. *Salix* ($\bar{x}$ = 3%) is at 2% post-Mazama, reaching 4% by 2500 cal yr BP, declining to 2% by 670 cal yr BP, and ending at 4.5% current-day. *Alnus* averages 1%, but does not appear until 2500 through 670 cal yr BP. There is no *Alnus* in the current-day assemblage. Ericaceae is recorded once (1%) at 6844 cal yr BP, and Betula is identified once (1%) at 3700 cal yr BP.

Upland herb percentages are dominated by Poaceae ($\bar{x}$ = 15%), with Cyperaceae ($\bar{x}$ = 4%) a distant second. Poaceae began at 11%, increasing to 23% by 3700 cal yr BP, 22% by 2500 cal yr BP, then declined to 9% by 670 cal yr BP. Current-day Poaceae is at 13%. Cyperaceae started at 4%, then, with the exception of 0.5% at 2500 cal yr BP, remained steady at 5% through to current-day. *Chenopodium*-types maintained a similar average (2.5%) as Zone 1, with percentages ranging between 2% at 6844 cal yr BP, highest at 670 cal yr BP (4%) and current-day at <1%. Asteroideae-type ($\bar{x}$ = 2.4%) pollen began at 3% and decreased to 2% by the end of Zone 1. Averages for remaining herbaceous taxa include Urticaceae (1%), Apiaceae (0.95%), Campanulaceae (0.10%), and Fabaceae (0.10%).

Typha was the only hydrophyte identified from Zone 2, with values of 1% at 6844 cal yr BP and 0.60 at current-day. Equisetaceae appears in both Zone 1 and 2, however, values are higher for Zone 1 (5%) than for Zone 2 (3%).

3.3. Fire History

WPMA fire history is sharply divided into two distinct periods (Fig. 23A). Raw charcoal counts of WPMA were plotted by age and by concentrations, and by age and uninterpolated accumulation rates. This approach preserves the features of the raw charcoal and accumulation rates between the two different cores while providing a visualization of the data over the same length of time (Long et al., 1998; Mohr et al., 2000). Average raw charcoal counts are 167 pieces cm^3. Charcoal concentrations range from 1 to 630 pieces/cm^3 with an average of 85 pieces/cm^3. Previous to the Mazama eruption charcoal concentrations at WPMA were variable and increased between 9600 and 7640 cal yr BP. High concentrations and charcoal frequency previous to the Mazama eruption abruptly decrease at or immediately after tephra deposition and remain low for the remainder of the assemblage. Post-Mazama charcoal concentrations were graphed separately to better illustrate deposition patterns (Fig. 23B). Pre- and post-Mazama charcoal is primarily wood, with some herbaceous charcoal present as well. The only time this changes is from 2600 to 1900 cal yr BP when the charcoal record is dominated by herbaceous charcoal. Charcoal concentrations increased at 8800 cal yr BP and continued to increase up to the Mazama eruption,

but the accumulation rate decreased during that same time. Charcoal concentrations post Mazama appear smoothed between peaks and <100 pieces cm^{-2}.

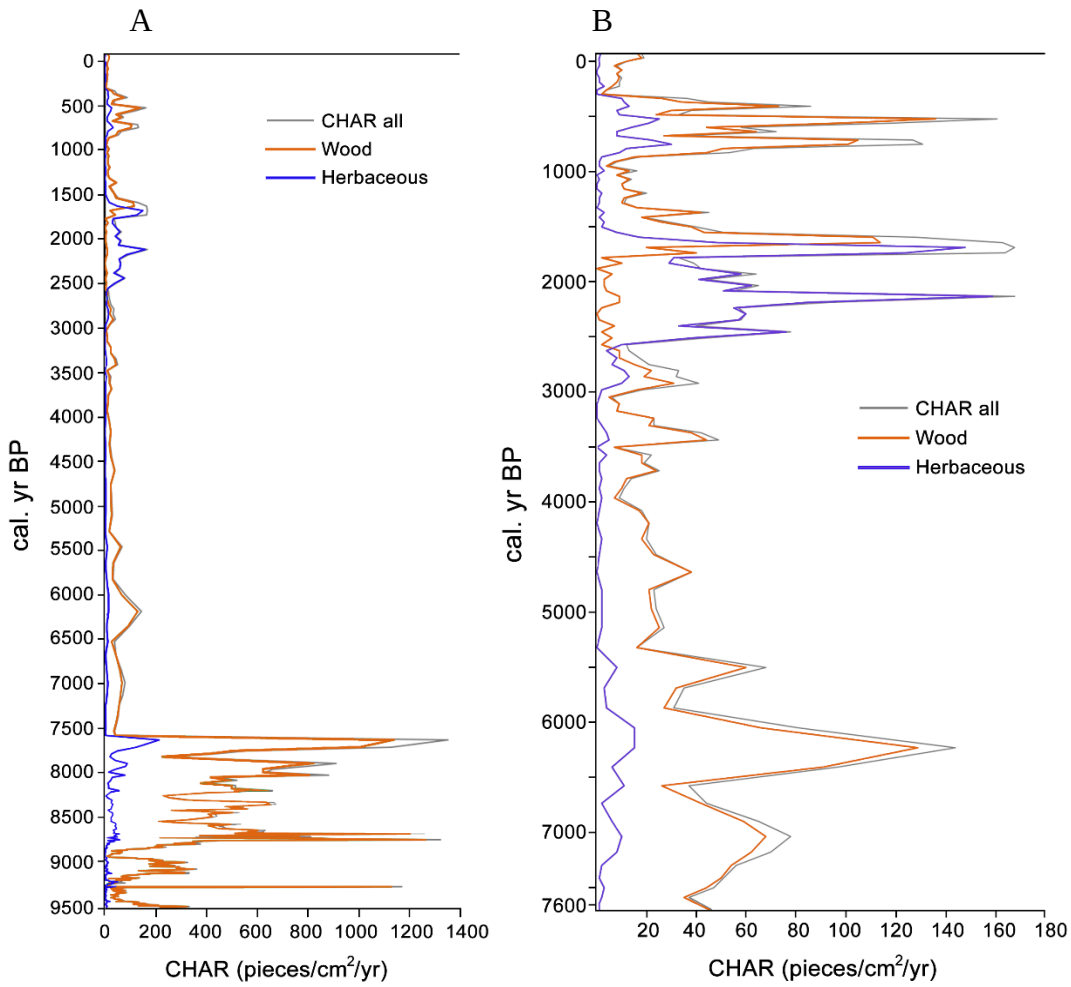

Figure 23. A) Charcoal accumulation rates for White Pine Marsh. B) Enlargement of the post-Mazama eruption tephra core section.

Both charcoal concentrations and accumulation rates are higher at WPMA than Dog Lake (Fig. 24), although post-Mazama fire intervals appear to be shorter at Dog Lake than WPMA. The timing of larger concentration events appears to be offset between WPMA and Dog Lake, with charcoal deposition at WPMA occurring previous to a large concentration event at Dog Lake.

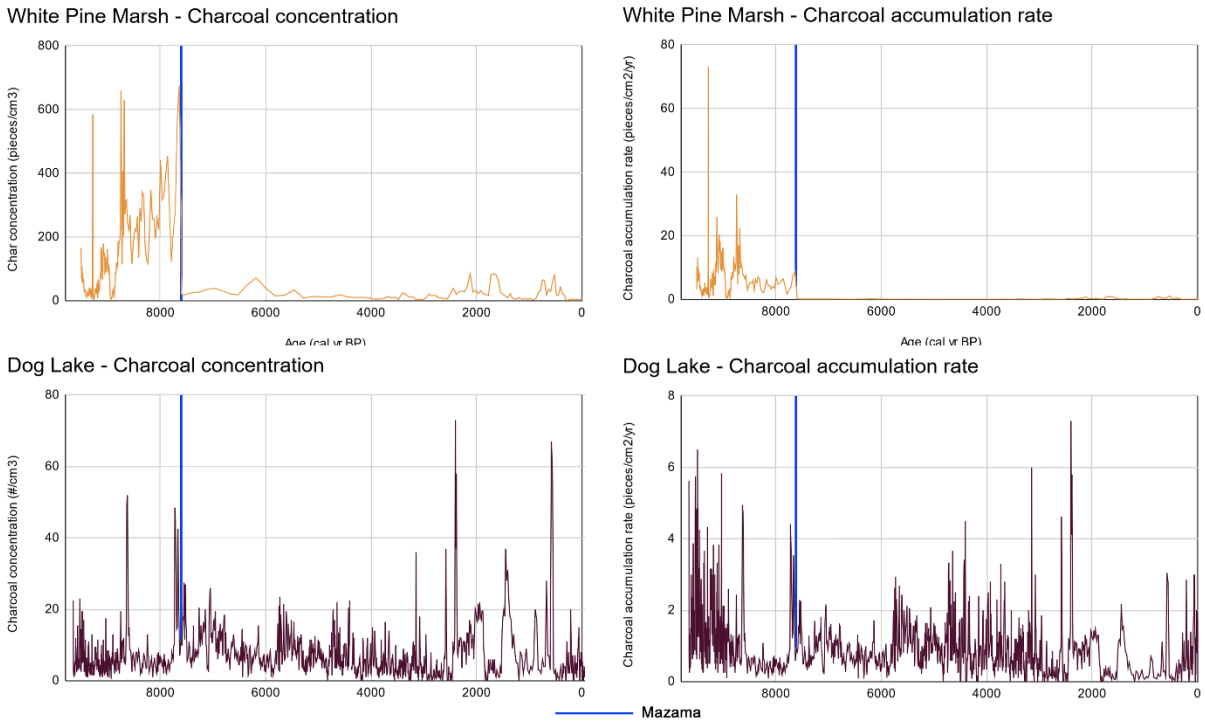

Figure 24. Charcoal concentrations and accumulation rates for White Pine Marsh and Dog Lake. Larger figure also in Appendix 38.

Tephra deposition at Dog Lake resulted in a decrease in charcoal concentrations and accumulations, similar to WPMA. Between 5700 to 3000 cal yr BP fires intervals are very short at Dog Lake (Fig. 24) in contrast to WPMA which saw overall much lower charcoal values.

4. DISCUSSION

The vegetative and sedimentation history of WPMA was heavily impacted by the Mazama eruption. The sediment record shows the development of a perennial marsh post-Mazama as a result of tephra added to the WPMA basin and raising the marsh floor by 30 cm. Sediments and vegetation covered the tephra, forming WPMA. Currently there is no evidence that the marsh has ever desiccated since 7640 cal yr BP. The sedimentation rate rose sharply

previous to 9000 cal yr BP to almost 0.0829 cm/yr, declining steeply until ca. 8300 cal yr BP leveling off somewhat at 8000 cal yr BP, then dropping post-Mazama and remaining very low at ca. 0.0022 cm/yr until 3700 cal yr BP, after which the sedimentation rate has increased slowly from 0.0030 to 0.0100 cm/yr current-day.

The pollen record shows abrupt changes resulting from the Mazama eruption. Trees increased slightly post-Mazama, primarily *Pinus,* but also *Abies* which went from <5% of the record to >6% for the remainder of the record. The conifer that fared poorly immediately following the tephra was *Pseudotsuga,* which persisted in the basin until ca. 2500 cal yr BP. *Tsuga* increased briefly immediately following the eruption but disappeared from the record by ca. 4000 cal yr BP. *Tsuga* is still present in the region, occasionally identified at lower elevations further south near Dog Lake. Cupressaceae never went above 2% post-Mazama, and even pre-Mazama Cupressaceae remained between 2-5%. *Alnus* is present in the earliest portion of the record but established itself in the basin between 3500 and 220 cal yr BP. *Populus tremuloides* has been consistently present in the WPMA basin for the entirety of the pollen 8900-year-long record. Mazama did not appear to affect *P. tremuloides,* between 6800 - 3300 cal yr BP a period of short fire intervals. Rosaceae, probably *Cercocarpus ledifolius*, was interrupted by the tephra down from 5% to <2% and recovering to >5% ca. 6000 cal yr BP. Poaceae thrived post-deposition, increasing up to >25% beginning at 6800 through to 2500 cal yr BP, after which it declined to ca 10%. Cyperaceae increased immediately post-deposition, going from 5% up to 10% for the remainder of the record.

Charcoal concentrations and accumulation rates were higher for WPMA and Dog Lake pre-Mazama eruption, with concentrations at WPMA higher than at Dog Lake, perhaps due to the smaller basin area of WPMA. Fire events were frequent at both WPMA and Dog Lake during

the early Holocene, with charcoal concentrations increasing steadily from 8800 to 7640 cal yr BP at WPMA, although Dog Lake went through a period where fires were less frequent or severe between 8700 and 8200 cal yr BP.

When comparing the synchrony of fire frequency post-Mazama between Dog Lake and WPMA the timing of higher charcoal concentrations appears staggered in time by 200-300 years, with WPMA experiencing concentration peaks before Dog Lake. This may be due to elevational climatic shifts, where the higher elevations see more rapid changes to vegetation and moisture patterns before lower elevations do.

An inverse pattern is clear in the early Holocene in that WPMA experienced long fire intervals and high-intensity fires, whereas Dog Lake experienced shorter fire intervals of perhaps more of medium to low intensity as a result of frequent fires. The difference may be due to the types of fuel at the two sites. At WPMA, conifers are present at the marsh edge with seasonally dry herbaceous fuel directly exposed to lightning and resulting in trees igniting easily. At Dog Lake, the trees were more distant to the lake edge, which was surrounded by wetlands. However, wider tree spacing at Dog Lake resulted in more herb and shrub vegetation than at WPMA, thus supporting a more frequent-fire regime.

Both WPMA and Dog Lake showed larger charcoal peaks previous to the Mazama tephra, with the contrast being peaks decreased after 8300 cal yr BP at Dog Lake while peaks increased up to the Mazama eruption at WPMA. Fire events were more frequent at Dog Lake, but charcoal peaks were larger at WPMA when they did occur. In comparison, Lily Lake, a small lake 47 km south of WPMA and at a similar elevation (2044 masl), has a charcoal record (Minckley et al., 2007) showing continuous fire throughout the Holocene, more similar to Dog Lake (1585 masl). Lily Lake receives slightly higher winter precipitation than WPMA (OSU-

PRISM), so it may be that although it is at the same elevation as WPMA, Lily Lake fires are climate-limited more akin to mid-elevation Dog Lake than fuel-limited like WPMA.

The dominant tree type at WPMA is currently *Pinus ponderosa*, although *Pinus contorta* is also present in far fewer numbers. This may indicate a fire history of infrequent medium severity fires or mixed severity. Mixed stands from the southern Cascades used fire-scars to determine fire frequency and severity over the last 400 years (Forrestel et al., 2017), with results showing mixed severity for mixed conifer forest types.

The continuous presence of *Populus tremuloides* may support this conclusion, as this is a disturbance-dependent species and the current population of seep-fed *P. tremuloides* on the south slope of WPMA basin are all of even age (C. Saban, personal observation), indicating a possible high severity fire resulting in *P. ponderosa* mortality. The area has been logged, as well, so it may also be that the *P. tremuloides* has populated a previously clear-cut area.

5. CONCLUSIONS

Several conclusions can be drawn from this research. First, fire regimens, vegetation history, and marsh hydrology of WPMA were all altered by tephra deposition from the eruption of Mount Mazama 7640 cal yr BP. The wetland became established at the time of the eruption, raising the marsh floor 25 cm in a single event. The charcoal, and pollen sequences all showed some reaction to the tephra deposition, but in the case of pollen, there is a lag of approximately 100 years in reaction timing.

Vegetation at WPMA pre-Mazama showed low pollen concentrations that began with high herbaceous counts and lower tree and shrub counts, shifting at ca. 8800 cal yr BP towards higher tree and shrub counts and lower herbaceous. This pattern stayed steady until 7640 cal yr

BP. There is a division in pollen assemblage composition within Zone 1 directly at 7640, but sum of squares analysis shows the primary division between Zone 1 & 2 at ca 3700 cal yr BP, a period of increased mesic conditions in the NGB. Herbaceous plants, including Poaceae, increased to their highest levels during the late Holocene between 2600 and 1700 cal yr BP. During this time herbaceous charcoal outnumbered wood charcoal, the only period in the core when this occurs.

Tephra may have had a profound effect on fire occurrence at WPMA. Tephra would have reduced grass and other herbaceous fuel availability resulted in longer fire intervals and higher intensity fires. We found this to be the opposite at Dog Lake, where fire was more frequent and of lower severity than at WPMA.

The inclusion of a fire-scar survey would help with late Holocene fire interpretations, however, much of the old-growth *P. ponderosa* has been logged since the turn of the century, so pollen and charcoal remain the best method for reconstructing past vegetation and fire patterns at WPMA.

CHAPTER IV

SUMMARY

The Paisley Caves are the low elevation NGB site (1380 masl) for this dissertation. The Paisley Caves study analyzed and contrasted pollen recovered from coprolites and from associated sediments to examine vegetation history and assess whether the coprolite pollen could provide unique information with respect to the coprolite producer, such as the use of specific habitats, foods, or water sources. We found that the dissimilarity of pollen assemblages between coprolites and associated sediments was greater than the serial dissimilarity between stratigraphically adjacent samples within either group. Serial dissimilarity within types was not greater for coprolites than sediments, as would be expected if there were unique pollen signatures derived from a short ingestion period of 1-2 days represented by each coprolite. Compared to the sediment pollen, the coprolites exhibited higher abundances of lighter pollen types and some individual samples were high in wetland taxa (particularly *Typha*). The results were consistent with coprolite pollen representing short time periods collected as a mammal moves on the landscape, whereas sediment pollen reflects longer time periods and more regional vegetation indicators.

Dog Lake is a perennial mid-elevation (1554 masl) freshwater lake located in south-central Oregon on the western periphery of the hydrologic Northern Great Basin. The 9600 year old landslide-formed lake has a current mean depth of approximately 6 m and is surrounded by extensive wetlands and is near the lower elevation limit of conifer forests. The 1282 cm long, highly organic sediment core was analyzed for δC, CMAR, δN, pollen and charcoal for the

purpose of understanding lake and fire history as well as detecting droughts during the Holocene. Periods of increased aridity were determined using indicators of lake level (aquatic macrophytes and sediment composition) and pollen assemblages. Lake levels between 1 - 3 m deep persisted between 9200 to 8700 cal yr BP, supporting the development of 122 cm of a dense algal mat. Between 8700 to 8200 cal yr BP the core materials shifted to show very shallow water and lower C:N indicating greater relative aquatic productivity, indicating a sluggish stream as opposed to a lake. High detrital silt input was also present due likely to increased dust resulting from severe regional drought and reduced terrestrial productivity.

The pollen assemblage record was synchronous with lake-level history (Hudson et al., 2020) by showing vegetation trending toward drier conditions previous to 8200 cal yr BP becoming more mesic after 8200 cal yr BP, with periods of high aridity at 5700 and 3700 cal yr BP. Fire activity was also low between 8700 and 8200 cal yr BP, consistent with reduced herbaceous vegetation. Following 8200 cal yr BP lake levels increased and silt levels declined, resulting in high planktonic productivity that persisted to present-day. Fires increased during the mid-Holocene between 6000 and 4000 cal yr BP, a period coinciding with cooler conditions in the NGB than the early Holocene, supporting fuel limitation of the fire regime at this site. Though low sedimentation rate after 2.0 ka greatly reduced the resolution of the charcoal record. While our findings matched well with other regional paleodrought findings, the timing of extreme drought present in the Northern Great Basin occurred several millennia earlier than that detected in eastern and Central Great Basin.

Charcoal was the primary material used to reconstruct the Holocene fire history of high-elevation White Pine Marsh (2050 masl) and to contrast WPMA fire history to mid-elevation Dog Lake fire history. Results found a reverse pattern of fire frequency between the two sites,

with the period between 10,000 to 7640 cal yr BP seeing increased biomass burn frequency at WPMA and very low fire frequency at Dog Lake during the same time period. The period following the eruption of Mount Mazama at 7640 cal yr BP saw biomass burning significantly reduced at WPMA compared to Dog Lake, which saw a significant increase in fire frequency.

Drought conditions were not clearly apparent through the sedimentary pollen at low-elevation Paisley Caves, and not at all in the coprolite pollen, but increased arid conditions were instead apparent through lake level studies (Cohen et al., 2001; Hudson et al., 2020), or through changes in human plant use as observable through paleoethnobotanical studies (Kennedy 2018). The fluctuations in vegetation types supported previous drought findings. Variability in species composition and fire history were in response to changes in precipitation at the middle elevation site of Dog Lake, while fuel availability was the primary fire limiter at high elevation site WPMA. Dog Lake is considered fuel limited as the upland herbs in the basin respond to changes in precipitation and increased fire frequencies were tied to increased precipitation (which produced more fuel), particularly during the middle-Holocene. White Pine Marsh, however, was likely climate-limited previous to 7640 cal yr BP, but became fuel-limited in response to post-Mazama tephra deposition, both by altering the soil of the area and in the formation of the marsh. In contrast, results from Lily Lake (2044 masl) 40 km south of WPMA (Minckley et al., 2007) showed Holocene fire event frequency more similar to that of Dog Lake than WPMA. Lily Lake experienced less tephra deposition than WPMA (Buckland et al., 2022), resulting in a more climate-limited fire regimen.

Early Holocene high aridity at Dog Lake resulted in upland herbaceous vegetation becoming much reduced, indicating low understory fuel availability. This perhaps in combination with too little moisture resulting in no convection storms resulted in fire frequency

and severity greatly reduced at Dog Lake between 8700 and 8200 cal yr BP. Fire events and severity were opposite at high-elevation White Pine Marsh, with fires increasing in frequency and severity up to the Mazama eruption. Middle Holocene conditions were generally cooler at all sites, with increased precipitation, resulting in increased fire events at mid-elevation sites, and very probably at high elevation sites with less tephra. Finally, drought conditions are apparent between 8700 to 8200 cal yr BP at mid- and high elevation sites, with less severe drought conditions at Dog Lake at 5100 and 3700 cal yr BP. This sets drought conditions as occurring earlier in the NGB than sites further south and east in the Great Basin. These changes could have influenced faunal and cultural activities.

This research would benefit further by plotting cultural activities in the NGB to identified drought timings. This study would also benefit by including more core sites within the NGB, as well as applying diatom and chironomid studies, especially during the late Pleistocene lake periods as I postulate that lake-effect off of the pluvial lakes such as Lake Chewaucan, Warner Lake, Alkalai Lake, Fort Rock Lake, and Goose Lake would have a measurable impact on local vegetation relative to drier areas of the NGB at that time. For the time being, locating suitable coring sites remains a challenge, but discovery of more sites with high resolution stratigraphy will improve the paleoenvironmental interpretations in the ecologically diverse Northern Great Basin.

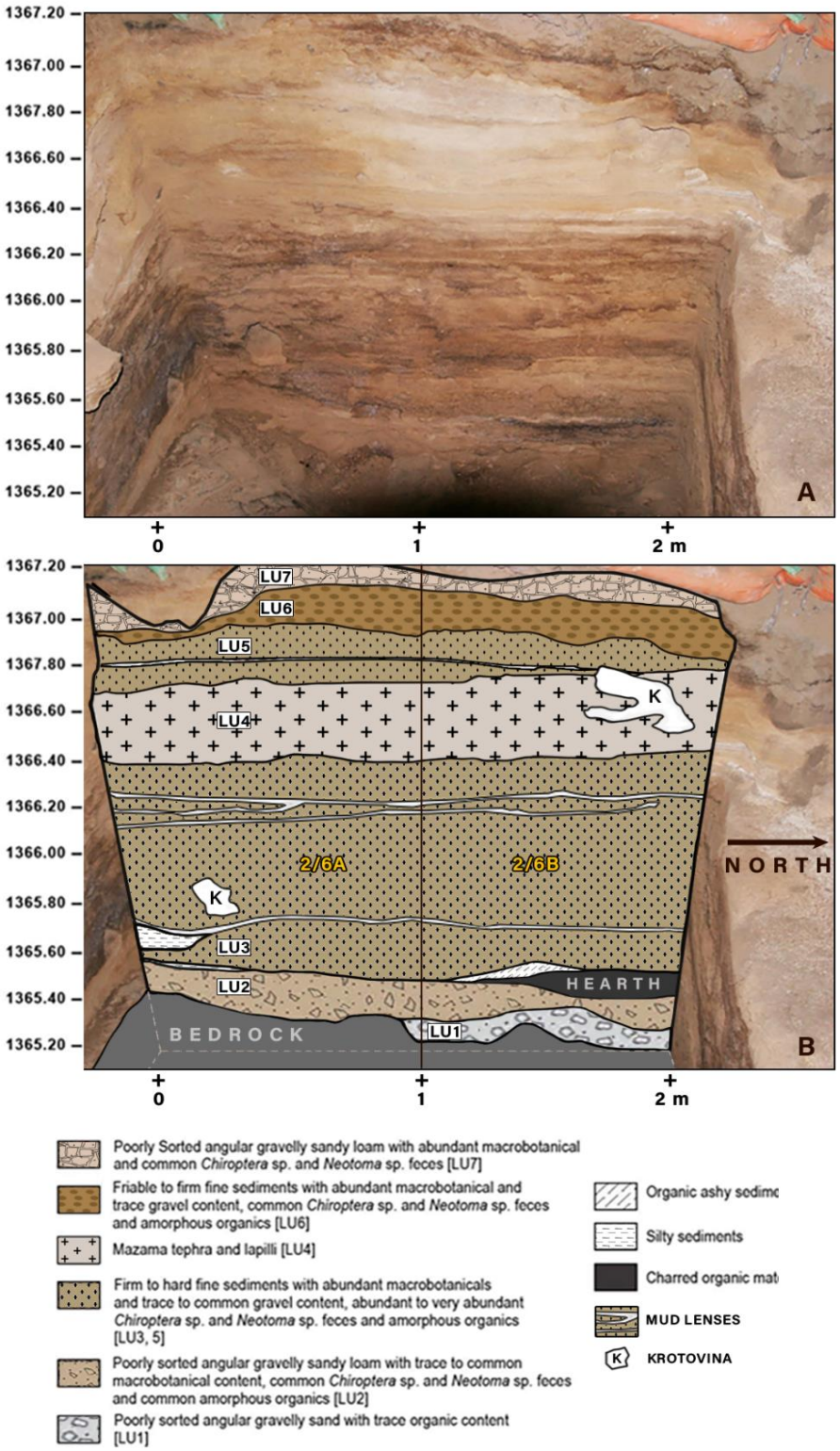

Figure 15. Paisley Caves west wall Figure 3 in text.

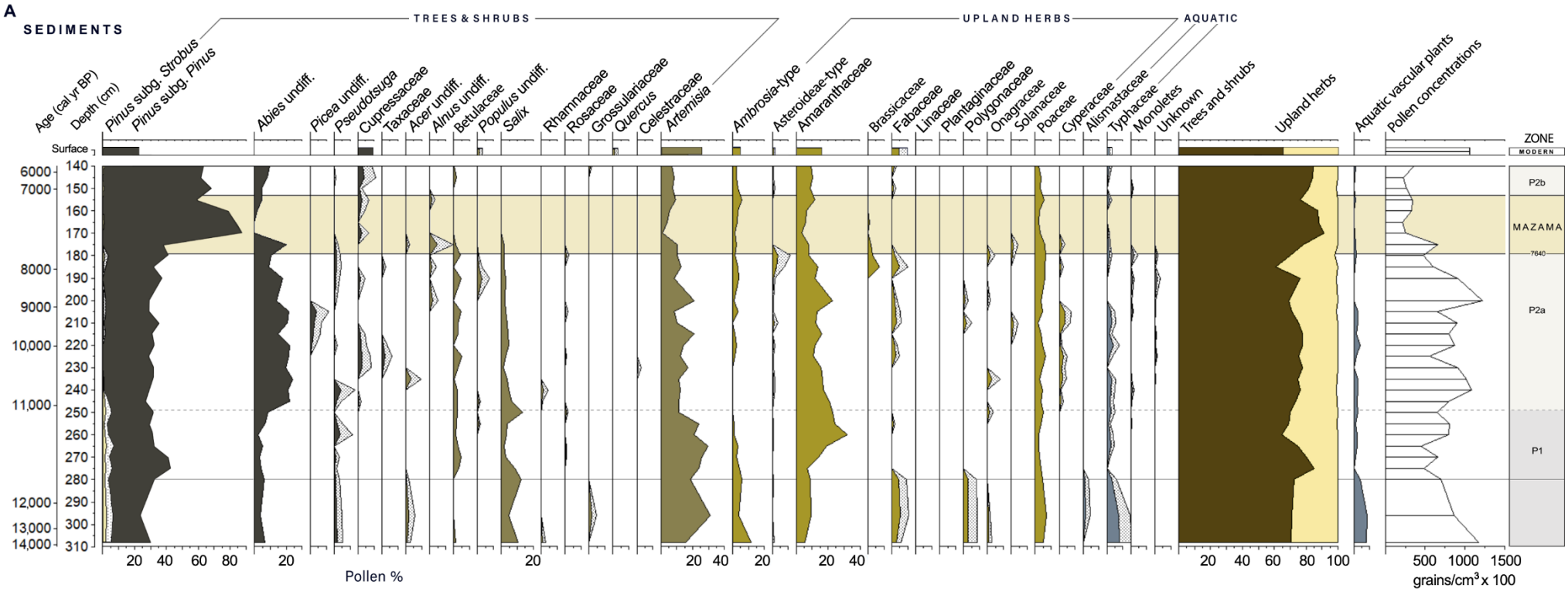

Figure 26. Sediment pollen diagram, Figure 6A in text.

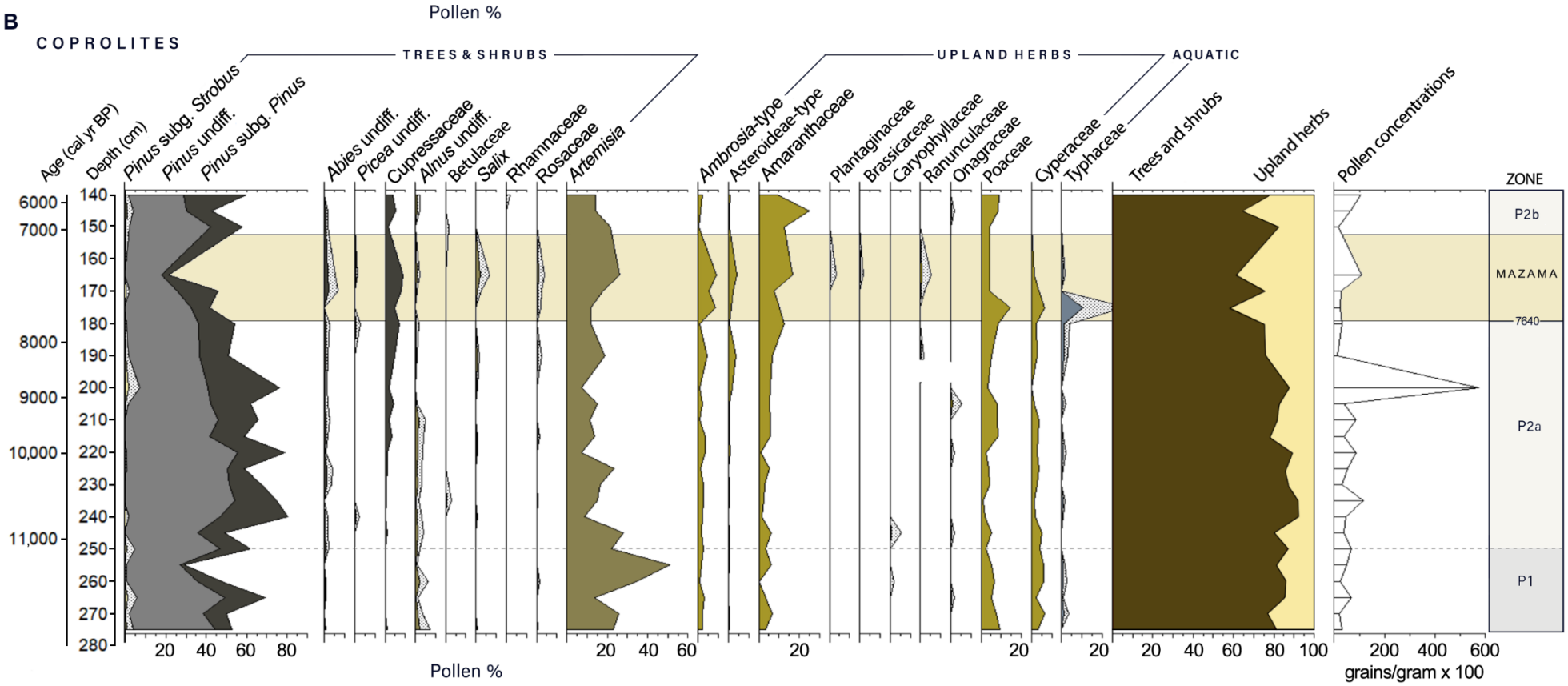

Figure 27. Coprolite pollen diagram, Figure 6B in text.

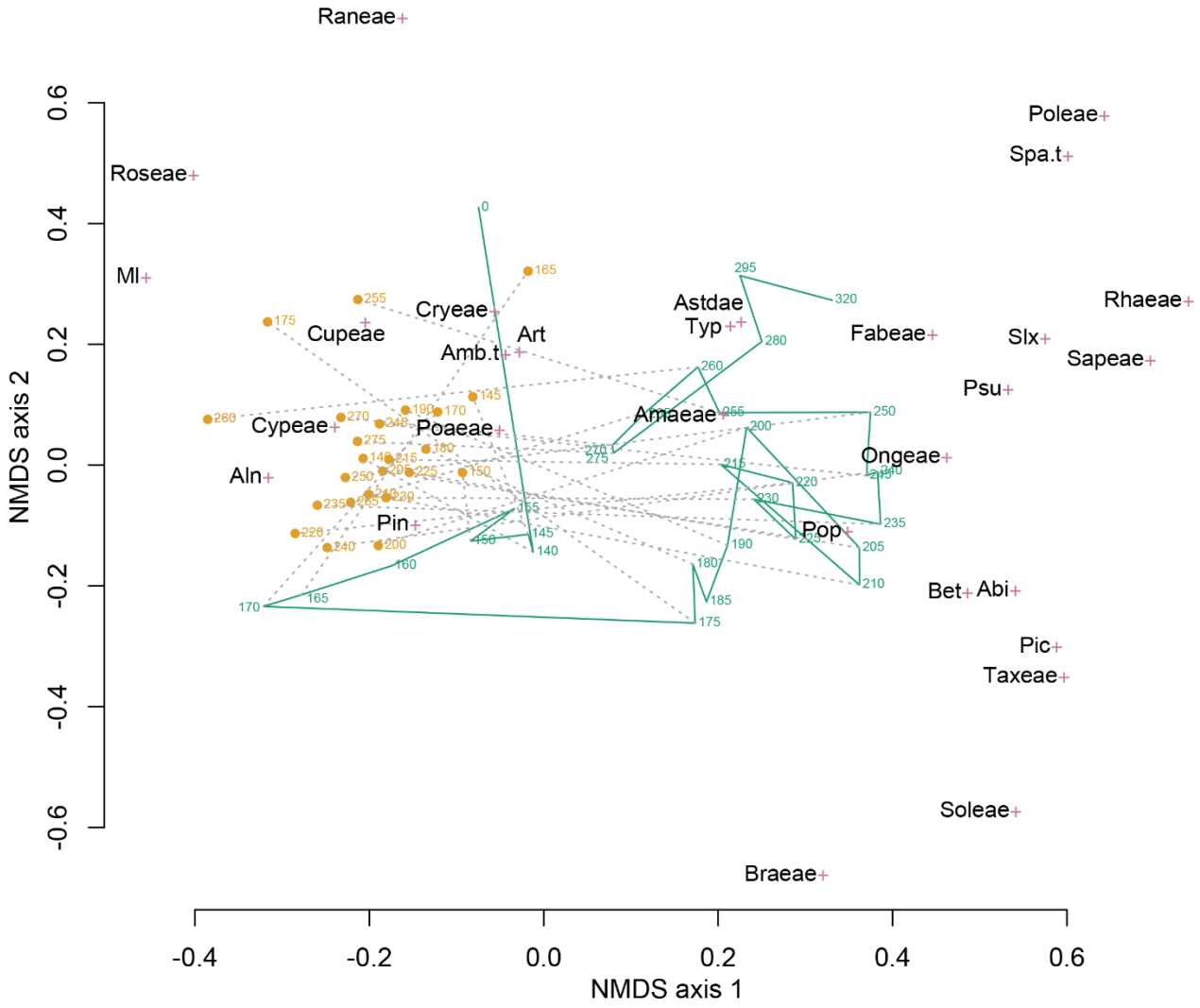

Figure 28. Non-metric multidimensional scaling (NMDS). From Figure 7 in text.

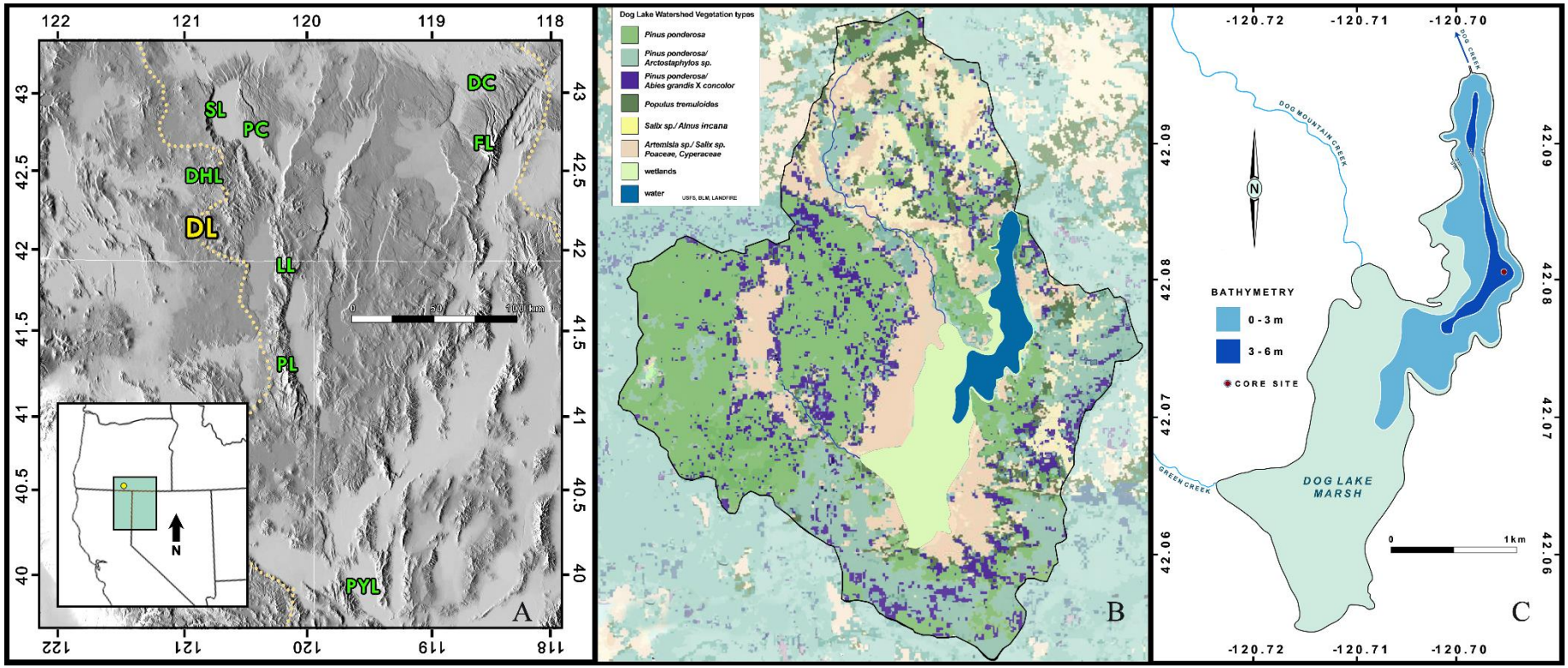

Figure 29. Maps Dog Lake from text Figure 10

Figure 30. Panoramas of Dog Lake from in text Figures 11A and B.

Figure 31. Dog Lake core.

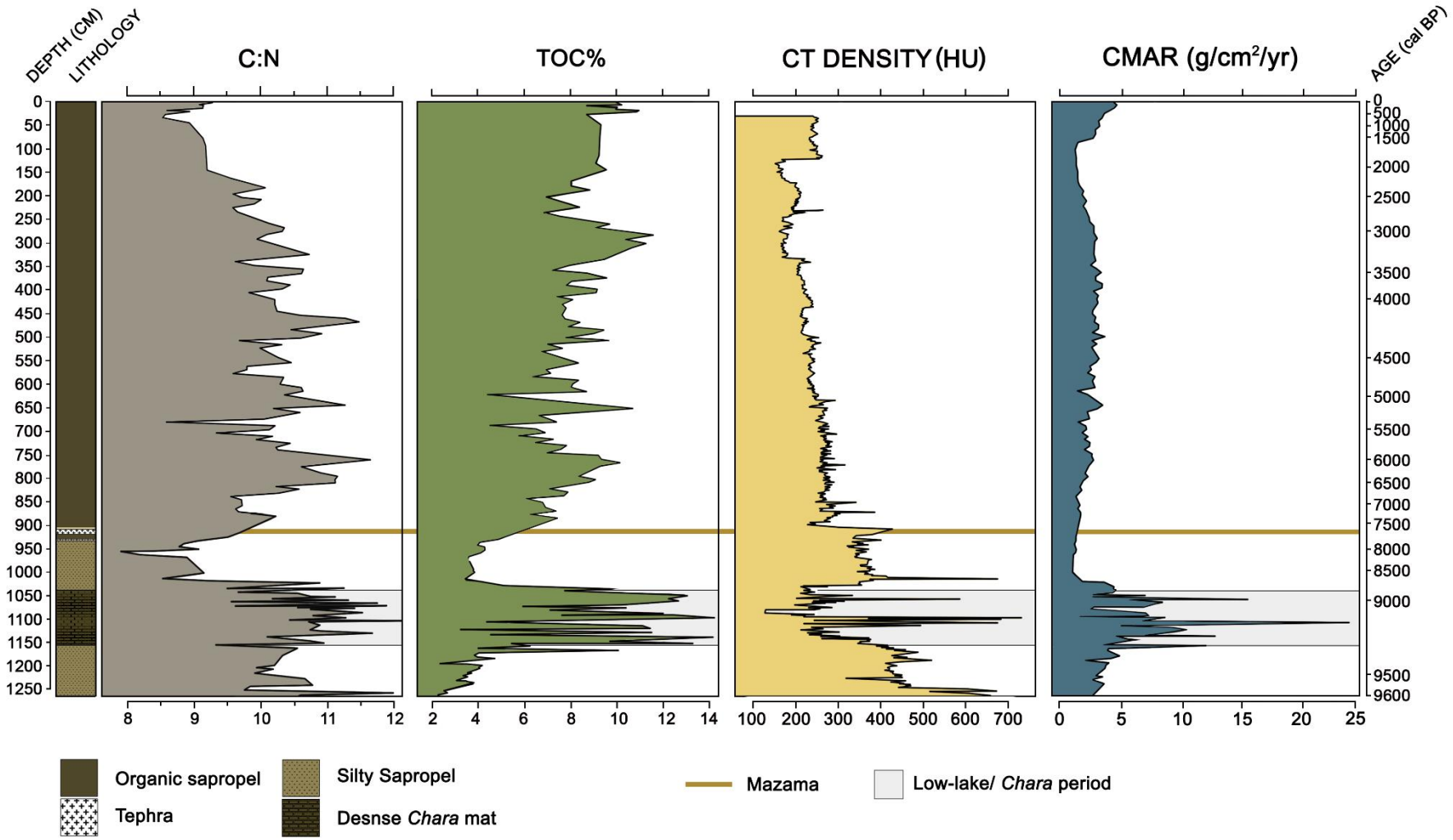

Figure 32. Lithology, C:N ratio, TOC, density and carbon mass accumulation rate (CMAR). From Dog Lake text Figure 12.

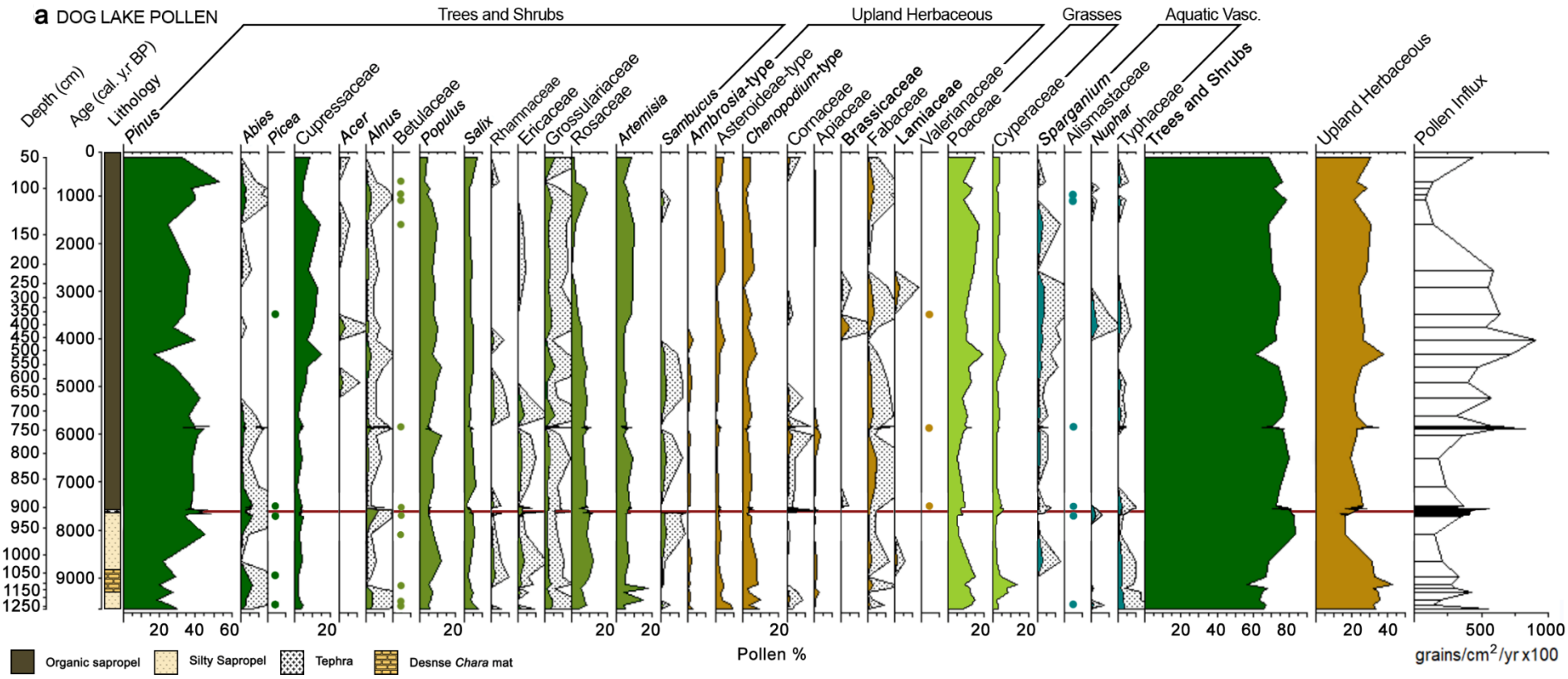

Figure 33. Dog Lake pollen with lithology. From text Figure 14A

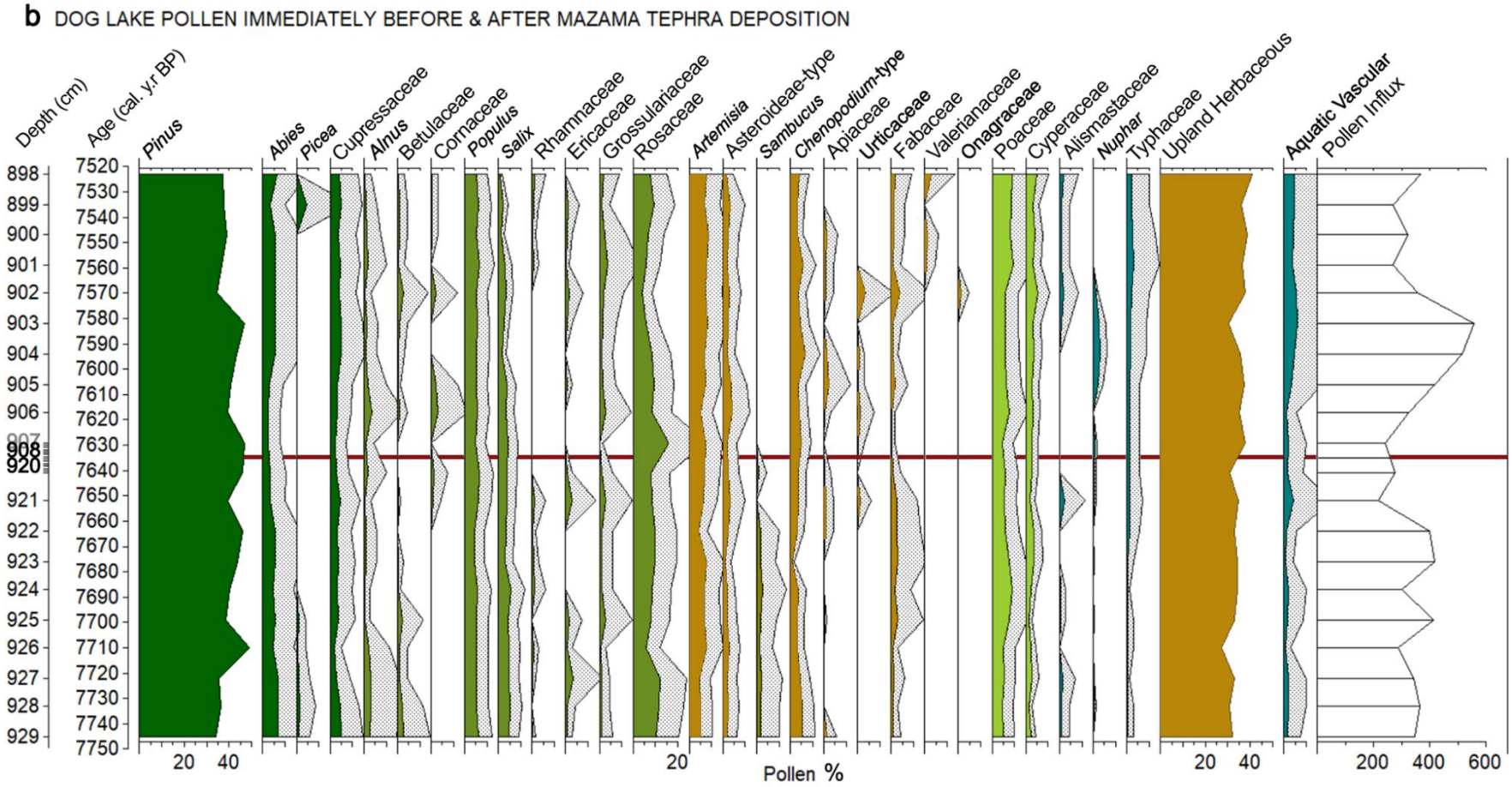

Figure 34. Dog Lake pollen before and after Mazama tephra deposition. No obvious changes from tephra deposition except for *Sambucus.* From text Figure 14B

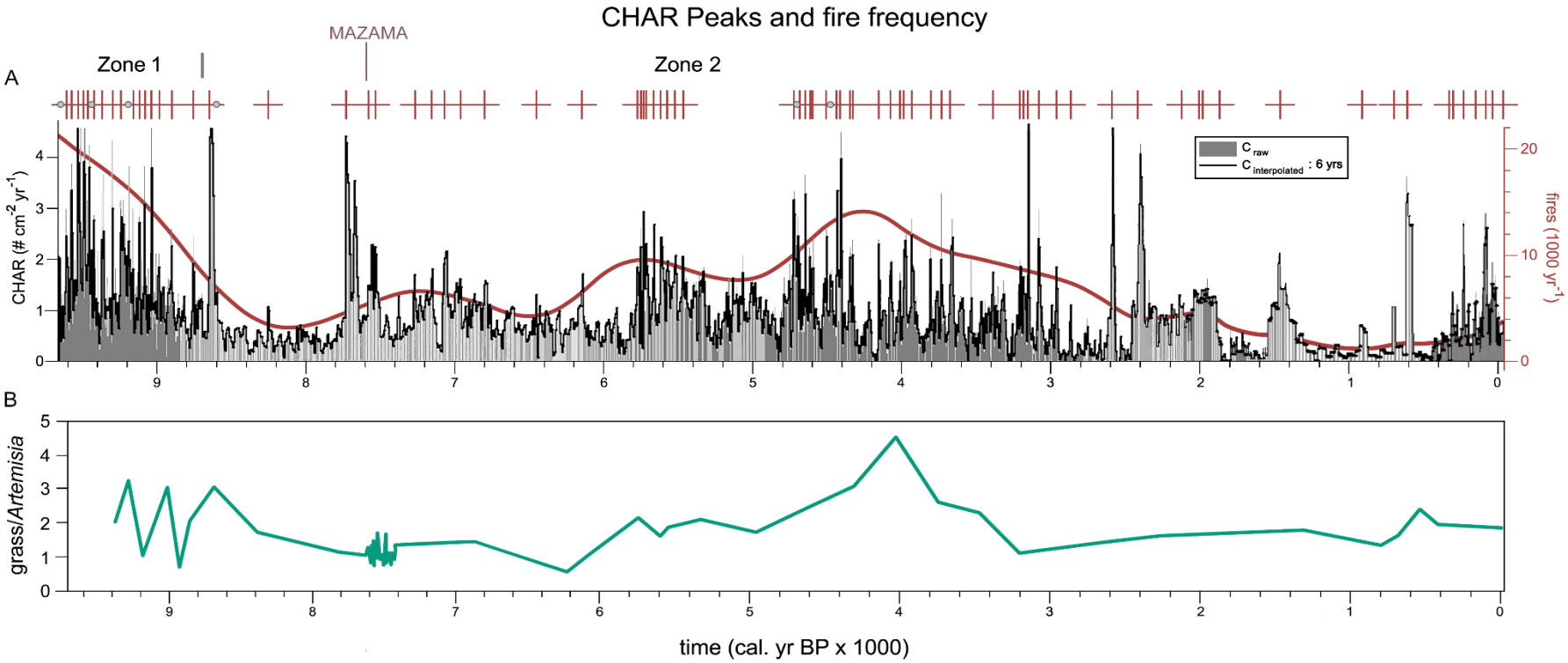

Figure 35. Peak frequency and B. Poaceae (grass)-*Artemisia* fuel ratio. From text Figure 15.

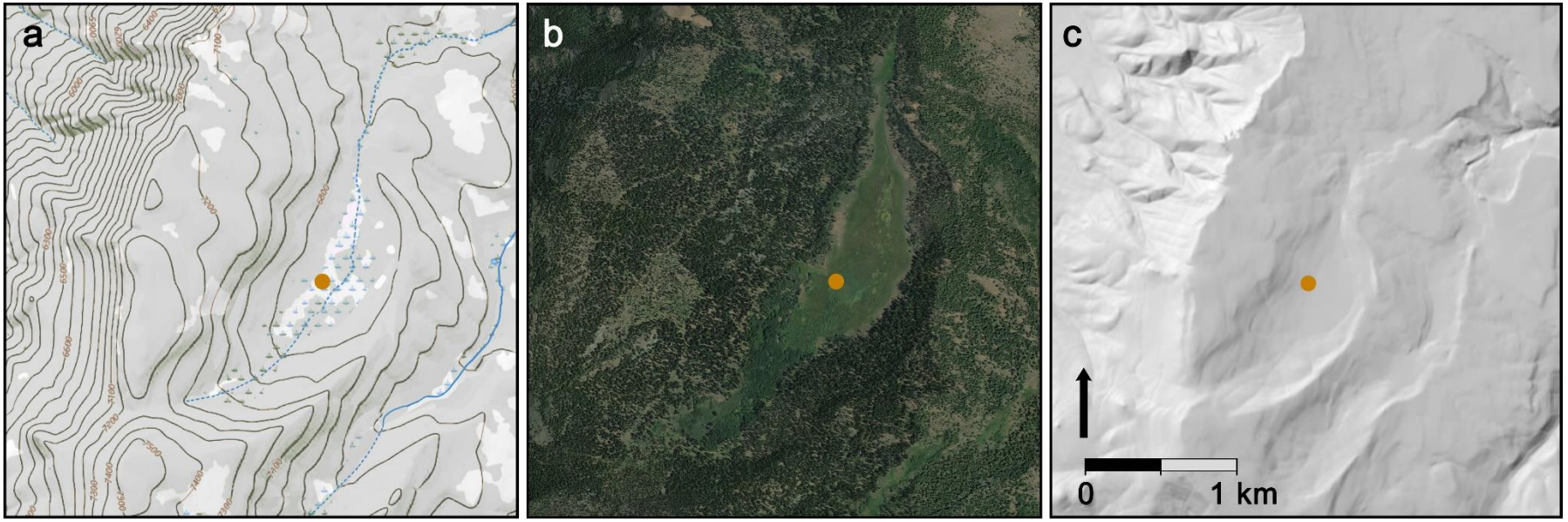

Figure 36. Three views of White Pine Marsh basin with coring site marked in orange. From in text Figure 17.

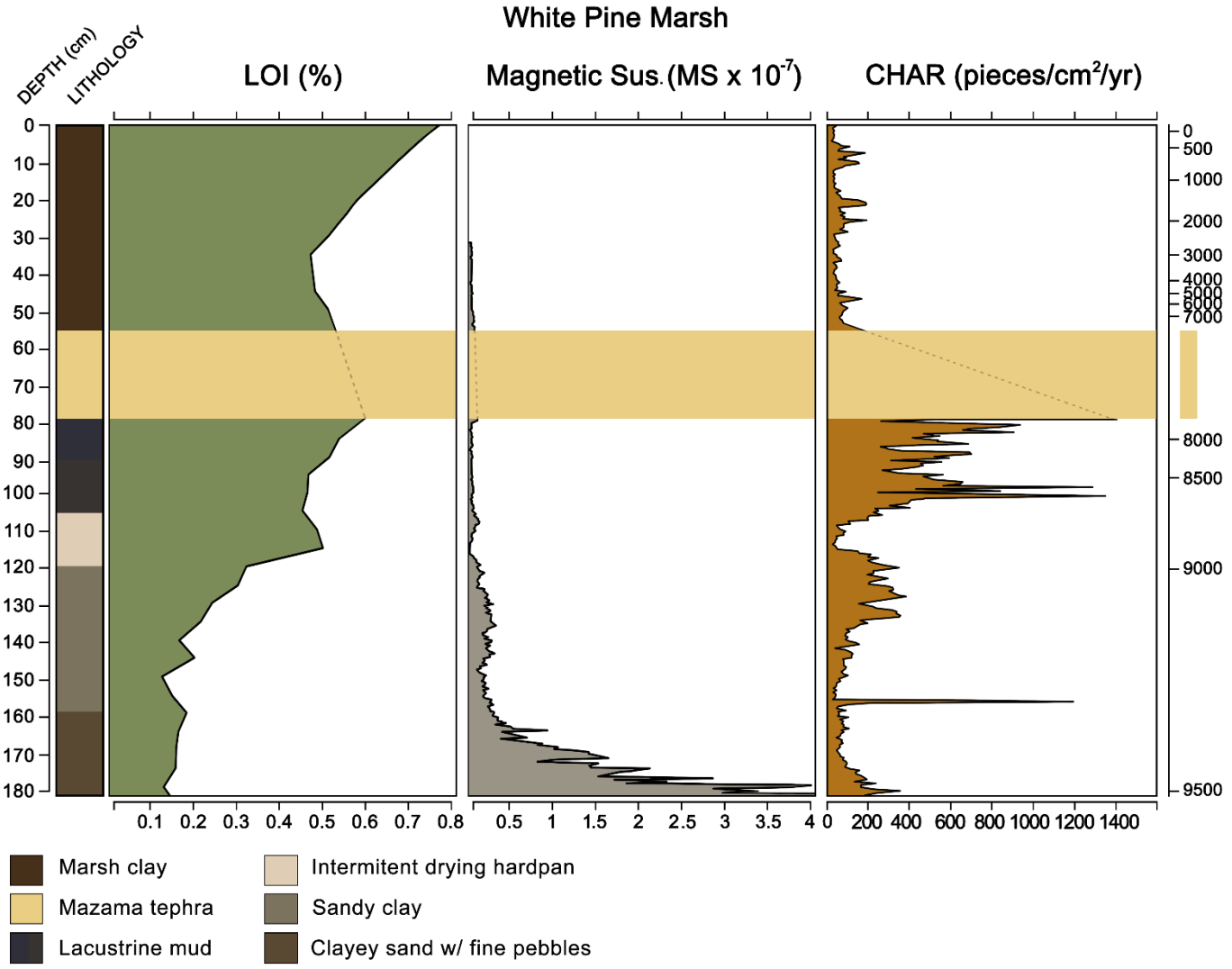

Figure 37. LOI, magnetic susceptibility and charcoal counts from White Pine Marsh. Yellow bar is Mazama tephra. From in text Figure 21

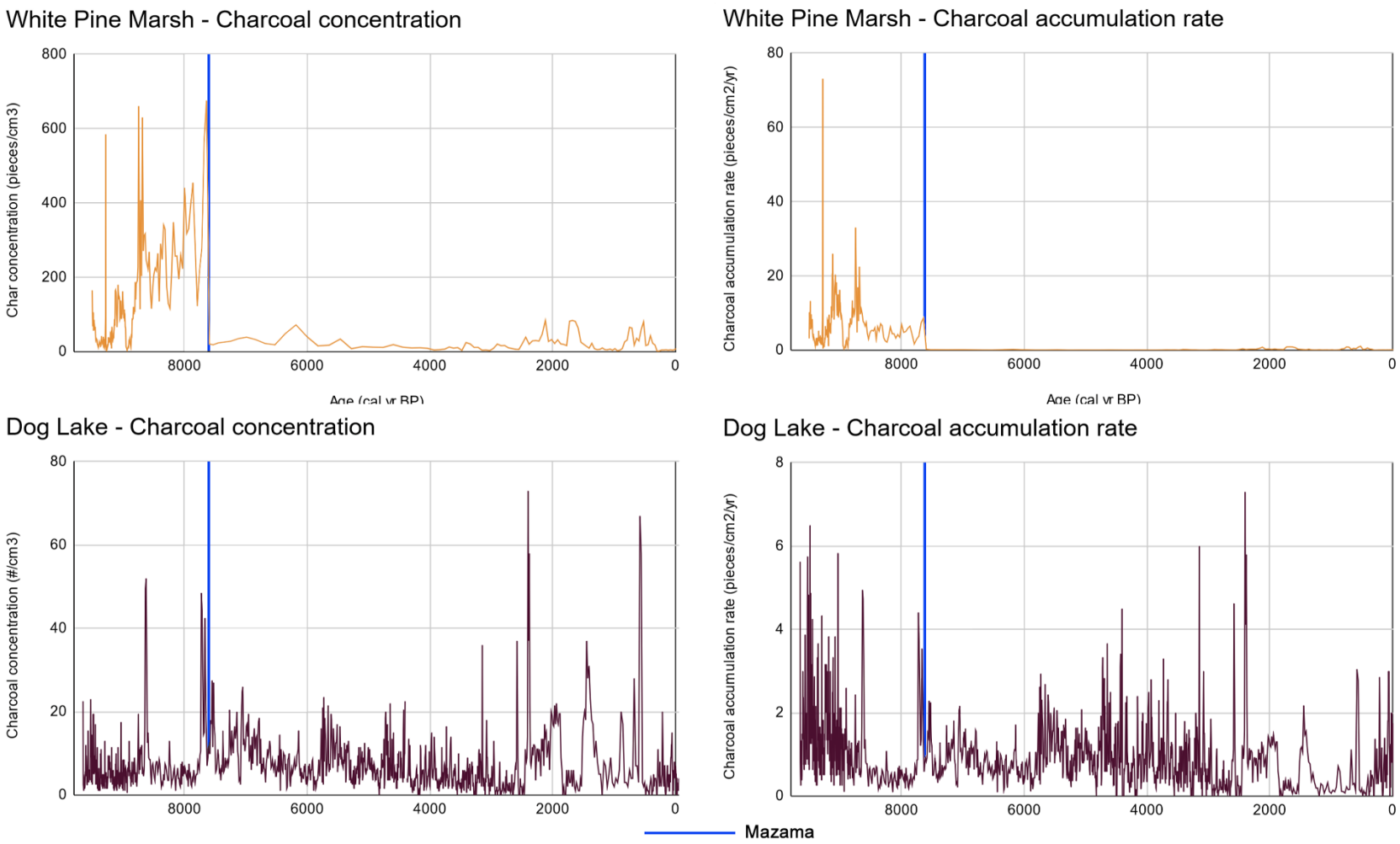

Figure 38. Charcoal comparison between White Pine Marsh and Dog Lake. From in text Figure 24.

REFERENCES CITED

Adams, K.D., & Rhodes, E.J., 2019. Late Pleistocene to present lake-level fluctuations at Pyramid and Winnemucca lakes, Nevada, USA. *Quaternary Research*, 92(1), 146–164. https://doi.org/10.1017/qua.2018.134

Adams, R.P., 2019. Juniperus of Canada and the United States: Taxonomy, key and distribution. *Lundellia* 21, 1–34. https://doi.org/10.25224/1097-993X-21.1

Allison, I.S., 1982. *Geology of pluvial Lake Chewaucan, Lake County, Oregon*. Oregon State University Press. Corvallis. ir.library.oregonstate.edu/xmlui/handle/1957/21983

Anderson, E.W., Borman, M.M., Krueger, W.C., 1998. *The Ecological Provinces of Oregon: A Treatise on the Basic Ecological Geography of the State*. Technical Report. Oregon Agricultural Experiment Station. Corvallis, Oregon.

Anderson, R.Y., 1955. Pollen analysis, a research tool for the study of cave deposits. *American Antiquity* 21, 84–85. https://doi.org/10.2307/276114

Arno, S.F., 2007. *Northwest Trees*. 2nd ed. Mountaineers Books. Seattle.

Anderson, P.M., Barnosky, C.W., Bartlein, P.J., Behling, P.J., Brubaker, L., Cushing, E.J., Dodson, J., Dwortesky, B., Guetter, P.J., Harrison, S.P., Huntley, B., Kutzbach, J.E., Markgraf, V., Marvel, R., McGlone, M.S., Mix, A., Moar, N.T., Morley, J., Perrott, R.A., Wright Jr, H.E., 1988. Climatic Changes of the Last 18,000 Years: Observations and Model Simulations. *Science*, 241(4869), 1043–1052. JSTOR.

Badger, T.C., Watters, R.J., 2004. Gigantic seismogenic landslides of Summer Lake basin, south-central Oregon. *Geological Society of America Bulletin* 116, 687–697. https://doi.org/10.1130/B25333.1

Bagnell, C.R., Jr., 1975. Species distinction among pollen grains of Abies, Picea, and Pinus in the rocky mountain area (A scanning electron microscope study). *Review of Palaeobotany and Palynology* 19, 203–220. https://doi.org/10.1016/0034-6667(75)90041-X

Baig, J., & Gavin, D.G., 2023. Vegetation and fire history with high-resolution analysis of tephra impacts in the High Cascade Range, Oregon. *Quaternary Science Reviews*, 303:107970.

Bartlein, P.J., Anderson, K.H., Anderson, P.M., Edwards, M.E., Mock, C.J., Thompson, R.S., Webb, R.S., Webb III, T., & Whitlock, C., 1998. Paleoclimate simulations for North America over the past 21,000 years: Features of the simulated climate and comparisons with paleoenvironmental data. *Quaternary Science Reviews*, 17(6), 549–585. https://doi.org/10.1016/S0277-3791(98)00012-2

Bartlein, P.J., Harrison, S.P., Brewer, S., Connor, S., Davis, B.A.S., Gajewski, K., Guiot, J., Harrison-Prentice, T.I., Henderson, A., Peyron, O., Prentice, I.C., Scholze, M., Seppa, H., Shuman, B., Sugita, S., Thompson, R.S., Viau, A.E., Williams, J., Wu, H., 2011. Pollen-based continental climate reconstructions at 6 and 21 ka: a global synthesis. *Climate Dynamics* 37, 775–802. https://doi.org/10.1007/s00382-010-0904-1

Beck, C.W., Bryant, V.M., Jenkins, D.L., 2018. Analysis of Younger Dryas—Early Holocene Pollen in Sediments of Paisley Cave 2, South-Central Oregon. *Palynology* 42(2), 168-169. https://doi.org/10.1080/01916122.2017.1319883

Beck, C.W., Bryant, V.M., Jenkins, D.L., 2020. Comparison of Neotoma (Packrat) Feces to Associated Sediments from Paisley Caves, Oregon, U.S.A. *Palynology* 44, 723–741. https://doi.org/10.1080/01916122.2019.1702118

Bennett, K.D., 1996. Determination of the number of zones in a biostratigraphic sequence. *New Phytologist* 132, 155–170. doi.org/10.1111/j.1469-8137.1996.tb04521.x

Benson, L., Burdett, J., Lund, S., Kashgarian, M., & Mensing, S., 1997. Nearly synchronous climate change in the Northern Hemisphere during the last glacial termination. *Nature*, 388(6639), Article 6639. https://doi.org/10.1038/40838

Benson, L., Kashgarian, M., Rye, R., Lund, S., Paillet, F., Smoot, J., Kester, C., Mensing, S., Meko, D., Lindström, S., 2002. Holocene multidecadal and multicentennial droughts affecting Northern California and Nevada. *Quaternary Science Reviews* 21, 659–682. https://doi.org/10.1016/S0277-3791(01)00048-8

Blaauw, M., Christen, J.A., 2011. Flexible paleoclimate age-depth models using an autoregressive gamma process. *Bayesian Analysis* 6, 457–474. doi.org/10.1214/11-BA618

Blong, J.C., Adams, M.E., Sanchez, G., Jenkins, D.L., Bull, I.D., Shillito, L.M., 2020. Younger Dryas and early Holocene subsistence in the Northern Great Basin: multiproxy analysis of coprolites from the Paisley Caves, Oregon, USA. *Archaeological and Anthropological Sciences* 12, 224. https://doi.org/10.1007/s12520-020-01160-9

Booth, R.K., Jackson, S.T., Forman, S.L., Kutzbach, J.E., Bettis, E.A., Kreigs, J., & Wright, D. K., 2005. A severe centennial-scale drought in midcontinental North America 4200 years ago and apparent global linkages. *The Holocene*, 15(3), 321–328. https://doi.org/10.1191/0959683605hl825ft

Briles, C.E., Whitlock, C., & Bartlein, P.J., 2005. Postglacial vegetation, fire, and climate history of the Siskiyou Mountains, Oregon, USA. *Quaternary Research*, 64(1), 44–56. https://doi.org/10.1016/j.yqres.2005.03.001

Brown, K.J., Clark, J.S., Grimm, E.C., Donovan, J.J., Mueller, P.G., Hansen, B.C.S., & Stefanova, I., 2005. Fire cycles in North American interior grasslands and their relation to prairie

drought. *Proceedings of the National Academy of Sciences*, 102(25), 8865–8870. https://doi.org/10.1073/pnas.0503621102

Bryant, V.M., 1974. Prehistoric diet in southwest Texas: The coprolite evidence. *American Antiquity* 39, 407–420. https://doi.org/10.2307/279430

Bryant, V.M., Jr., Holloway, R.G., 1983. The role of palynology in archaeology. *Advances in Archaeological Method and Theory* 6, 191–224. https://doi.org/www.jstor.org/stable/20210068

Bryant, V.M., Reinhard, K.J., 2012. Coprolites and archaeology: The missing links in understanding human health. In: Hunt, A.P., Milan, J., Lucas, S.G., Spielmann, J.A. (Eds.), *Vertebrate Coprolites, Bulletin 57*. New Mexico Museum of Natural History and Science, Albuquerque, pp. 379–387.

Buckland, H.M., Cashman, K.V., Engwell, S.L., Rust, A.C., 2020. Sources of uncertainty in the Mazama isopachs and the implications for interpreting distal tephra deposits from large magnitude eruptions. *Bulletin of Volcanology*,82(23). https://doi.org/10.1007/s00445-020-1362-1

Burns, R.M., and Honkala, B.H., 1990. Silvics Manual Volume 1-Conifers. Agriculture Handbook 654, Forest Service, United States Department of Agriculture, Washington DC. srs.fs.usda.gov/pubs/misc/ag_654/table_of_contents.htm

Carlson, A.E., 2013. Paleoclimate: The Younger Dryas Climate Event. In: Elias, S.A. (Ed.), *Encyclopedia of Quaternary Science vol. 3*, Elsevier, Amsterdam, pp. 126–134. doi.org/10.1016/B978-0-444-53643-3.00029-7

Carrión, J.S., Riquelme, J.A., Navarro, C., Munuera, M., 2001. Pollen in hyaena coprolites reflects late glacial landscape in southern Spain. *Palaeogeography, Palaeoclimatology, Palaeoecology* 176, 193–205. https://doi.org/10.1016/S0031-0182(01)00338-8

Carter, V.A., Brunelle, A., Minckley, T.A., Shaw, J.D., DeRose, R.J., Brewer, S., 2017. Climate variability and fire effects on quaking aspen in the central Rocky Mountains, USA. *Journal of Biogeography* 44, 1280–1293. https://doi.org/10.1111/jbi.12932

Chame, M., 2003. Terrestrial mammal feces: a morphometric summary and description. *Methods and Techniques* 98, 71–94. https://doi.org/10.1590/S0074-02762003000900014

Cohen, A., Palacios-Fest, M., Negrini, R., Wigand, P., & Erbes, D., 2000. A Paleoclimate Record for the Past 250,000 Years from Summer Lake, Oregon, USA: II. Sedimentology, Paleontology and Geochemistry. *Journal of Paleolimnology*, 24(2), 151–182. https://doi.org/10.1023/A:1008165326401

Cook, B.I., Smerdon, J.E., Cook, E.R., Williams, A.P., Anchukaitis, K.J., Mankin, J.S., Allen, K., Andreu-Hayles, L., Ault, T.R., Belmecheri, S., Coats, S., Coulthard, B., Fosu, B., Grierson, P., Griffin, D., Herrera, D.A., Ionita, M., Lehner, F., Leland, C., Wise, E.K., 2022.

Megadroughts in the Common Era and the Anthropocene. *Nature Reviews Earth & Environment*, 3(11), Article 11. https://doi.org/10.1038/s43017-022-00329-1

Cook, J.G., & Irwin, L.L., 1992. Climate-vegetation Relationships between the Great Plains and Great Basin. *The American Midland Naturalist*, 127(2), 316–326. https://doi.org/10.2307/2426538

Cowardin, L.M., Carter, V., Golet, F.C., & LaRoe, E.T., 1979. *Classification of Wetlands & Deepwater Habitats of the United States*. Fish and Wildlife Service, US Dept of the Interior.

Crawford, J.N., Mensing, S.A., Lake, F.K., & Zimmerman, S.R., 2015. Late Holocene Fire & Vegetation Reconstruction from the Western Klamath Mountains, California, USA: A Multi-disciplinary Approach for Examining Potential Human Land-use Impacts. *The Holocene*, 25(8), 1341–1357. https://doi.org/10.1177/0959683615584205

Cressman, L.S., 1940. Studies on Early Man in South Central Oregon. In: *Carnegie Institution of Washington Year Book No. 39*. Washington D.C.

Cronin, T.M., 2009. *Paleoclimates: Understanding Climate Change Past and Present*. Columbia University Press.

Cronquist, A., Holmgren, A.H., Holmgren, N.H., Reveal, J.L., 1972. *Intermountain Flora; Vascular Plants of the Intermountain West, U.S.A.* Hafner Publishing Company, New York Botanical Garden.

Dennis, L.R.J., & Halse, R.R., 2008. *Aquatic and Wetland Plants of Oregon with Vegetative Key* (1st ed.). Uncial Press. Beaverton.

Dennison-Budak, C.W., 2010. *Ostracodes as Indicators of the Paleoenvironment in the Pliocene Glenns Ferry Formation, Glenns Ferry Lake, Idaho*. Masters Thesis, Kent State University. https://etd.ohiolink.edu/acprod/odb_etd/ws/send_file/send?accession=kent1271442702&disposition=inline.

Dexter, J., & Saban, C.V., 2014. Assessing Late Pleistocene to Early Holocene diet breadth in the northern great basin through paleoethnobotanical analysis. Presented at the 79th Annual Meeting of the Society for American Archaeology, April 23–27, 2014, Austin, Texas.

Di Orio, A.P., Callas, R., & Schaefer, R.J., 2005. Forty-eight year decline and fragmentation of aspen (Populus tremuloides) in the South Warner Mountains of California. *Forest Ecology and Management*, 206(1), 307–313. https://doi.org/10.1016/j.foreco.2004.11.011

Dodson, S.I., 2005. *Introduction to Limnology* (1st ed.). McGraw-Hill.
Egan, J., Staff, R., & Blackford, J. 2015. A high-precision age estimate of the Holocene Plinian eruption of Mount Mazama, Oregon, USA. *The Holocene*, 25(7), 1054–1067. https://doi.org/10.1177/0959683615576230

Egger, A.E., Ibarra, D.E., Weldon, R., Langridge, R.M., Marion, B., Hall, J., 2021. Influence of pluvial lake cycles on earthquake recurrence in the northwestern Basin and Range, USA. In: Starratt, S.W., Rosen, M.R. (Eds.), *From Saline to Freshwater: The Diversity of Western Lakes in Space and Time*. Geological Society of America 1-28. https://doi.org/10.1130/2018.2536(07)

Euler, R.C., 1986. The Great Basin. In: D'Azevedo, W.L., Sturtevant, W.C. (Eds.), *Handbook of North American Indians*. Vol. 11, pp. .79, 474. Smithsonian Institution Press,. Washington, D.C.

Faegri, K., Kaland, P.E., & Krzywinski, K., 1989. *Textbook of Pollen Analysis* (4th ed.). Wiley.
Falk, D. A., Heyerdahl, E. K., Brown, P. M., Farris, C., Fulé, P. Z., McKenzie, D., Swetnam, T. W., Taylor, A. H., & Van Horne, M. L. 2011. Multi-scale controls of historical forest-fire regimes: New insights from fire-scar networks. *Frontiers in Ecology and the Environment*, 9(8), 446–454. https://doi.org/10.1890/100052

Forrestel, A. B., Andrus, R. A., Fry, D. L., & Stephens, S. L., 2017. Fire History and Forest Structure along an Elevational Gradient in the Southern Cascade Range, Oregon, USA. *Fire Ecology*, 13(1), Article 1. https://doi.org/10.4996/fireecology.1301001

Franklin, J.F., & Dyrness, C.T., 1973. *Natural Vegetation of Oregon and Washington*. Gen. Tech. Rep. PNW-GTR-008. U.S. Department of Agriculture, Forest Service, Pacific Northwest Research Station. 8(427). Oregon State University Press.
https://www.fs.usda.gov/treesearch/pubs/26203

Friedel, D.E., 1993. *Chronology and Climatic Controls of Late Quaternary Lake-level Fluctuations in Chewaucan, Fort Rock, and Alkali basins, South-central Oregon*. Dissertation. University of Oregon, Eugene.

Gasche, H., Tunca, Ö., 1983. Guide to Archaeostratigraphic Classification and Terminology: Definitions and Principles. *Journal of Field Archaeology* 10, 325–335. doi.org/10.2307/529547

Gavin, D.G., Hallett, D.J., Hu, F. S., Lertzman, K.P., Prichard, S.J., Brown, K.J., Lynch, J.A., Bartlein, P., & Peterson, D.L., 2007. Forest fire and climate change in western North America: Insights from sediment charcoal records. *Frontiers in Ecology and the Environment,* 5(9), 499–506. https://doi.org/10.1890/060161

Geologic Map of Oregon. 2023, June 6). [Maps]. Oregon Geology.
https://www.oregongeology.org/geologicmap/index.htm

Gilbert, M.T.P., Jenkins, D.L., Gotherstrom, A., Naveran, N., Sanchez, J.J., Hofreiter, M., Thomsen, P.F., Binladen, J., Higham, T.F.G., Yohe, R.M., Parr, R., Cummings, L.S., Willerslev, E., 2008. DNA from Pre-Clovis human coprolites in Oregon, North America. *Science* 320, 786–789. https://doi.org/10.1126/science.1154116

Grayson, D. K., 1993. *The Desert's Past: A Natural Prehistory of the Great Basin* (1st Edition. edition). Smithsonian.

Grayson, D. K., 2011. *The Great Basin: A Natural Prehistory*. University of California Press. http://ebookcentral.proquest.com/lib/uoregon/detail.action?docID=675858

Grigg, L.D., & Whitlock, C., 1998. Late-Glacial Vegetation and Climate Change in Western Oregon. *Quaternary Research,* 49(3), 287–298. https://doi.org/10.1006/qres.1998.1966

Grimm, E.C., 1987. CONISS: A FORTRAN 77 program for stratigraphically constrained cluster analysis by the method of incremental sum of squares. *Computers & Geosciences*, 13(1), 13–35. https://doi.org/10.1016/0098-3004(87)90022-7

Gruell, G.E., 1982. Fires' influence on vegetative succession—Wildlife habitat implications and management opportunities. *The Wildlife Society*, 43–50.

Gucker, C.L., 2006. Cercocarpus ledifolius (Fire Effects Information System, p. online). Forest Service, Rocky Mountain Research Station, *Fire Sciences Laboratory*. https://www.fs.usda.gov /database/feis/plants/tree/cerled/all.html

Heizer, R.F., 1969. Analysis of Human Coprolites from a Dry Nevada Cave. *Papers in Great Basin Archaeology*, California Archaeological Survey Report 70, 1–20.

Heizer, R.F., Napton, L.K., Dunn, F.L., Follett, W.I., Morbeck, M.E., Radovsky, F.J., Watkins, R., 1970. *Archaeology and the Prehistoric Great Basin Lacustrine Subsistence Regime as Seen from Lovelock Cave, Nevada.* Contributions of the University of California Archaeological Research Facility, 10. University of California. Berkeley. escholarship.org/uc/item/0p60j7gf

Hermann, N.W., Oster, J.L., & Ibarra, D.E., 2018. Spatial patterns and driving mechanisms of mid-Holocene hydroclimate in western North America. *Journal of Quaternary Science*, 33(4), 421–434. https://doi.org/10.1002/jqs.3023

Herweijer, C., Seager, R., Cook, E.R., & Emile-Geay, J., 2007. North American Droughts of the Last Millennium from a Gridded Network of Tree-Ring Data. *Journal of Climate*, 20(7), 1353–1376. https://doi.org/10.1175/JCLI4042.1

Heusser, C.J., Denton, G.H., Hauser, A., Andersen, B.G., Lowell, T.V., 1995. Quaternary pollen record from the Archipiélago de Chiloé in the context of glaciation and climate. *Revista Geolocica de Chile* 22, 25–46. doi.org/10.5027/andgeoV22n1-a02

Higuera, P.E., Gavin, D. G., Bartlein, P. J., & Hallett, D. J., 2010. Peak detection in sediment-charcoal records: Impacts of alternative data analysis methods on fire-history interpretations. *International Journal of Wildland Fire* 19(8) 996-1014 https://doi.org/10.1071/WF09134

Higuera, P.E., Peters, M. E., Brubaker, L. B., & Gavin, D.G., 2007. Understanding the origin and analysis of sediment-charcoal records with a simulation model. *Quaternary Science* Reviews, 26(13), 1790–1809. https://doi.org/10.1016/j.quascirev.2007.03.010

Hirschboeck, K.K., 1991. Hydrology of Floods and Droughts: Climate and Floods (National Water Summary 1988–89 — Hydrologic Events and Floods and Droughts 2375; US Geological Survey Water Supply Paper 2375, 65–88, pp. 65–88). USGS. https://doi.org/10.3133/wsp2375

Hitchcock, C.L., Cronquist, A., 2018. *Flora of the Pacific Northwest: An Illustrated Manual* 2nd Edition. University of Washington Press. Seattle.

Hofreiter, M., Poinar, H.N., Spaulding, W.G., Bauer, K., Martin, P.S., Possnert, G., Pääbo, S., 2000. A molecular analysis of ground sloth diet through the last glaciation. *Molecular Ecology* 9, 1975–1984. doi.org/10.1046/j.1365-294X.2000.01106.x

Hopkins, W.E., 1979. *Plant Associations of the Fremont National Forest* (Technical Report R6-ECOL-79–004; p. 145). USDA Forest Service Pacific Northwest Region

Howard, J.L., Aleksoff, K.C., 2000. *Abies grandis*. In: *Fire Effects Information System*, [Online]. U.S. Department of Agriculture, Forest Service, Rocky Mountain Research Station, Fire Sciences Laboratory (Producer). Available: https://www.fs.usda.gov /database/feis/plants/tree/abigra/all

Howard, J.L., 2018. *Fire regimes of quaking aspen communities of the Sierra Nevada and Southern Cascades*. FEIS USDA. Fire Effects Information System. https://www.fs.fed.us/database/feis/fire_regimes/Sierra_Nevada_quaking_aspen/all.html

Hudson, A.M., Hatchett, B.J., Quade, J., Boyle, D.P., Bassett, S.D., Ali, G., & De los Santos, M. G., 2019. North-south dipole in winter hydroclimate in the western United States during the last deglaciation. *Scientific Reports*, 9(1), 4826. https://doi.org/10.1038/s41598-019-41197-y

Hudson, A.M., Emery-Wetherell, M.M., Lubinski, P.M., Butler, V.L., Grimstead, D.N., & Jenkins, D.L., 2021. Reconstructing paleohydrology in the northwest Great Basin since the last deglaciation using Paisley Caves fish remains (Oregon, U.S.A.). *Quaternary Science Reviews*, 262, 106936. https://doi.org/10.1016/j.quascirev.2021.106936

Jenkins, D.L., Connolly, T.J., Aikens, C.M., 2004. Early and Middle Holocene archaeology in the Northern Great Basin: Dynamic natural and cultural ecologies. In: Jenkins, D.L., Connolly, T.J., Aikens, C.M. (Eds.), *Early and Middle Holocene Archaeology of the Northern Great Basin, University of Oregon Anthropological Papers 62*. Museum of Natural History and Department of Anthropology, University of Oregon, Eugene, pp. 1–20.

Jenkins, D.L., Davis, L.G., Stafford, T.W., Campos, P.F., Hockett, B., Jones, G.T., Cummings, L.S., Yost, C., Connolly, T.J., Yohe, R.M., Gibbons, S.C., Raghavan, M., Rasmussen, M., Paijmans, J.L., Hofreiter, M., Kemp, B. M., Barta, J. L., Monroe, C., Thomas, G.M., 2012. Clovis age western stemmed projectile points and human coprolites at the Paisley Caves. *Science* 337, 485–510. doi.org/10.1126/science.1218443

Jenkins, D.L., Davis, L.G., Stafford Jr, T., Campos, P.F., Connolly, T.J., Cummings, L.S., Hofreiter, M., Hockett, B., McDonough, K., Luthe, I., O'Grady, P.W., Swisher, M.E., White, F.,

Yates, B., Yohe II, R.M., Yost, C., Willerslev, E., 2013. Geochronology, archaeological context, and DNA at the Paisley Caves. In: Graf, K.E., Ketron, C.V., Waters, M.R. (Eds.), *Paleoamerican Odyssey*. Texas A and M Publishing, College Station, pp. 173–197.

Jenkins, D.L., Davis, L.G., Jr., Stafford, T.W., Jr., Connolly, T.J., Jones, G.T., Rondeau, M., Cummings, L.S., Hockett, B., McDonough, K., O'Grady, P.W., Reinhard, K.J., Swisher, M.E., White, F., Yohe II, R.M., Yost, C., Willerslev, E., 2016. Younger Dryas archaeology and human experience at the Paisley Caves in the northern Great Basin. In: Kornfeld, M., Huckell, B.B. (Eds.), *Stones, Bones, and Profiles: Exploring Archaeological Context, Early American Hunter-Gatherers, and Bison*. University Press of Colorado, Denver. pp. 127–205. doi.org/10.5876/9781607324539.C006

Johnson, D. M., Lycan, D. R., Petersen, R. R., Sweet, J. W., Neuhaus, M. E., & Schaedel, A. L., 1985. *Atlas of Oregon Lakes.* Oregon State University Press.

Kelso, G.K., 1971. *Hogup Cave, Utah: Comparative Pollen Analysis of Human Coprolites and Cave Fill.* M.A. Thesis. University of Arizona, Tuscon.

Kelso, G., Solomon, A., 2006. Applying modern analogs to understand the pollen content of coprolites. *Palaeogeography, Palaeoclimatology, Palaeoecology* 237, 80–91. doi.org/10.1016/j.palaeo.2005.11.036

Kennedy, J., 2018. *A Paleoethnobotanical Approach to 14,000 Years of Great Basin Prehistory: Assessing Human-Environmental Interactions Through the Analysis of Archaeological Plant Data at Two Oregon Rockshelters*. Ph.D. Dissertation. University of Oregon, Eugene. scholarsbank.uoregon.edu/xmlui/handle/1794/23918

Kovalchik, B.L., Chitwood, L.A., 1990. Use of geomorphology in the classification of riparian plant associations in mountainous landscapes of central Oregon. *Forest Ecology and Management* 33-34, 405–418. doi.org/10.1016/0378-1127(90)90206-Q

Kutzbach, J., Gallimore, R., Harrison, S., Behling, P., Selin, R., Laarif, F., 1998. Climate and biome simulations for the past 21,000 years. *Quaternary Science Reviews* 17, 473–506. https://doi.org/10.1016/S0277-3791(98)00009-2

Lanner, R.M., 1984. *Trees of the Great Basin: A Natural History*. University of Nevada Press. Reno.

Licciardi, J.M., 2001. Chronology of latest Pleistocene lake-level fluctuations in the pluvial Lake Chewaucan basin, Oregon, USA. *Journal of Quaternary Science* 16, 545–553. doi.org/10.1002/jqs.619 1

Long, C.J., Shinker, J.J., Minckley, T.A., Power, M.J., & Bartlein, P.J., 2019. A 7600 yr vegetation and fire history from Anthony Lake, northeastern Oregon, USA, with linkages to modern synoptic climate patterns. *Quaternary Research*, 91(2), 705–713. https://doi.org/10.1017/qua.2018.124

Long, C., Whitlock, C., Bartlein, P., & Millspaugh, S., 1998. A 9000-year fire history from the Oregon Coast Range, based on a high-resolution charcoal study. *Canadian Journal of Forest Research*, 28(5), 774–787. https://doi.org/10.1139/cjfr-28-5-774

Longland, W.S., Ostoja, S.M., 2013. Ecosystem services from keystone species: Diversionary seeding and seed-caching desert rodents can enhance Indian ricegrass seedling establishment. *Restoration Ecology* 2, 285–291. doi.org/10.1111/j.1526-100X.2012.00895.x

Loud, L.L., Harrington, M.R., 1929. *Lovelock Cave*. University of California Press. Berkeley. archive.org/details/LovelockCaveLoudAndHarrington1929

Lyle, M., Barron, J., Bralower, T.J., Huber, M., Olivarez Lyle, A., Ravelo, A.C., Rea, D.K., & Wilson, P.A., 2008. Pacific Ocean and Cenozoic evolution of climate. *Reviews of Geophysics*, 46(2). https://doi.org/10.1029/2005RG000190

Marlon, J.R., Bartlein, P.J., Walsh, M.K., Harrison, S.P., Brown, K.J., Edwards, M.E., Higuera, P.E., Power, M.J., Anderson, R.S., Briles, C., Brunelle, A., Carcaillet, C., Daniels, M., Hu, F.S., Lavoie, M., Long, C., Minckley, T., Richard, P.J.H., Scott, A.C., Field, C.B., 2009. Wildfire Responses to Abrupt Climate Change in North America. *Proceedings of the National Academy of Sciences of the United States of America*, 106(8), 2519–2524.

Mayewski, P.A., Meeker, L.D., Whitlow, S., Twickler, M.S., Morrison, M.C., Alley, R.B., Bloomfield, P., Taylor, K., 1993. The atmosphere during the Younger Dryas. *Science* 261, 195–197. doi.org/10.1126/science.261.5118.195

McDonough, K., Luthe, I., Swisher, M.E., Jenkins, D.L., O'Grady, P., White, F., 2012. ABCs at the Paisley Caves: Artifact, Bone, and Coprolite Distributions in Pre-Mazama Deposits. *Current Archaeological Happenings in Oregon* 37, 7–12.

McDonough, K.N., 2019. Middle Holocene menus: Dietary reconstruction from coprolites at the Connley Caves, Oregon, USA. *Archaeological and Anthropological Sciences*, 11(11), 5963–5982. https://doi.org/10.1007/s12520-019-00828-1

McDonough, K., Kennedy, J., Rosencrance, R., Holcomb, J., Jenkins, D.L., Puseman, K., 2022. Expanding Paleoindian diet breadth: Paleoethnobotany of Connley Cave 5, Oregon, USA. *American Antiquity* 87, 303–332. doi.org/10.1017/aaq.2021.141

Mehringer, P., 1986. Prehistoric Environments. In: D'Azevedo, W.L., Sturtevant, W.C. (Eds.), *Handbook of North American Indians Vol. 11*. Smithsonian Institution Press. Washington D.C., pp. 31–50.

Mehringer, P.J., Arno, S.F., Petersen, K.L., 1977. Postglacial History of Lost Trail Pass Bog, Bitterroot Mountains, Montana. *Arctic and Alpine Research* 9, 345–368. doi.org/10.2307/1550528

Mehringer, P. J., 1987. *Late Holocene environments on the northern periphery of the Great Basin:*

Final report. Report to the Bureau of Land Management, Oregon State Office. Pullman, Wash.: Departments of Anthropology and Geology, Washington State University. http://archive.org/details/lateholoceneenvi9157mehr

Mehringer, P.J., & Wigand, P.E., 1986. Holocene History of Skull Creek Dunes, Callow Valley, Southeastern Oregon, U.S.A. *Journal of Arid Environments*, 11, 117–138.

Mensing, S.A., Benson, L.V., Kashgarian, M., & Lund, S., 2004. A Holocene pollen record of persistent droughts from Pyramid Lake, Nevada, USA. *Quaternary Research*, 62(1), 29–38. https://doi.org/10.1016/j.yqres.2004.04.002

Mensing, S., Smith, J., Burkle Norman, K., & Allan, M., 2008. Extended drought in the Great Basin of western North America in the last two millennia reconstructed from pollen records. *Quaternary International*, 188(1), 79–89. https://doi.org/10.1016/j.quaint.2007.06.009

Mensing, S.A., Sharpe, S.E., Tunno, I., Sada, D.W., Thomas, J.M., Starratt, S., Smith, J., 2013. The Late Holocene Dry Period: Multiproxy evidence for an extended drought between 2800 and 1850 cal yr BP across the Central Great Basin, USA. *Quaternary Science Reviews* 78, 266–282. doi.org/10.1016/j.quascirev.2013.08.010

Meyers, P.A., & Teranes, J.L., 2001. Sediment Organic Matter. In W. M. Last & J. P. Smol (Eds.), *Tracking Environmental Change Using Lake Sediments: Physical and Geochemical Methods*. 2(239–269). Kluwer Academic Publishers. 10.1007/0-306-47669-X

Miller, R.F., Rose, J.A., 1995. Historic Expansion of *Juniperus occidentalis* (western juniper) in Southeastern Oregon. *The Great Basin Naturalist* 55, 37–45. jstor.org/stable/41712862

Miller, R.F., & Rose, J.A., 1999. Fire History and Western Juniper Encroachment in Sagebrush Steppe. *Journal of Range Management*, 52(6), 550–559. https://doi.org/10.2307/4003623
Minckley, T. A., Whitlock, C., & Bartlein, P. J. 2007. Vegetation, fire, and climate history of the northwestern Great Basin during the last 14,000 years. *Quaternary Science Reviews*, 26(17–18), 2167–2184. https://doi.org/10.1016/j.quascirev.2007.04.009

Minckley, T.A., Bartlein, P.J., Whitlock, C., Shuman, B.N., Williams, J.W., Davis, O.K., 2008. Associations among modern pollen, vegetation, and climate in western North America. *Quaternary Science Reviews* 27, 1962–1991. doi.org/10.1016/j.quascirev.2008.07.006

Mitchell, V.L., 1976. The regionalization of climate in the western United States. *Journal of Applied Meteorology* 15, 920–927. doi.org/10.1175/1520-0450(1976)015<0920:TROCIT>2.0.CO;2

Mohr, J.A., Whitlock, C., & Skinner, C.N., 2000. Postglacial vegetation and fire history, eastern Klamath Mountains, California, USA. *The Holocene*, 10(5), 587–601. https://doi.org/10.1191/095968300675837671

Mudie, P.J., Marret, F., Aksu, A.E., Hiscott, R.N., Gillespie, H., 2007. Palynological evidence for climatic change, anthropogenic activity and outflow of Black Sea water during the late Pleistocene and Holocene: Centennial-to decadal-scale records from the Black and Marmara Seas. *Quaternary International* 167–168, 73–90. doi.org/dx.doi.org/10.1016/j.quaint.2006.11.009

North, M., Collins, B., Safford, H., & Stephenson, N.L., 2016. *Montane Forests*. In H. Mooney, E. Zavaleta, & M. C. Chapin (Eds.), Ecosystems of California (1st ed., pp. 553–557). University of California Press. https://www.jstor.org/stable/10.1525/j.ctv1xxzp6

Northwest Alliance for Computational Science & Engineering. 2016. PRISM Climate Group OSU: Explorer. http://prism.oregonstate.edu/

Nowak, C.L., Nowak, R.S., Tausch, R.J., Wigand, P.E., 1994. Tree and shrub dynamics in northwestern Great Basin woodland and shrub steppe during the late-Pleistocene and Holocene. *American Journal of Botany* 81, 265–277. https://doi.org/10.2307/2445452

Oksanen, J., Blanchet, F.G., Kindt, P., McGlinn, D., Minchin, P.R., O'Hara, R.B., Simpson, G. L., Solymos, P.M., Stevens, H.H., Szoecs, E., Wagner, H., 2020. *vegan: Community Ecology Package* (2.5-7). CRAN.R-project.org/package=vegan

Orr, E.L., Orr, W.N., 2012. *Oregon Geology*. 6th ed. Oregon State University Press. Corvallis.

Osmond, C.B., Hidy, G.M., Pitelka, L.F., 1990. *Plant Biology of the Basin and Range*. Ecological Studies, vol. 80. Springer. link.springer.com/book/10.1007/978-3-642-74799-1

Pearsall, D.M., 2016. *Paleoethnobotany: A Handbook of Procedures*. 3rd ed. Routledge. New York, NY.

Pilliod, D.S., Welty, J.L., & Arkle, R.S., 2017. Refining the cheatgrass–fire cycle in the Great Basin: Precipitation timing and fine fuel composition predict wildfire trends. *Ecology and Evolution*, 7(19), 8126–8151. https://doi.org/10.1002/ece3.3414

Rasmussen, S.O., Bigler, M., Blockley, S.P., Blunier, T., Buchardt, S.L., Clausen, H.B., Cvijanovic, I., Dahl-Jensen, D., Johnsen, S.J., Fischer, H., Gkinis, V., Guillevic, M., Hoek, W. Z., Lowe, J.J., Pedro, J.B., Popp, T., Seierstad, I.K., Steffensen, J.P., Svensson, A.M., Winstrup, M., 2014. A stratigraphic framework for abrupt climatic changes during the Last Glacial period based on three synchronized Greenland ice-core records: Refining and extending the INTIMATE event stratigraphy. *Quaternary Science Reviews* 106, 14–28. doi.org/10.1016/j.quascirev.2014.09.007

Reimer, P.J., Austin, W.E.N., Bard, E., Bayliss, A., Blackwell, P.G., Ramsey, C.B., Butzin, M., Cheng, H., Edwards, R. L., Friedrich, M., Grootes, P.M., Guilderson, T.P., Hajdas, I., Heaton, T. J., Hogg, A.G., Hughen, K.A., Kromer, B., Manning, S. W., Muscheler, R., Talamo, S., 2020. The IntCal20 northern hemisphere radiocarbon age calibration curve (0–55 cal kBP). *Radiocarbon* 62, 725–757. doi.org/10.1017/RDC.2020.41

Reinemann, S.A., Porinchu, D.F., Bloom, A.M., Mark, B.G., Box, J.E., 2009. A multi-proxy paleolimnological reconstruction of Holocene climate conditions in the Great Basin, United States. *Quaternary Research* 72, 347–358. doi.org/10.1016/j.yqres.2009.06.003

Riley, T., 2008. Diet and seasonality in the Lower Pecos: Evaluating coprolite data sets with cluster analysis. *Journal of Archaeological Science* 35, 2726–2741. doi.org/10.1016/j.jas.2008.04.022

Quigley, T.M. (Ed.)., 1999. *Linking vegetation patterns and landscape vulnerability to potential insect and pathogen disturbances* (General Technical Report PNW-GTR-458; Historical and Current Forest and Range Landscapes in the Interior Columbia River Basin and Portions of the Klamath and Great Basins, Part I, p.388). Department of Agriculture, Forest Service, Pacific Northwest Research Station. https://www.fs.usda.gov/pnw/pubs/pnw_gtr458.pdf

Reilly, B.T., Stoner, J. S., & Weist, J., 2017. SedCT: MATLAB tool for standardized and quantitative processing of sediment core computed tomography (CT) data collected using a medical CT scanner [Computer software]. Geochemistry, Geophysics, Geosystems. doi:10.1002/2017GC006884

Reimer, P.J., Austin, W.E.N., Bard, E., Bayliss, A., Blackwell, P. G., Ramsey, C.B., Butzin, M., Cheng, H., Edwards, R.L., Friedrich, M., Grootes, P.M., Guilderson, T.P., Hajdas, I., Heaton, T. J., Hogg, A.G., Hughen, K. A., Kromer, B., Manning, S.W., Muscheler, R., Talamo, S., 2020. The IntCal20 Northern Hemisphere Radiocarbon Age Calibration Curve (0–55 cal kBP). *Radiocarbon*, 62(4), 725–757. https://doi.org/10.1017/RDC.2020.41

Reinemann, S.A., Porinchu, D. F., Bloom, A.M., Mark, B.G., & Box, J.E., 2009. A multi-proxy paleolimnological reconstruction of Holocene climate conditions in the Great Basin, United States. *Quaternary Research*, 72(3), 347–358. https://doi.org/10.1016/j.yqres.2009.06.003

Rhodes, A.N., 1998. A method for the preparation and quantification of microscopic charcoal from terrestrial and lacustrine sediment cores. *The Holocene*, 8(1), 113–117. https://doi.org/10.1191/095968398671104653

Saban, C.V., 2015. *Palynological Perspectives On Younger Dryas to Early Holocene Human Ecology At Paisley Caves, Oregon.* Masters Thesis, Oregon State University, Corvallis. https://ir.library.oregonstate.edu/concern/graduate_thesis_or_dissertations/2801pk70d

Schnurrenberger, D., Russell, J., & Kelts, K., 2003. Classification of lacustrine sediments based on sedimentary components. *Journal of Paleolimnology*, 29(2), 141–154. https://doi.org/10.1023/A:1023270324800

Schwörer, C., Gavin, D.G., Walker, I.R., & Hu, F.S., 2017. Holocene tree line changes in the Canadian Cordillera are controlled by climate and topography. *Journal of Biogeography*, 44(5), 1148–1159. https://doi.org/10.1111/jbi.12904

Sea, D.S., & Whitlock, C., 1995. Postglacial vegetation history of the high Cascade Range, central Oregon. *Quaternary Research*, 43, 370–381.

Shillito, L-M., Bull, I.D., Matthews, W., Almond, M.J., Williams, J.M., Evershed, R.P., 2011. Biomolecular and micromorphological analysis of suspected faecal deposits at Neolithic Çatalhöyük, Turkey. *Journal of Archaeological Science* 38, 1869–1877. doi.org/10.1016/j.jas.2011.03.031

Shillito, L-M., Blong, J.C., Green, E.J., & van Asperen, E.N., 2020. The what, how, and why of archaeological coprolite analysis. *Earth-Science Reviews* 207, 103196. doi.org/10.1016/j.earscirev.2020.103196

Shinker, J. 2010. Visualizing Spatial Heterogeneity of Western U.S. Climate Variability. *Earth Interactions*. 14(10). https://doi.org/10.1175/2010EI323.1

Shuman, B., Henderson, A. K., Colman, S. M., Stone, J. R., Fritz, S. C., Stevens, L. R., Power, M. J., & Whitlock, C., 2009. Holocene lake-level trends in the Rocky Mountains, U.S.A. *Quaternary Science Reviews*, 28(19), 1861–1879. https://doi.org/10.1016/j.quascirev.2009.03.003

Smith, S. J., 1998. *Processing Pollen Samples from Archaeological Sites in the Southwestern United States: An Example of Differential Recovery from Two Heavy Liquid Gravity Separation Proceedures.* New Developments in Palynomorphic Sampling, Extraction and Analysis, 29–34. American Association of Stratigraphic Palynologists Foundation.

Sowers, T., Bender, M., 1995. Climate records covering the last deglaciation. *Science* 269, 210–214. doi.org/10.1126/science.269.5221.210

Spooner, I.S., Barnes, S., Baltzer, K.B., Raeside, R., Osborn, G.D., Mazzucchi, D., 2003. The impact of air mass circulation dynamics on Late Holocene paleoclimate in northwestern North America. *Quaternary International* 108, 77–83. doi.org/10.1016/S1040-6182(02)00196-9

St. Louis, M., 2021. *Summer Lake Wildlife Area Management Plan*. State Wildlife Management Assessment. Oregon Department of Fish and Wildlife. dfw.state.or.us/wildlife/management_plans/wildlife_areas/docs/2021_SLWA%20Management%20Plan_Revision%20Final%20Draft.pdf

Stein, J.K., 1987. Deposits for Archaeologists. *Advances in Archaeological Method and Theory*, 11, 337–395. doi.org/128.223.129.241

Thomas, D.H., Davis, J.O., Grayson, D.K., Melhorn, W.N., Thomas, T., Trexler, D.T., Adovasio, J.M., Andrews, R.L., Bennyhoff, J.A. Bierwirth, S.L., Casteel, R.W., Hattori, E.M., Hughes, R.E., Kautz, R.R., Kramer, K., Lanner, R.M., Mayer, D., Mead, J.I., Rhode, D., Williams, L.R., 1983. *The Archaeology of Monitor Valley 2, Gatecliff Shelter*. Anthropological Papers of the American Museum of Natural History, 59. doi.org/hdl.handle.net/2246/267

Thompson, R.S., Whitlock, C., Bartlein, P.J., Harrison, S.P., & Spaulding, W.G., 1993. In H. E. Wright, J.E. Kutzbach, T. Webb, W.F. Ruddiman, F.A. Street-Perrott, & P. J. Bartlein (Eds.), *Global Climates since the Last Glacial Maximum*. (468–513). University of Minnesota Press. http://www.jstor.org/stable/10.5749/j.ctttsqhb.21

Thompson, R.S., 1996. Pliocene and early Pleistocene environments and climates of the western Snake River Plain, Idaho. *Marine Micropaleontology* 27, 141–156. doi.org/10.1016/0377-8398(95)00056-9

Thompson, R., Clark, R.M., Boulton, G.S., 2012. Core Correlation. In: Birks, H., Lotter, A., Juggins, S., Smol, J. (eds) Tracking Environmental Change Using Lake Sediments. *Developments in Paleoenvironmental Research*, vol 5. Springer, Dordrecht. https://doi-org.uoregon.idm.oclc.org/10.1007/978-94-007-2745-8_13

USDA Web Soil Survey. Soil Survey Staff, Natural Resources Conservation Service, United States Department of Agriculture. Official Soil Series Descriptions. Accessed April 12, 2023.

Vacco, D., Clark, P., Mix, A., Cheng, H., Edwards, R., 2005. A speleothem record of Younger Dryas cooling, Klamath Mountains, Oregon, USA. *Quaternary Research* 64, 249–256. doi.org/10.1016/j.yqres.2005.06.008

Vale, T.R., 1977. Forest Changes in the Warner Mountains, California. *Annals of the Association of American Geographers*, 67(1), 28–45.

Walker, G.W., 1963. Reconnaissance geologic map of the eastern half of the Klamath Falls (AMS) quadrangle, Lake and Klamath Counties, Oregon. Map 3565; *Mineral Investigations Field Studies Map* MF-260). USGS; https://doi.org/10.3133/mf260. https://pubs.er.usgs.gov/publication/mf260

Walsh, M.K., Whitlock, C., & Bartlein, P.J., 2008. A 14,300-year-long record of fire–vegetation–climate linkages at Battle Ground Lake, southwestern Washington. *Quaternary Research*, 70(2), 251–264. https://doi.org/10.1016/j.yqres.2008.05.002

Walsh, M.K., Whitlock, C., & Bartlein, P.J., 2010. 1200 years of fire and vegetation history in the Willamette Valley, Oregon, and Washington, reconstructed using high-resolution macroscopic charcoal and pollen analysis. *Palaeogeography, Palaeoclimatology, Palaeoecology*, 297(2), 273–289. https://doi.org/10.1016/j.palaeo.2010.08.007

White, W.B., 2007. *Cave Sediments and Paleoclimate*. Journal of Cave and Karst Studies, 69(1), 76–93. caves.org/pub/journal/PDF/v69/cave-69-01-76.pdf

Wigand, P.E., 1987. Diamond Pond, Harney County, Oregon: Vegetation history and water table in the eastern Oregon desert. *Great Basin Naturalist*, 47, 427–458. scholarsarchive.byu.edu/gbn/vol47/iss3/7

Wigand, P.E., Rhode, D., 2002. Great Basin Vegetation History and Aquatic Systems: The Last 150,000 Years. In: Herschler, R., Madsen, D.B., Currey, D.R. (Eds.), *Great Basin Aquatic Systems History.* Smithsonian Institution Press. Washington D.C., pp. 309–367. loc.gov/catdir/toc/fy036/2002026685.html

Williams-Dean, G., and Bryant, V.M., 1975. *Pollen Analysis of Human Coprolites from Antelope House.* Kiva, 41(1), 97–111. jstor.org/stable/30246610

Wolf, EC., & Cooper, D.J., 2015. Fens of the Sierra Nevada, California, USA: patterns of distribution and vegetation. Mires and Peat, 15(8), 1–22.

Wood, J.R., Wilmshurst, J.M., 2012. Wetland soil moisture complicates the use of *Sporormiella* to trace past herbivore populations. *Journal of Quaternary Science* 27, 254–259. doi.org/10.1002/jqs.1539

Wood, J.R., Wilmshurst, J.M., 2016. A protocol for subsampling Late Quaternary coprolites for multi-proxy analysis. *Quaternary Science Reviews* 138, 1–5. Doi.org/10.1016/j.quascirev.2016.02.018

Wood, J.R., Wilmshurst, J.M., Wagstaff, S.J., Worthy, T.H., Rawlence, N.J., Cooper, A., 2012. High-resolution coproecology: Using coprolites to reconstruct the habits and habitats of New Zealand's extinct upland moa (*Megalapteryx didinus*). *PLOS ONE* 7, e40025. https://doi.org/10.1371/journal.pone.0040025

Worona, M.A., & Whitlock, C., 1995. Late Quaternary vegetation and climate history near Little Lake, central Coast Range, Oregon. *Geological Society of America Bulletin*, 107(7), 867–876. https://doi.org/10.1130/0016-76061995107<0867:LQVACH>2.3.CO;2

Wriston, T., Smith, G.M., 2017. Late Pleistocene to Holocene history of Lake Warner and its prehistoric occupations, Warner Valley, Oregon (USA). *Quaternary Research* 88, 491–513. doi.org/10.1017/qua.2017.59